

CRITICAL MEMBER ANALYSIS OF  
WELLHEAD OFFSHORE PLATFORM DUE TO  
EL CENTRO EARTHQUAKE

LENG YEE HUI

B. ENG(HONS.) CIVIL ENGINEERING

UNIVERSITI MALAYSIA PAHANG

## UNIVERSITI MALAYSIA PAHANG

### DECLARATION OF THESIS AND COPYRIGHT

Author's Full Name : LENG YEE HUI

Date of Birth : 22 DECEMBER 1994

Title : CRITICAL MEMBER ANALYSIS OF WELLHEAD  
OFFSHORE PLATFORM DUE TO EL CENTRO  
EARTHQUAKE

Academic Session : 2017/2018

I declare that this thesis is classified as:

- CONFIDENTIAL (Contains confidential information under the Official Secret Act 1997)\*
- RESTRICTED (Contains restricted information as specified by the organization where research was done)\*
- OPEN ACCESS I agree that my thesis to be published as online open access (Full Text)

I acknowledge that Universiti Malaysia Pahang reserves the following rights:

1. The Thesis is the Property of Universiti Malaysia Pahang
2. The Library of Universiti Malaysia Pahang has the right to make copies of the thesis for the purpose of research only.
3. The Library has the right to make copies of the thesis for academic exchange.

Certified by:

\_\_\_\_\_  
(Student's Signature)

\_\_\_\_\_  
(Supervisor's Signature)

941222-02-5241  
New IC/Passport Number  
Date: 11 JUN 2018

IR.DR SAFFUAN BIN WAN  
AHMAD  
Name of Supervisor  
Date: 11 JUN 2018

NOTE : \* If the thesis is CONFIDENTIAL or RESTRICTED, please attach a thesis declaration letter.



## **SUPERVISOR'S DECLARATION**

I hereby declare that I have checked this project and in my opinion, this project is adequate in terms of scope and quality for the award of the Bachelor Degree in Civil Engineering

---

(Supervisor's Signature)

Full Name : IR.DR SAFFUAN BIN WAN AHMAD  
Position : Lecturer  
Date : 11 JUN 2018



## **STUDENT'S DECLARATION**

I hereby declare that the work in this thesis is based on my original work except for quotations and citations which have been duly acknowledged. I also declare that it has not been previously or concurrently submitted for any other degree at Universiti Malaysia Pahang or any other institutions.

---

(Student's Signature)

Full Name : LENG YEE HUI

ID Number : AA 14246

Date : 11 JUN 2018

CRITICAL MEMBER ANALYSIS OF WELLHEAD OFFSHORE  
DUE TO AL CENTRO EARTHQUAKE

LENG YEE HUI

Thesis submitted in fulfillment of the requirements  
for the award of the  
Bachelor Degree in Civil Engineering

Faculty of Civil Engineering and Earth Resources  
UNIVERSITI MALAYSIA PAHANG

JUNE 2018

## **DEDICATION**

**This thesis is proudly dedicated to**

**My beloved parent**

**Leng So Hua and Yeoh Ley Peng**

**For their great support, pray, love and care**

**My supervisor**

**Ir. Dr. Saffuan**

**For his excellent guidance, advice, and motivation**

**Making me who I am today**

## ACKNOWLEDGEMENTS

I would like to take this opportunity to thank my university, University Malaysia Pahang for providing me the good condition of facilities and equipment to complete this study.

I would also like to express my sincere gratitude to my supervisor, Ir. Dr. Saffuan Bin Wan Ahmad, who has been very supportive in guiding and providing me informative discussion and recommendation throughout the programme. His undeviating encouragement and motivation allowed me to perform and unleash my potentiality in this research field.

In addition, I would like to express my gratitude to my panel, Dr. Fadzil bin Mat Yahaya, and En. Khalimi Johan bin Abd Hamid for their valuable suggestions and comments on my work to allow me to improve my research outcome and meet the objectives of this study.

Apart from that, I would like to thank all the lecturers who have taught me in every semester. They have indeed helped me to reinforce my basic knowledge and theories in this field. A special thanks to my friend, Lee Jia Qing, for his willingness to share their precious knowledge and resources with me in completing this research work.

Finally, I am also grateful to my family Mr. Leng So Hua, Ms. Yeoh Ley Peng, and Ms. Wendy Lee Jiang Wen for their love, support, care, and encouragement all the way to the completion of my task in this programme.

## ABSTRAK

Kajian ini berkenaan dengan analisis seismik ahli struktur luar pesisir yang kritikal di Malaysia dengan matlamat untuk mengira maklum balas dan menilai kapasiti rintangan struktur untuk memuatkan gempa bumi. Walau bagaimanapun, keadaan sempadan struktur luar pesisir dianggap sebagai tetap kepada tanah dan interaksi tanah telah diabaikan. Kajian ini dijalankan kerana gegaran berlaku di Malaysia telah dilaporkan beberapa kali yang disebabkan oleh gempa Sumatra dan Filipina. Oleh itu, jurutera-jurutera bimbang tentang kelemahan seismik struktur luar pesisir kerana kekurangan pertimbangan pemuatan seismik dalam prosedur reka bentuk bangunan Malaysia. Dengan ini, platform luar pesisir telah dianalisis dengan menggunakan SAP2000 di bawah pelbagai jenis analisis termasuk Analisis Getaran Bebas (FVA), Spektrum Respon (RS) dengan menggunakan lengkung spektrum tindak balas Eurocode 8 dan Analisis Sejarah Masa (THA) memandangkan data gempa El Centro 1940. Kod reka bentuk yang digunakan untuk struktur keluli ialah Eurocode 3. Data-data faktor alam sekitar yang dipertimbangkan adalah seperti ketinggian gelombang, tempoh gelombang, halaju arus dan pecutan gerak tanah. Angkutan alam sekitar seperti gelombang dan beban angin telah direka dengan merujuk kepada kriteria reka bentuk API (American Petroleum Institute). Sebagai kesimpulannya, struktur luar pesisir adalah stabil dan mampu menahan kepada gempa bumi. Reka bentuk struktur luar pesisir dapat memberikan ketahanan yang mencukupi terhadap kesan seismik dan sebahagian besar strukturnya berada dalam keadaan baik.



## **ABSTRACT**

The paper deals with the seismic analysis of a critical member of wellhead offshore platform in Malaysia with the aim to compute the response and assess the resistance capacity of the structure to earthquake loading. However, the boundary condition of the offshore structure is assumed as fixed to the ground and soil interaction has been neglected. This study is conducted due to tremors occurred in Malaysia caused by Sumatra and Philippine earthquakes have been reported several times. Thus, engineers are concerned about the seismic vulnerability of offshore structures due to lack of earthquake consideration in Malaysia's building design procedure. With this, wellhead offshore platform is analyzed using Finite Element Modelling (FEM) by SAP2000 software under different types of analyses including Free Vibration Analysis (FVA), Response Spectrum (RS) by using response spectra curves of Eurocode 8 and Time History Analysis (THA) considering El Centro 1940 earthquake data. The design code for the steel frame is Eurocode 3. All the environmental factors data are given such as ranges of wave height, wave period, current velocity and ground motion acceleration. The environmental loadings such as wave and wind load have been designed by referring API (American Petroleum Institute) design criteria. In conclusion, wellhead offshore platform is stable and capable to withstand the earthquake. It can be concluded that the design of the offshore structures can provide sufficient resistance against seismic effects and most of the part of the structure was in good condition.

## TABLE OF CONTENT

<b>DECLARATION</b>	
<b>TITLE PAGE</b>	
<b>DEDICATION</b>	<b>ii</b>
<b>ACKNOWLEDGEMENTS</b>	<b>iii</b>
<b>ABSTRAK</b>	<b>iv</b>
<b>ABSTRACT</b>	<b>v</b>
<b>TABLE OF CONTENT</b>	<b>vi</b>
<b>LIST OF TABLES</b>	<b>ix</b>
<b>LIST OF FIGURES</b>	<b>x</b>
<b>LIST OF SYMBOLS</b>	<b>xiii</b>
<b>LIST OF ABBREVIATIONS</b>	<b>xiv</b>
<b>CHAPTER 1 INTRODUCTION</b>	<b>1</b>
1.1 Background of Study	1
1.2 Problem Statement	4
1.3 Objectives	6
1.4 Scope of Study	6
1.5 Significance of Study	7
<b>CHAPTER 2 LITERATURE REVIEW</b>	<b>9</b>
2.1 Introduction	9
2.2 Earthquake	9
2.2.1 Plates Tectonics Theory	10

2.2.2	Fault	13
2.2.3	Seismic Waves	14
2.2.4	Earthquake Measurement	16
2.3	El Centro Earthquake, 1940	22
2.4	Seismicity in Malaysia	23
2.5	Offshore Structure	26
2.5.1	Offshore Wellhead Platform Support Frame	27
2.6	Code of Practices for Offshore Structure	28
2.6.1	Seismic Design Guideline	29
2.6.2	Environmental Load Design Guideline	32
2.6.3	Structural Design Guideline for Steel Structure	33
2.7	Design Criteria for Offshore Structure	33
2.7.1	Dead Load	34
2.7.2	Live Load	34
2.7.3	Wind Load	34
2.7.4	Waves Load	35
2.7.5	Current Load	36
2.7.6	Earthquake Load	36
2.8	Seismic Response of the Structure	37
<b>CHAPTER 3 METHODOLOGY</b>		<b>41</b>
3.1	Planning of Study	41
3.2	Information and Data Collection	43
3.2.1	Detailing Description	43
3.2.2	Material Description	45
3.2.3	Loads Description	45

3.3	Load Combination	51
3.4	Resistance Capacity for Structural member	51
3.4.1	The resistance of Cross Sections	52
3.4.2	Buckling Resistance of Members	53
3.5	SAP2000 Computational Program	55
3.5.1	Checklist of SAP2000 Modelling and Analysis	56
3.5.2	Steps in SAP2000 Modelling and Analysis	56
<b>CHAPTER 4 RESULTS AND DISCUSSION</b>		<b>70</b>
4.1	Summary of Analysis	70
4.2	Wellhead Offshore Modelling	71
4.3	Free Vibration Analysis	72
4.4	Time History Analysis	75
4.5	Response Spectrum Analysis	80
4.6	Linear Analysis	82
4.7	Result Comparison of SAP 2000 and Manual Calculation	87
4.8	Summary of Analysis	88
<b>CHAPTER 5 CONCLUSION</b>		<b>104</b>
5.1	Conclusion	104
5.2	Recommendations	106
<b>REFERENCES</b>		<b>108</b>
<b>APPENDIX A Grid system data</b>		<b>112</b>
<b>APPENDIX B Modal Shape of offshore platform</b>		<b>113</b>
<b>APPENDIX C Manual Calculation</b>		<b>116</b>

## LIST OF TABLES

Table 2.1	Richter scale	19
Table 2.2	Modified Mercalli intensity (MMI) scale	20
Table 2.3	Local earthquake occurrences in Malaysia	24
Table 2.4	Result of dynamic response from different input in the analysis	40
Table 3.1	Dead loads and live load description	46
Table 3.2	Environmental criteria used at Terengganu	46
Table 3.3	Shape Coefficient, $C_s$	47
Table 3.4	Drag coefficient, $C_d$ and Inertia Coefficient, $C_m$	49
Table 3.5	Imperfection factors fro buckling factors, $\alpha$	55
Table 4.1	Modal period and frequencies	72
Table 4.2	Time History Displacement, Velocities, and Acceleration of Joint 37 in 3 directions	75
Table 4.3	Shear force diagram for several load combination at element 25	84
Table 4.4	Shear stress and allowable capacity check for several load combination at element 25	84
Table 4.5	Bending moment diagram for several load combination at element 25	86
Table 4.6	Bending stress and allowable capacity check for several load combination at element 25	86
Table 4.7	PMM Demand/Capacity Ratio between manual calculation and SAP2000	88
Table 4.8	Unity Ratio of Structure Member	89
Table 4.9	Joint Displacement in different load combination at joint 37	99
Table 4.10	Joint Velocities in different load combination at joint 37	100
Table 4.11	Joint Acceleration in different load combination at joint 37	101

## LIST OF FIGURES

Figure 1.1	Gross Domestic Products First Quarter 2018	1
Figure 1.2	Relationship of crude oil to other fossil fuels	2
Figure 1.3	a) Onshore drilling and b) offshore drilling	3
Figure 1.4	Plate Tectonic	4
Figure 1.5	Earthquake-prone region of Malaysia	5
Figure 2.1	General illustration of an earthquake rupture scenario	10
Figure 2.2	Inner earth	11
Figure 2.3	Major Plates	11
Figure 2.4	Conventional current below Earth	12
Figure 2.5	Types of interplates boundaries	13
Figure 2.6	Types of fault	14
Figure 2.7	Seismic wave types	16
Figure 2.8	Strong motion record from El Centro, 1940.	21
Figure 2.9	The collapse of these walls in the business district of Imperial caused the deaths of four people.	22
Figure 2.10	The collapse of the 100,000 gallon city water tank at Imperial.	22
Figure 2.11	Earthquake hazard zonation	25
Figure 2.12	Type of offshore structure	27
Figure 2.13	Fixed offshore platform	28
Figure 2.14	Seismic design procedure	31
Figure 2.15	Loads on offshore platform. ( $V$ , self-weight of topside; $M_v$ , moment with eccentric loading of platform; $L_b$ , lateral wind load; $L_c$ , lateral current load; $L_w$ , lateral wave load, $M_b$ & $M_c$ & $M_w$ , moment related to lateral loadings, and $E$ , seismic load)	33
Figure 2.16	Waves characteristic	35
Figure 2.17	Damped and undamped oscillations	38
Figure 3.1	Flow Chart of Methodology	42
Figure 3.2	Side view of wellhead support frame	44
Figure 3.3	Plan view of wellhead support frame	44
Figure 3.4	Data of material properties	45
Figure 3.5	Transferring earthquake data from East direction in MS Excel	50
Figure 3.6	Time (s) vs Acceleration (g) in E-direction	50
Figure 3.7	Selection of buckling curve for a cross section	55
Figure 3.8	Select the modal type and unit	57

Figure 3.9	Define grid system data	57
Figure 3.10	Define material types	58
Figure 3.11	Material properties data	58
Figure 3.12	Define pipe section	59
Figure 3.13	3D modelling of the structure	59
Figure 3.14	Restraint at the base	60
Figure 3.15	Define load pattern for each loading	60
Figure 3.16	Define all load cases	61
Figure 3.17	Dead load & live load	61
Figure 3.18	Dead load case data	61
Figure 3.19	Live load case data	62
Figure 3.20	Wind load pattern data	62
Figure 3.21	Wind load case data	63
Figure 3.22	Wave load pattern	63
Figure 3.23	Wave characteristics	64
Figure 3.24	Current profile data	64
Figure 3.25	Wave plot	65
Figure 3.26	Wave load case data	65
Figure 3.27	Define time history function	66
Figure 3.28	Linear modal history case data	66
Figure 3.29	Response spectrum EuroCode 8 function	67
Figure 3.30	Response spectrum load case data	67
Figure 3.31	Modal load case	68
Figure 3.32	Define load combination	68
Figure 3.33	Set load case to run	69
Figure 3.34	Result output table	69
Figure 4.1	3D model of the wellhead support frame	71
Figure 4.2	Modal periods	73
Figure 4.3	Three modes of vibration (a) mode shape 1 (0.1060 sec) (b) mode shape 2 (0.0878 sec) (c) mode shape 3 (0.0776 sec)	74
Figure 4.4	Time (sec) versus Acceleration (g)	75
Figure 4.5	Comparison of displacement history in x, y and z direction at Joint 37	77
Figure 4.6	Comparison of velocity history in x, y and z direction at Joint 37	78
Figure 4.7	Comparison of acceleration history in x, y and z direction at Joint 37	80
Figure 4.8	Pseudo Spectral Acceleration in x, y and z direction at Joint 37	82

Figure 4.9	PMM Demand/Capacity Ratio of Wellhead Offshore Structure	89
Figure 4.10	Graph of Bending Stress versus Load Cases	98
Figure 4.11	Graph of Shear Stress versus Load Cases	98
Figure 4.12	Graph of Joint Displacement versus Load Cases in Three Directions	99
Figure 4.13	Graph of Joint Velocities versus Load Cases in Three Directions	100
Figure 4.14	Graph of Joint Acceleration versus Load Cases in Three Directions	101
Figure 4.15	Deformed shape of DL + LL	101
Figure 4.16	Deformed shape of EL	102
Figure 4.17	Deformed shape of DL + LL + EL + TH_AC	102
Figure 4.18	Deformed shape of RS	103



## LIST OF SYMBOLS

km	kilometer
cm/yr	centimeter per year
$m/s^2$	metre per square second
Hz	hertz
m	meter
Nm	Newton meter
Mm	Millimetre
N	Newton
$Kg/m^3$	kilogram per cubic meter
m/s	meter per second
$m^2$	square meter
MPA	Mega Pascal
G	Gal
Hz	Hertz
$N/m^3$	Newton per cubic meter
MN	Mega newton
s	second

## LIST OF ABBREVIATIONS

GDP	Gross Domestic Product
BS	British Standard
EC	Eurocode
ISO	International Organization for Standardization
API	American Petroleum Institute
P	Primary
S	Secondary
L	Love
R	Rayleigh
$\nu$	Poisson's ratio
$E$	Young's modulus
$G$	Shear modulus
$P$	Density
$M_L$	Local magnitude
$m_b$	Body wave magnitude
$A$	Maximum amplitude (in microns)
$T$	Period (in seconds)
$M_s$	Surface wave magnitude
$M_w$	Moment magnitude
$A$	Fault area
$U$	longitudinal displacement of fault (in m)
$M_o$	Seismic moment (in Nm)
MMI	Modified Mercalli Intensity
PGA	Peak ground acceleration
PGV	Peak ground velocity
US	United State
ATC	Applied Technology Council
FPU	Floating production unit
FPSO	Floating production, storage and offloading
DLE	Ductility Level Earthquake
PSHA	Probabilistic Seismic Hazard Assessment
DSHA	Deterministic Seismic Hazard Assessment
CEN	European Committee for Standardization
ELE	Extreme level Earthquake
ALE	Abnormal Level Earthquake
ULS	Ultimate limit state
V	Self-weight of topside
$M_v$	Moment with eccentric loading of platform
$L_b$	Lateral wind load
$L_c$	Lateral current load
$L_w$	Lateral wave load
$M_b$	Moment related to wave loadings
$M_c$	Moment related to current loadings
$M_w$	Moment related to wind loadings
D, $\emptyset$	Diameter
L	Length
$\omega$	Circular frequency (in rad/sec)
$f$	Number of vibration (Hertz or cycle/sec)

$T$	Time required to complete one cycle of vibration
W.T	Wall thickness
$u(z, t)$	Design wind speed
$z$	Height above sea level
$U(z)$	1 hour mean wind speed
$I_u(z)$	Turbulence intensity
F	Wind drag force
P	Density of air
U	Wind speed
$C_s$	Shape coefficient
A	Area of object
$F_w$	Hydrodynamic force vector per unit length
$F_D$	Drag force per unit length
$C_d$	Drag coefficient
$C_m$	Inertia coefficient
$U_{mo}$	Maximum horizontal particle velocity at storm mean water level
$T_{app}$	Apparent wave period
$D$	Platform leg diameter at storm mean water level
$G$	Gravity acceleration
FVA	Free vibration analysis
DL	Dead load
LL	Live load
EL	Environmental load
TH	Time history
RS	Response spectrum
$f_y$	Yield strength
$f_u$	Ultimate strength
$\gamma_{M0}, \gamma_{M1}, \gamma_{M2}$	Partial factor
$W_{pl}$	Plastic section modulus
$M_{c,Rd}$	Design bending resistance
$M_{pl,Rd}$	Design plastic bending resistance
$V_{c,Rd}$	Design shear resistance
$V_{pl,Rd}$	Design plastic shear resistance
$\chi$	Reduction factor for buckling mode
$\lambda$	Non-dimensional slenderness
$\lambda_1$	Relative slenderness
$\varepsilon$	Strain
$L_{cr}$	Buckling length
$i$	Radius of gyration
$\alpha$	Imperfection factor
$V_{Ed}$	Design shear force
$f_v$	Shear stress
$V_{b,RD}$	Allowable shear force
$F_v$	Allowable shear stress
$M_{Ed}$	Design moment
$f_b$	Bending stress
$M_{b,RD}$	Allowable bending moment
$F_b$	Allowable bending stress

# CHAPTER 1

## INTRODUCTION

### 1.1 Background of Study

Malaysia is the third-largest exporter of liquefied natural gas in the world and the second largest oil and natural gas manufacturer in Southeast Asia (US. Energy, Information Administration, 2011). In spite of the low price of global crude oil, Oil and Gas sector is still playing a crucial role in our country because it subsidizes around 20 to 30 % to the Gross Domestic Product (GDP) in Malaysia. It recognized as an important and priority sector by Petroliaam Nasional Bhd (PETRONAS, the National Oil Company) and Malaysia's Government due to the massive multiplier effect developed by this sector with more than 3,500 companies that work in oil and gas (O&G) in Malaysia (PWC, 2016). This showed that the petroleum industry is still a major element of the worldwide economy.

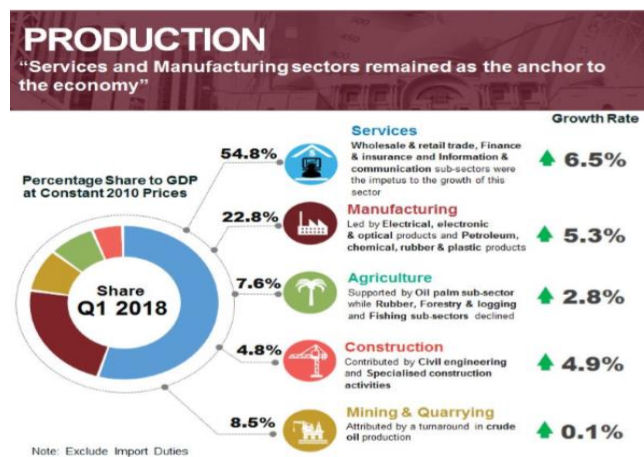


Figure 1.1 Gross Domestic Products First Quarter 2018  
Sources: Department of Statistic Malaysia, 2018

The processes involved in petroleum industry are exploration, extraction, refining, transporting, and marketing of petroleum product. Petroleum, as known as

crude oil and natural gas which are a mixture of hydrocarbon molecules that made up by the dead bodies of plants and animals, mostly was the small marine life that had lived millions of years ago. Basically, these petroleum reservoirs are located at thousands of feet below the surface. Hence, drilled wells are required to install to the reservoirs in order to reveal or determine oil and gas for multiple functions development and economic uses. Generally, one or more exploratory wells and several development wells may require for a sizable petroleum reservoir. An exploratory well is to identify petroleum reservoir purposes while development well is to manufacture discovered oil and gas. Oil and gas reserves is the volumes of oil and gas discovered within the petroleum reservoir (Light, 2011).

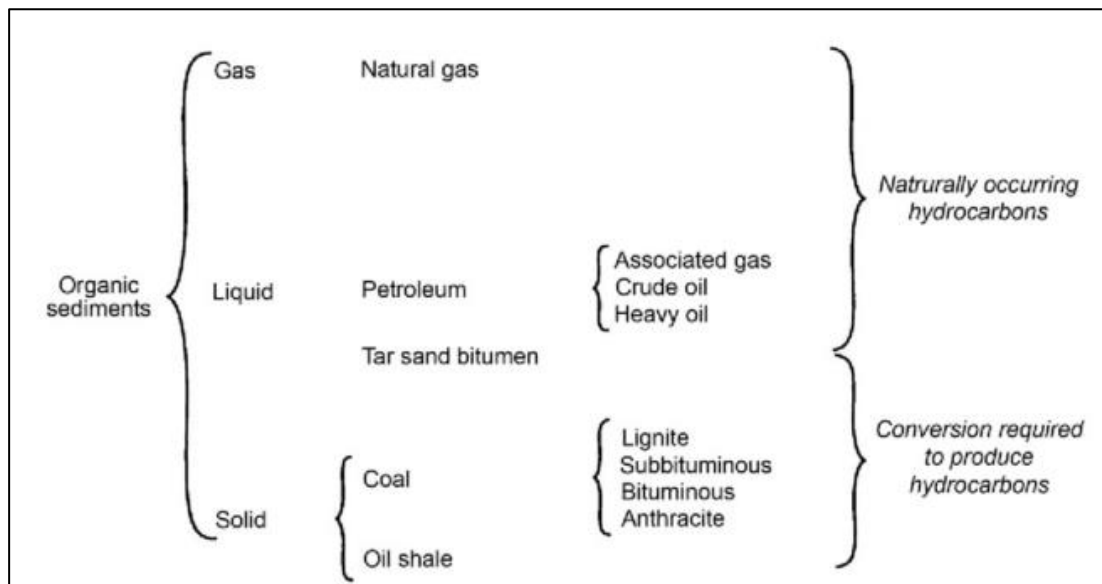


Figure 1.2 Relationship of crude oil to other fossil fuels  
Sources: (Speight, 2015)

There are two advanced drilling techniques for oil and gas: offshore drilling and onshore drilling. Onshore drilling indicates that the deep holes are drilling under the earth's surface while offshore drilling refers to drilling underneath the seabed. In term of cost, onshore drilling will be more economical than offshore drilling as the timeline of the contract is often shorter. However, offshore drilling is adopted in Malaysia as most of the reserves are discovered beneath the seabed (US. Energy, Information Administration, 2011). Unlike onshore drilling, offshore drilling will be facing more challenges on the stability issues due to the shear depth of water before reaching the seabed. Hence, the platform must remain stable and secure by facilitating some anchoring to the ocean floor. These platforms use either in the fixed or floating platform.

The types of offshore drilling platforms including fixed platform, compliant towers, sea star, floating production system, tension leg platform, subsea platform and SPAR platform (Devold, 2002).



(a)



(b)

Figure 1.3 a) Onshore drilling and b) offshore drilling

Sources: Devold, 2002; Speight, 2015

The design lifetime of the offshore structures must be at least 25 years or more depending on the reservoir capacity. Offshore platforms are either constructed in huge steel or concrete structures to explore and extract the oil and gas from the petroleum reservoir. In terms of the response of the structure and loading system, it leads to the construction of offshore structures is more complicated compared with onshore structures. This is because of the high level of uncertainties and high dependency on the environment condition that increases the complexity of design and construction process as the offshore structure used have been extended from shallow to deep water (Mukhlas et al., 2016). This is the most challenging and inventive task for the engineers to design the best offshore structure platform that is reconcilable with that tremendous environmental condition (A S Kharade; and S V Kapadiya, 2014).

However, there are some design considerations that are crucial for engineers to be taken humourlessly such as the peak loads created by cyclone wind, strong waves and seismic load as well. According to Marto, Tan, Kasim, & Mohd.Yunus, (2013), although Malaysia is considered as relatively low seismicity but it is important for engineers to take into account to the design as Malaysia is bordered by the most two seismically active plate boundaries which are on the west and east from the inter-plate boundary between the Indo-Australian and Eurasian Plates and the inter-plate boundary

between the Eurasian and Philippines Sea Plates respectively. Most of the earthquakes came from these plate boundaries have been felt in Malaysia. Tremors felt in the west coast of Peninsular Malaysia are generated from large earthquakes in the seismic area of Sumatra and the Andaman Sea whereas East Malaysia is affected by tremors from large earthquakes at Southern Philippines and Northern Sulawesi. Besides, Peninsular Malaysia (e.g., Bukit Tinggi, Jerantut, Temenggor, and Kuala Pilah) and East Malaysia have experienced few of earthquakes from the local origin which are considered as an active fault that exists in Peninsular Malaysia, Sabah and Sarawak (Malaysian Meteorological Service, 2009).

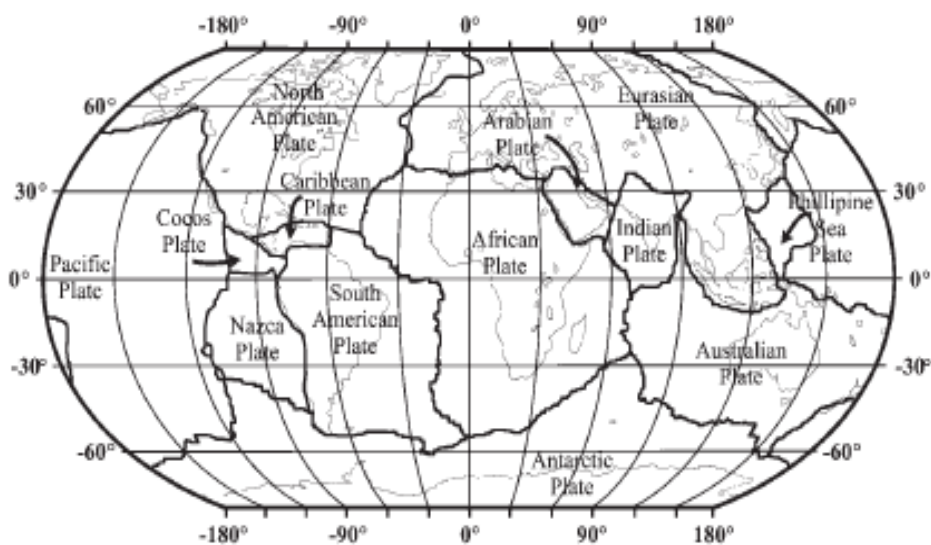


Figure 1.4 Plate Tectonic

Sources: (Hatheway, 1996)

As a consequence, these structures are necessary to be analyzed in all possible manners to prevent structural failure and loss of life of workers as they are located long away from the shoreline (A S Kharade; and S V Kapadiya, 2014). The objective is to design a structure which is durable and indestructible that can resist the unfavorable conditions of high winds, wave's effect, earthquakes, and tsunami.

## 1.2 Problem Statement

Malaysia is inching closer to seismic zones and will not immune to earthquake forever. Although Malaysia is located on the stable Sunda plate, it still affected by earthquake tremors as it is near to seismically active earthquake sources of Sumatra (Manafizad, Pradhan, & Abdullahi, 2016). Besides that, the pressure on the land is

accumulating due to the Australian, Eurasian and Philippine plates are moving and pushing into us. Hence, it seems unpreventable to investigate the hazard and risk from earthquake and consider earthquake-resistant in the building design due to reformation in the core of Sunda-land.

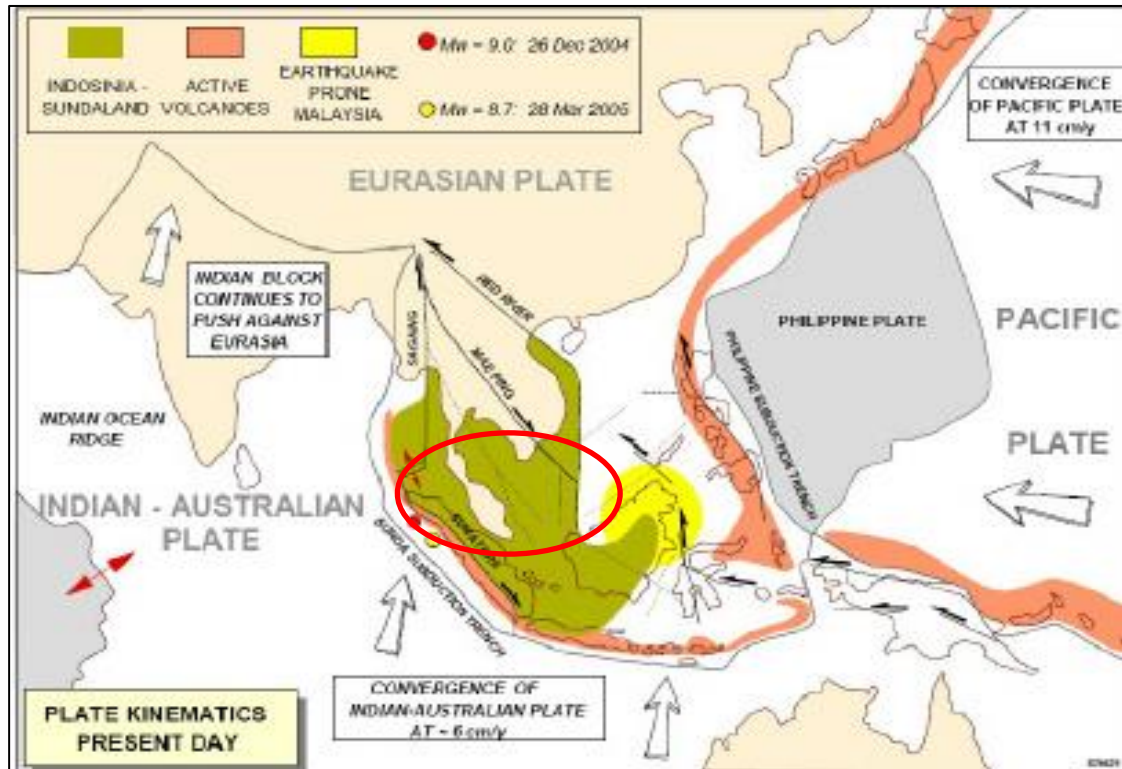


Figure 1.5 Earthquake-prone region of Malaysia

Sources: (Marto, Tan, Kasim, & Mohd.Yunus, 2013)

Repeated earthquake or multi-event earthquake is defined as the first tremor is followed by other tremors. This is because of the nature of earthquake and it can occur in a few hours after the first one, and extend to a few days. Therefore, buildings are against to the seismic action loads more than one time during a great earthquake event. The buildings may subject to the damages from minor to moderate after undergoes the first tremor, followed by another tremor, resulting in stiffness and strength degradation of the overall system.

Moreover, in Malaysia, structural steelwork buildings were designed according to the BS5950 code of practice or Eurocode 3: Design of steel structure, which does not specify any provisions for seismic forces. Although the references of Uniform Building by-laws have stated that to be considered seismic forces in the building design it does not state what values and measures should be used. After experienced several tremors,



the Malaysian start to questionnaire about the integrity and the structural capacity of existing structures in Malaysia to resist earthquake load in future without fail. In addition, they also interested in how vulnerable a building to the seismic effect or the seismic responses from the structure depends on the ground motion modeling. Therefore, it is important to determine the necessity of seismic design consideration for wellhead offshore structure to prevent structural failure.

### **1.3 Objectives**

The main objectives of this research are:

- i. To obtain the earthquake resistance capacity of wellhead offshore platform in Malaysia due to El Centro earthquake by using SAP 2000.
- ii. To compute the seismic performance of wellhead offshore platform in Malaysia by considering El Centro earthquake.
- iii. To provide a desirable result for performance evaluation parameters of wellhead offshore platform in Malaysia by identifying specific demand parameters.

### **1.4 Scope of Study**

This research is about the seismic response of wellhead offshore structure due to surrounding earthquake. Hence, there are some scopes that need to be followed, reviewed from time to time in order to the objective of this research. The research scopes are as follows:

- i. The offshore structure is located on East Coast of Peninsular Malaysia, Terengganu.
- ii. The study will only consider wind load, wave's buoyant forces, current loading and earthquake load from surrounding as the lateral and vertical forces that act on the structure.
- iii. The software used for computational analysis and structural modeling of the structure is SAP2000 version 18.

- iv. The analysis of seismic is conducted as follows to determine the seismic response of a wellhead offshore structure by utilizing the available historical seismic data from El Centro earthquake:
  - Free vibration analysis is to obtain the natural frequency, period and the deformed shape of the wellhead offshore structure
  - Time history seismic analysis is to be carried out by referring to the time history of the earthquake in El Centro 1940.
  - The response spectrum seismic analysis is to be carried out by using response spectra curves of Eurocode 8, EC8.
- v. The structure is considered to be fully fixed at the base restraint and soil interaction has been neglected in the analysis. The connection in the member is assumed as rigid as the details in the drawing are confidential.
- vi. ISO 19901-2:2004 (Modified), Petroleum and natural gas industries – Part 2: Seismic design procedure and criteria of the American Petroleum Institute, API 2014 are used for the consideration of seismic design procedure and criteria to the structure (ANSI/API-RP 2EQ).
- vii. The consideration of design criteria for loading are referred to American Petroleum Institute: Recommended Practice for Planning, Designing and Constructing Fixed Offshore Platform – Working Stress Design, 21<sup>st</sup> Edition, December 2000 (API-RP2A).
- viii. The consideration of the structural design is referred to Eurocode 3: Design of steel structure – Part 1-1: General rules and rule for the building.

## **1.5 Significance of Study**

The knowledge about the seismic actions and structural response based on the fundamental concept of earthquake engineering nowadays was created in 70 years ago. Today, the transformation of the new seismic knowledge to practice is not completely done as there are many initial concepts keep changing and updating due to the progress

in research works for achieving a satisfactory level of seismic design. For the development of Engineering Seismology and Earthquake Engineering, structural response analysis is the most common method used by major researchers as the structural response can be fairly predicted from the modeling. However, the uncertainties in the ground motion are the major challenge in seismic design due to unforeseen forces at an unpredicted time as these events occur below the earth. Hence, it is necessary to reassess the seismic resistance of the building.

Studies like this are meant to determine the seismic structural response of wellhead offshore platform structure that located in East Coast of Peninsular Malaysia based on model-based computer simulations. This may help to improve the seismic design of the structure to reach a satisfactory level and design a building that can withstand an earthquake without failure. Hence, the main objective of this research for identifying the necessity of the implementation of seismic designs consideration in designing offshore structure in Malaysia. Besides that, studies also contribute to reducing human and economic losses by solving the balance between earthquake demand and structural capacity of the structure.

Moreover, studies also help in improving the understanding of behavior and collapse mechanism of the structure under different types of the earthquake in order to establish new methodologies that able to consider different design knowledge for the structure located in low to moderate and string seismic area. In addition, the development of next-generation performance-based codes can be enhanced. This is because of accumulated results able to transfer from the research to design practice and to upgrade any existing gap between the studies. This may help consultants to aware of hazards and risks created by the earthquake and use locally developed parameters in their design assessments. Hence, implementation of the seismic design is important and helps to keep buildings steady during the next big earthquake.

## **CHAPTER 2**

### **LITERATURE REVIEW**

#### **2.1 Introduction**

This chapter will be emphasized on the causes of earthquakes for a good understanding of the overall geophysical process of the earthquake. The sources that induced the propagation and measurement of seismic waves through earth will briefly discuss. The next section will cover the details of offshore platform structure to provide a good understanding of the background. Design criteria considered used for the structure including the method of seismic analysis and current design practices in Malaysia are then briefly discussed. The final section will cover the seismic response from the structure of the seismic analysis.

#### **2.2 Earthquake**

Earthquakes are one of nature's greatest hazards that produced an unexpected and tremendous destruction of life and property. There are four modes of generation – tectonic, volcanic, collapse, or explosion. This natural hazard, however, did not kill people but the collapse of the structure caused by it can do. The structure can be damaged by an earthquake in three different ways: (a) ground failure, (b) other effects produced by the earthquake that may affect the structure indirectly, and (c) ground vibration on which the structure stays. As an example, some possible ground failures are ground cracking, landslides, soil liquefaction at surface faulting and the common indirect effect that may vandalize a structure is Tsunami. Among these three earthquake effects, ground shaking is the most destructing to structures as the ground is moving vertically and horizontally that caused the structure on the shaking ground oscillating according to these motion and experiences massive stress and deformation.

Basically, an earthquake is a phenomenon that involves the motion or vibrating of the earth's crust by waves that coming from a source of disturbance that sudden release of energy inside the earth. Figure 2.1 illustrated the energy is released by the brittle failure on faults and carried by the propagation of seismic waves. The initial point of earthquake rupture is known as focus or hypocentre. The epicentre is the point that directly above the hypocentre earth's surface. The earthquake focus is due to the sliding of Earth's mass takes places in pieces that called Tectonic Plates which will be briefly discussed in the following sub-chapters.

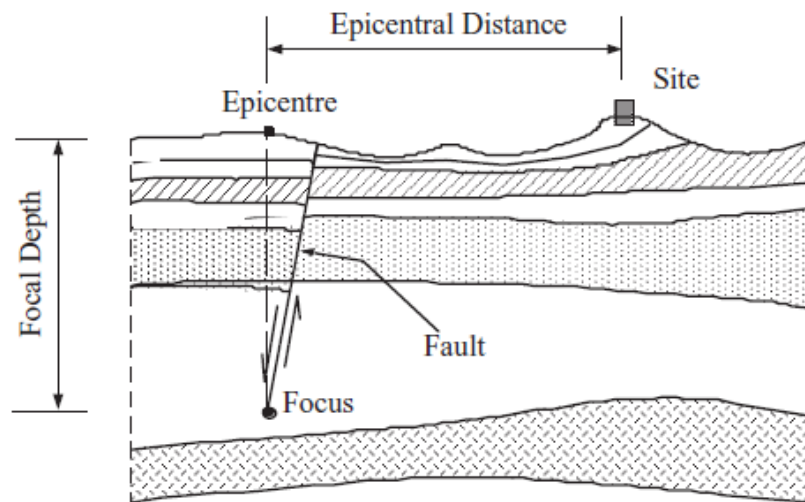


Figure 2.1 General illustration of an earthquake rupture scenario

Sources: (Hatheway, 1996)

### 2.2.1 Plates Tectonics Theory

Earth is made up of four layers: inner core, outer core, mantle, and crust. The upper part of the earth is divided into two different properties layers. The upper layer is rigid such as lithosphere that made up of crust and mantle whereas the lower layer known as asthenosphere which is at 700km depth. The Earth's crust was composed of continental crust and oceanic crust. Figure 2.2 below depicts the inner structure of the earth.

The theory of plate tectonics stated that lithosphere is divided into seven large segments known as major plates and a large number of minor plates. Both continental crust and oceanic crust are including in tectonic plate. The most important plates among the 52 important tectonic plates which are: African (continental plate), North and South

American (continental plate), Antarctic (continental plate), Indo-Australian (continental plate), Eurasian (continental plate) and Pacific plate (oceanic plate) which can be shown in Figure 2.3. The lithospheric plates can be floated in a complex pattern, moving with a velocity of about 2-10 cm/year on the soft rocks that underlying asthenosphere. This theory requires a source that can generate tremendous force is acting on the plates that offered by convection currents created by the thermos-mechanical behavior of the earth's subsurface.

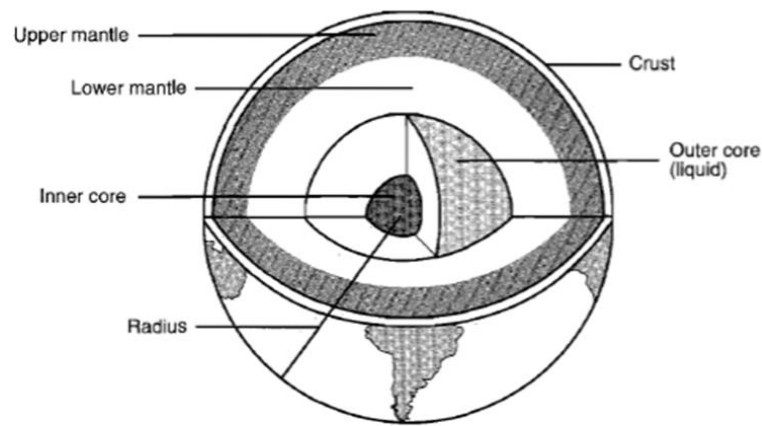


Figure 2.3 Internal structure of the earth.

Figure 2.2 Inner earth

Sources: (Kramer, 1996)

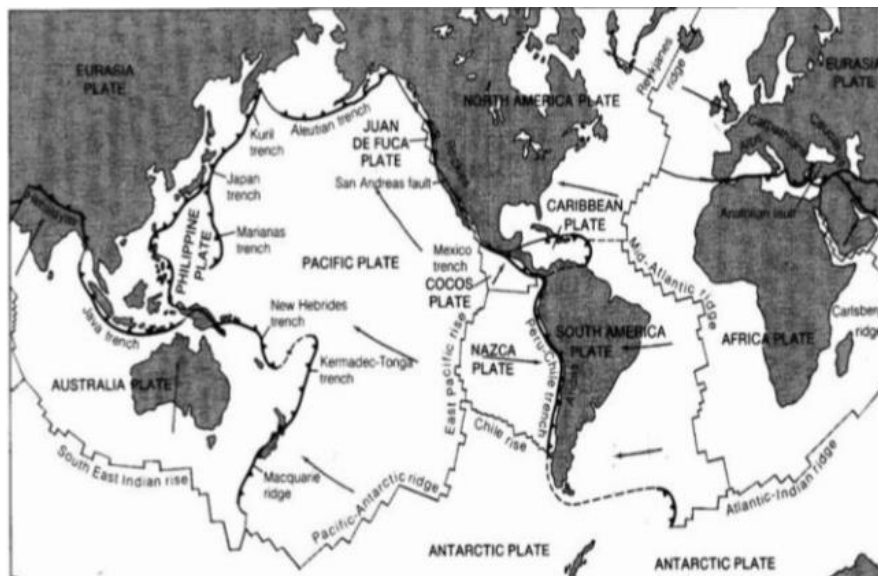


Figure 2.3 Major Plates

Sources: (Manafizad et al., 2016)

According to continental drift concept, it states that two lands with large masses are initial linked-in-chains but drift apart from each other, mid-ocean ridges is formed (underwater mountain system) due to a hot mantle move upward to the earth's surface at the ridges, then convective circulation occurs. Figure 2.4 showed the derivation of the energy of convective flow in the mantle, formed an extra crust on the lithosphere that flows on the asthenosphere and cools in the surface. The newly formed crust will eventually spread outwards as the continuously upwelling of molten rock and sink underneath the sea surface as it cools down. This phenomenon called seafloor spreading.

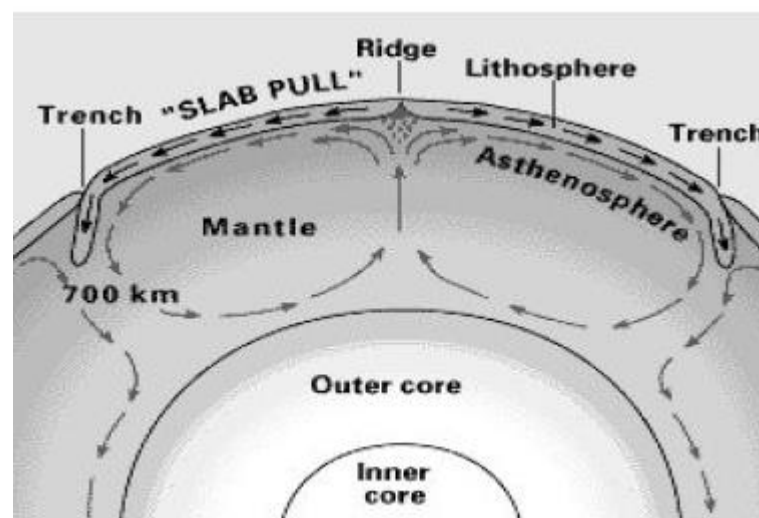


Figure 2.4 Conventional current below Earth

Sources: (Gioncu & Mazzolani, 2011)

As plate glides over the asthenosphere, the continents and ocean move with it. They may knock against their neighbors at boundaries. The great forces thus generated at plate boundary that caused earthquakes. There are two types of earthquakes, one is an inter-plate earthquake which occurs at the plate boundaries; another one is an intra-plate earthquake which occurs on the plate and far from plate boundaries. Basically, there are three types of plate boundaries can be grouped in inter-plate interaction:

i. Divergent boundaries

Divergent boundaries are areas that two plates are moving away from each other due to the rising of molten lava. One of the examples of divergent boundaries is The Mid Atlantic Ridge (mid-ocean ridges, also called spreading centres).

ii. Convergent boundaries

It happens when two plates are moving toward each other and collide as they are slowly moving in front or opposing to each other. Example of convergent plate boundaries is subduction zones. It can be ocean-ocean convergent boundaries, ocean-continent convergent boundaries, and continental-continental convergent plates.

iii. Transform boundaries

It can be formed by two plates slide to each other side-by-side along the same fault with opposite direction. Transform faults and other strike-strip faults are some examples of transform boundaries. One of the famous examples of transform boundaries is San Andreas Fault which located along the boundary of North America and Pacific plates.

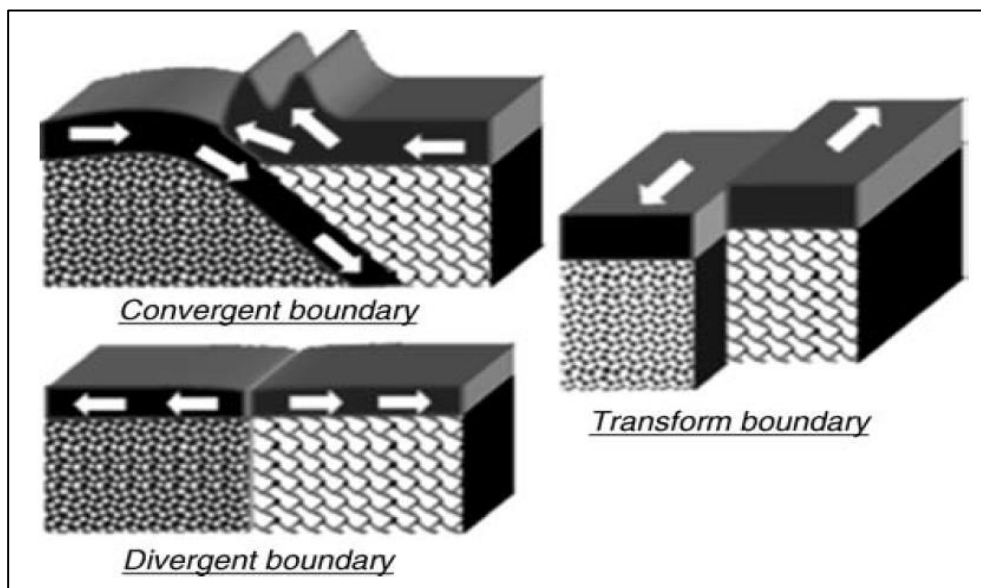


Figure 2.5 Types of interplates boundaries

Sources: (Datta, 2010)

### 2.2.2 Fault

Fault can be explained as the discontinuity in the rock mass and moved along with the movement which had occurred in the past. Large faults in the Earth's crust are caused by the action of plate tectonic forces from the boundaries forming in between the plates, for example, subduction zones or transform faults. Elastic strain energy is build upon a fault, by held statically by friction between the rocks, until the stress



accumulated and exceed the strength; the slip occurs along the fault line and released the energy stored in the waves form. This process can refer to Elastic Rebound theory. Most of the earthquakes are caused by the suddenly released energy and associated with rapid movement on active faults.

An active fault is the faults that have been undergoing deformation for a long time ago and can be continued to deform with time. As mentioned before, the focus or hypocentre of an earthquake is the point on the fault where rupture starts to occur. Earthquakes are classified into shallow focus, intermediate focus, and deep focus: but most of the dangerous earthquakes are from shallow focus. There are three types of fault movements which are normal, reverse, and strike-slip movements shown in figure 2.6. These movements involving the extension, compression, and lateral movement of the Earth's crust respectively.

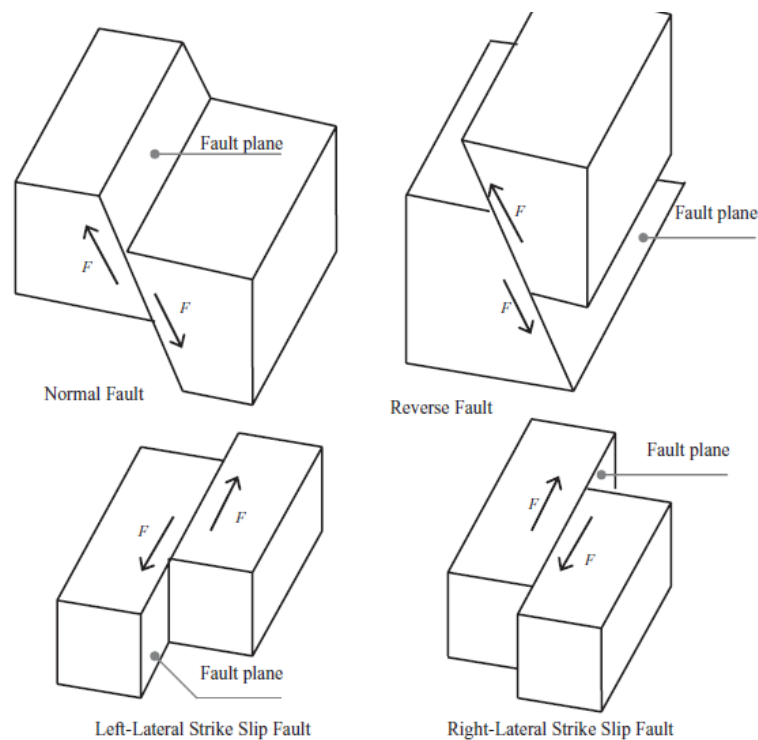


Figure 2.6 Types of fault

Sources: (Hatheway, 1996)

### 2.2.3 Seismic Waves

Seismic waves are the energy waves caused by the sudden breaking of rock in the Earth. These seismic waves carry the energy from one location of the earth to

another through many layers and finally to the surface and cause the destruction. Body waves and surface waves are two main types of seismic wave that radiating from the fault break (hypocentre sources) to the site. Body waves are waves that travel through the interior part of the earth with a period of 1 second and surface waves travel along the surface of the earth with a period of 20 seconds.

The body waves are P waves (primary) and S waves (secondary) that propagate through the Earth's crust. These two waves were recognized by Richard Dixon Oldham, a British geologist, and seismologist in early seismology. P wave will push and pull the rock by compression and expansion, caused the rock particle to oscillate backward and forward in the same direction as the waves transmit. Sound waves showed same properties which are short duration and small amplitudes which bring relatively little damage potential only. They are the fastest waves compared with other, having velocities of about 5-7 km/sec, and thereby this wave has a very high frequency. Since P wave is the first waves to arrive, they can be used for accurately recorded and determine the earthquake location.

S wave is the second type of body wave which moves the rock up and down (vertical, SV) or side to side (horizontal, SH) and vibrating perpendicularly to the direction of the wave propagates. This introduced the shear stresses in the rock along with their paths. They are slower and move with 3 to 4 km/sec but larger amplitudes and longer periods which may cause significant damage as compared to P wave. The velocity may be described by Navier's equation (Udias, 1999):

$$V_p = \sqrt{\frac{E(1-\nu)}{\rho(1+\nu)(1-2\nu)}} \quad 2.1$$

$$V_s = \sqrt{\frac{G}{\rho}} = \sqrt{\frac{E}{2\rho(1+\nu)}} \quad 2.2$$

Where

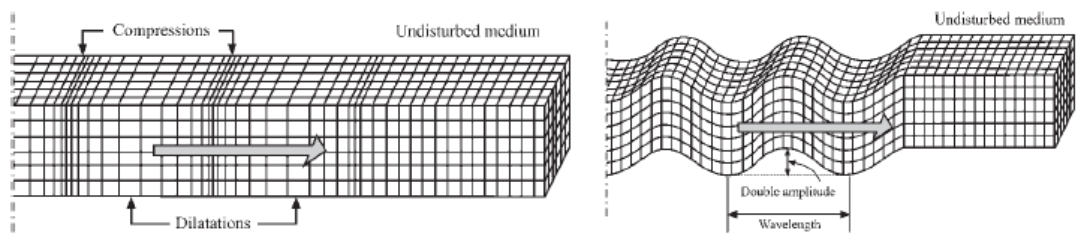
$\nu$  is the Poisson's ratio

$E$  is the Young's modulus of the elastic medium

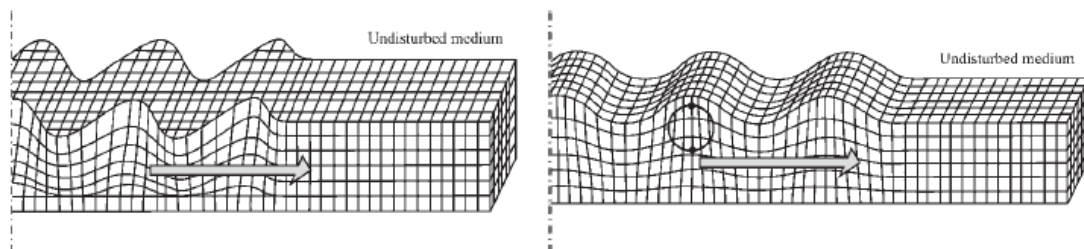
$G$  is the shear modulus

$P$  is the density

For surface waves, there are L waves (love) and R waves (Rayleigh), which travel along the Earth's surface. Kulhanek, 1990 has stated that surface waves can carry a massive amount of energy from shallow shock and are the main cause of the destruction of high population areas from the earthquake. Surface waves are more destructive due to low frequency, long duration, and large amplitude. L wave is caused by SH body waves and move the ground from side-to-side with a velocity of 2-4.4 km/sec while R wave is the combination of P and SV waves which move the ground up and down and side-to-side in the same direction as the wave is transmitting. To sum up, P waves is the first, followed by the S wave after some time; surface waves will be arriving after a short time with increasing of ground motion amplitude. All the seismic types will be shown in Figure 2.7.



(a) P-waves and S-waves



(b) L-waves and R-waves

Figure 2.7 Seismic wave types

Sources: (Hatheway, 1996)

## 2.2.4 Earthquake Measurement

### 2.2.4.1 Magnitude

Magnitude is one of the most fundamental parameters to describe an earthquake. It is a total energy released from an earthquake in the form of seismic waves that

including energy required forming new cracks in rocks, the energy dissipated through friction and energy elastically radiated through the Earth. However, we only interested in radiated energy as it can shake the building and recorded by seismographs. The seismic energy released by the earthquake is referring to a magnitude scale by seismologists. Each earthquake has their own unique amount of energy, but the magnitude values for the same event may vary due to different estimation methods.

There are a lot of definitions of magnitude: Richter magnitude or local magnitude, energy magnitude, moment magnitude, body-wave magnitude, etc. Hence, we must be very careful when we using the data of earthquake magnitude if the used scale is not declared. Among the magnitude scales, Richter scale is the most commonly used to express the seismic energy released by each earthquake. As a general guideline, an earthquake with a magnitude between 4.5 to 5.5 is considered as local; a seismic event with magnitude 6.0 to 7.0 is considered as large, and destructive earthquake is those magnitude larger than 8.0. The most common magnitude scales are described in the following section:

i. Local magnitude ( $M_L$ )

To measure the maximum seismic wave amplitude  $A$  (in microns) from a record of a seismic event that using Wood-Anderson seismograph located from the epicenter at a distance of 100 km. The natural frequency of seismograph is 0.8 s and it has a critical 0.8 damping ratio and 2800 for the amplification factor. This scale is applicable for the small and shallow earthquake in California and for epicenter distances less than 600km. Magnitude,  $M_L$  is calculated by the following:

$$M_L = \log(A) - \log(A_0) \quad 2.3$$

Where  $A$  is maximum amplitude (in microns) recorded on a standard short seismometer, and  $A_0$  is calibration factor that based on the distance where the distance  $\leq 100$ km.

ii. Body wave magnitude ( $m_b$ )

Gutenberg and Richter (1956) proposed  $m_b$  to measure the amplitude of P-waves with a period of 1.0 second. This scale is considered as worldwide scales and is suitable

for deep earthquakes that have few surface waves and for epicenter distances more than 1000km. It will not affect the depth of energy source and able to measure distance events not less than 600km. Magnitude,  $m_b$  that related to amplitude,  $A$  and period  $T$  of P-wave is given by:

$$m_b = \log\left(\frac{A}{T}\right) + \sigma(\Delta) \quad 2.4$$

Where  $A$  is the actual ground motion amplitude in microns,  $T$  is a corresponding period in seconds, and  $\sigma(\Delta)$  is a function of distance  $\Delta$  (in degrees).

iii. Surface wave magnitude ( $M_s$ )

It is a worldwide scale and to measure the period of the amplitude of LR-waves that have 20 seconds. Surface wave magnitude is normally used for great epicenter distances large earthquakes (>2000km). However, it is not suitable to be used for indicating relatively small and deep earthquake in specific regions. The relationship between amplitude  $A$ , period  $T$ , distance  $\Delta$  and  $M_s$  is given by:

$$M_s = \log\left(\frac{A}{T}\right) + 1.66 \log(\Delta) + 2.0 \quad 2.5$$

Where  $A$  is spectral amplitude in microns, the horizontal component of the Rayleigh wave with a period of the 20s,  $T$  is the period of the seismic wave in seconds, and  $\Delta$  is the epicenter distance in km.

iv. Moment magnitude ( $M_w$ )

This is the best measure of the size of an earthquake that introduced by Kanamori (1977) as it is used for measuring the whole spectrum of ground motion which can be defined as the seismic moment function,  $M_o$ . The seismic moment is

$$M_o = GAU \quad 2.6$$

Where  $G$  is the material's shear modulus surrounding the fault (approx. 32000MPa in the crust and 75000 MPa in the mantle);  $A$  is the fault area (length  $\times$  width) in  $m^2$ ;  $U$  is the longitudinal displacement of the fault in m.

The seismic moment is obtained from seismograph that using a fault with very large rupture area as the point source for a long time wave. Hence, a magnitude based on seismic moment will be the most accurately explains the size of the largest earthquake since the seismic moment is a strain energy measurement that released from the whole fracture area. Moment magnitude,  $M_w$  that has related to seismic moment is as following:

$$M_w = \frac{2}{3} \log_{10} M_o - 6.0 \quad 2.7$$

Where  $M_o$  is in Nm, or

$$M_w = \frac{2}{3} \log_{10} M_o - 10.7 \quad 2.8$$

Where  $M_o$  is in dyne-cm.

Table 2.1 Richter scale

Description	Magnitude	Average annually
Great	8 and higher	1
Major	7–7.9	18
Strong	6–6.9	120
Moderate	5–5.9	820
Light	4–4.9	6200 (estimated)
Minor	3–3.9	49 000 (estimated)
Very minor	<3.0	Magnitude 2–3 about 1000 per day Magnitude 1–2 about 8000 per day

Sources: (Datta, 2010)

#### 2.2.4.2 Intensity

Intensity is the measurement of the observed destruction at a particular location. This intensity is different from the location from the epicenter; it will be greater when it is nearer the site and lesser when it is far away. It is a qualitative description of the effects of an earthquake at a specified site and used for interpretation of historical data such as the establishment of location, the rate of recurrence, and earthquake size. Modified Mercalli Intensity (MMI) was used to describe the effect of earthquakes,

composed by twelve different grade denoted by Roman numerals I-XII. Each level of intensity and degree of intensity provide a qualitative description of earthquake effects and evaluation of destruction together with the magnitude Richter scale. The lowest intensity indicated the earthquake is insignificant and small whereas the highest intensity showed the destruction of an earthquake is under catastrophic level where the damage is nearly total and large rock masses are displaced. However, the measurement of earthquake size should be according to the released energy at the focus.

Table 2.2 Modified Mercalli intensity (MMI) scale

Intensity	Evaluation	Description	Magnitude (Richter scale)
I	Insignificant	Only detected by instruments	1–1.9
II	Very light	Only felt by sensitive people; oscillation of hanging objects	2–2.9
III	Light	Small vibratory motion	3–3.9
IV	Moderate	Felt inside buildings; noise produced by moving objects	4–4.9
V	Slightly strong	Felt by most people; some panic; minor damage	
VI	Strong	Damage to non-seismic resistant structures	5–5.9
VII	Very strong	People running; some damage in seismic resistant structures and serious damage to un-reinforced masonry structures	
VIII	Destructive	Serious damage to structures in general	
IX	Ruinous	Serious damage to well-built structures; almost total destruction of non-seismic resistant structures	6–6.9
X	Disastrous	Only seismic resistant structures remain standing	7–7.9
XI	Disastrous in extreme	General panic; almost total destruction; the ground cracks and opens	
XII	Catastrophic	Total destruction	8–8.9

Sources: (Datta, 2010)

### 2.2.4.3 Ground Motion

Ground motion is another important parameter for earthquake measurement. It is the movement of the earth's surface from the waves that generated by sudden slip on a fault. Characteristics that are covered by ground motion parameters are the amplitude of motion, the frequency of motion, and duration of motion. This seismic measurement parameter of ground motion including peak ground acceleration (PGA), peak ground velocity (PGV), the ground displacement which is shown in Figure 2.8. Peak ground acceleration is measured by the accelerogram where the velocity and displacement are obtained through direct integration of the accelerogram. Acceleration provides the most accurate measure of an earthquake's intensity. They can provide a basis for dynamic analyses of structures but they do not have any direct correlation to the seismic

coefficients that used in the engineering design. On the other hand, ground velocity is directly corresponding to the energy transmitted to the structure and the intensity of damage caused. It provides a more accurate estimation of the potential damage to the flexible structure such as tall building, bridges etc. Ground displacement is used for the design of underground structures. It cannot use to determine ground motion due to the displacement is related to the lower frequency range that is hardly determined.

Peak ground acceleration (PGA) is peak horizontal ground acceleration (PHA), that commonly used to determining the intensity of ground shaking and it is the highest value in the record. For example, a PGA value of 0.6g (g, the acceleration due to gravity,  $9.81 \text{ m/s}^2$ ) produced a movement of ground that exerts a maximum horizontal force that equal to 60% of its weight on a rigid structure. All points in the structure will experience the same PGA. Vertical acceleration is not considered due to static gravity load of the structure neutralize the dynamic vertical force created by vertical acceleration produced by an earthquake. Hence, in the design code, the vertical acceleration is taken as 1/3 to 2/3 of the horizontal acceleration and maximum horizontal acceleration in two horizontal directions is equal. Usually, strong ground motions carry powerful energy with high shaking frequency within the range from 0.03 to 30 Hz. The longer the duration of the earthquake, the bigger the stress it carries to the building.

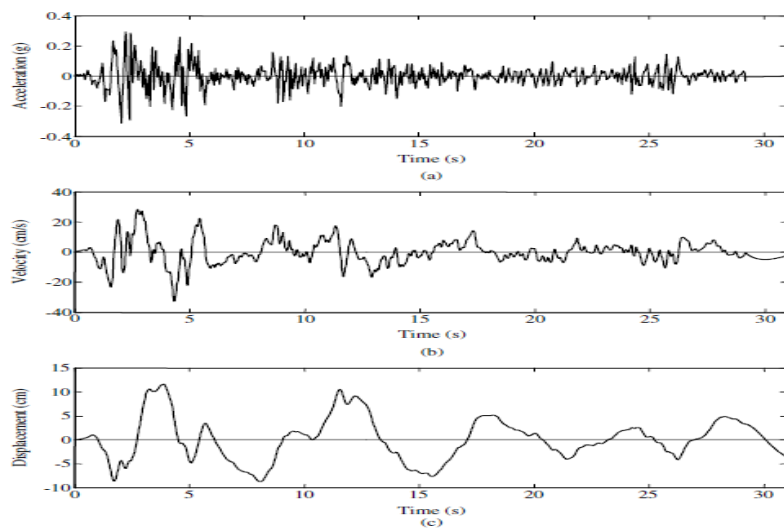


Figure 2.8 Strong motion record from El Centro, 1940.

Sources: (Datta, 2010)



### 2.3 El Centro Earthquake, 1940

The Imperial Valley in south-eastern Southern California was hit with a moment magnitude of 6.9 and extreme intensity of X based on the MMI scale on May 19, 1940. The earthquake was classified as a typical moderate-sized destructive event with a complicated energy release signature (Trifunac & Brune 1970). It was the strongest earthquake to be recorded to hit the Imperial Valley and caused widespread damage to irrigation systems and nine people are dead during the event. At the time; it had a population of about 40,000 and caused \$6 million worth of property damage (Southern California Earthquake Data Center, 2018).



Figure 2.9 The collapse of these walls in the business district of Imperial caused the deaths of four people.

Sources: (Southern California Earthquake Data Center, 2018)



Figure 2.10 The collapse of the 100,000 gallon city water tank at Imperial.

Sources: (Southern California Earthquake Data Center, 2018)

It was the first recorded major earthquake by a strong-motion seismograph located next to a fault rupture (Hough, S.E., 2004). According to Gioncu & Mazzolani, (2011), the ground motion of 1940 US El-Centro earthquake is crucial in the evolution of seismic design, being the first earthquake that recorded in the form of digital which could be used in structural analysis. Due to the limitation of the understanding about an actual attribute of different types of the earthquake, the record was applied for structural analysis and design throughout the world for many years. Hence, this accelerogram is then used and applied in this study to determine the critical member of an offshore platform in Malaysia.

## **2.4 Seismicity in Malaysia**

According to Malaysian Meteorological Department, Malaysia is located in inactive seismic fault zones, hence, mostly 90% of buildings in Malaysia were designed without considering any seismic provision. However, since Malaysia is surrounded by Indonesia and the Philippines, which are two of the most seismically active countries in this region with frequent earthquakes, therefore, Malaysia still facing a certain degree of earthquake threat from both distant earthquakes. Nowadays, the earthquake happened in Malaysia, for instances, the earthquake in Malaysia at Ranau, Sabah (2015), Lahad Datu, Sabah (2012), Tasik Kenyir, Terengganu (2010), and Bukit Tinggi, Pahang (2007). Those earthquakes have caused heavy damage to the property and crack to the building, supposedly the engineer should have designed the building with considering earthquake effects, yet, they still design the building without considering earthquake effects. Marto et al., (2013) has conducted a study about the seismic impact in Malaysia and stated that microzonation study should be conducted for current developing cities for future consideration of the reactivation of ancient fault in Malaysia.

Jabatan Mineral dan Geosains Malaysia (JMGM) undertook a study of the seismotectonic setting of Malaysia. They concluded that Malaysia is a low seismicity country except for Sabah. These earthquakes started to occur since 2007 as presented in Table 2.3. According to Marto et al., (2013) has commented that reactivations of ancient inactive fault due to the intraplate stress built up after 2004 Megaquake happened in Aceh, Indonesia. Although East Malaysia, especially Sabah is seismically active and known as earthquake-prone area of Malaysia, Peninsular has experienced

some tremors as well. The 2007 Bukit Tinggi earthquakes, of magnitudes 3.5 may have occurred along the Bukit Tinggi Fault Zone within Peninsular Malaysia.

Table 2.3 Local earthquake occurrences in Malaysia

No.	Location	Magnitude	Year
1	Ranau, Sabah	6.0	2015
2	Lahad Datu, Sabah	4.6	2012
3	Mersing	3.2	2012
4	Niah, Sarawak	3.3	2010
5	Tasik Kenyir, Terengganu	2.7	2010
6	Kuala Pilah, Negeri Sembilan	3.3	2009
7	Manjung, Perak	3.2	2009
8	Jerantut, Pahang	2.6	2009
9	Bukit Tinggi, Pahang	3.5	2007

Sources: (Bernama, 2010a, 2010b; Cheng, 2016; Noorliza Lat & Ibrahim, 2009; S.Bedi, 2012)

Based on historical records, subduction zone and strike-slip fault in Sumatran are two external sources that originated the earthquakes in Malaysia. According to Manafizad, Pradhan, & Abdullahi (2016), large earthquakes came from these two active areas did created ground motion to the western part of West Malaysia. Seismic source zones are considered within a radius of 500 km from the site. They stated that any outside of this radius may not significantly affect by the peak ground acceleration.

According to Malaysian Meteorological Service, 2009, Sarawak has experienced earthquakes of mainly local origin. Since 1874 up to now, a total of 21 earthquakes with magnitude ranging from 3.5 to 5.3 were recorded, with the MMI scale of VI, suggesting a frequency of an earthquake every 6-7 years. In Sabah, it had experienced 65 earthquakes of magnitude ranging from 3.3 to 6.5, with the Maximum Mercalli Intensity scale of VIII, suggesting a frequency of an earthquake every 1 year. Below figure 2.11 is the Earthquake and Tsunami Hazards Maps, it identified 5 Risk Zones based on Maximum Mercalli Intensity (MMI) and Peak Ground Acceleration (PGA) data: (i) Sabah has Zones 1 (in central and eastern Sabah with an MMI scale of VIII), Zones 2 (in central and eastern Sabah with an MMI scale of VII), and Zones 3 (in western Sabah with an MMI scale of VI); (ii) Sarawak was identified as having Zones 3 (in northern and central Sarawak with an MMI scale of VI), Zones 4 (over much of Sarawak with an MMI scale of V) and Zones 5 (in western and southwestern Sarawak with an MMI scale of IV); and (iii) Peninsular Malaysia was identified as having Zones

4 (in western Peninsular Malaysia with an MMI scale of V), Zones 5 (along the inner western Peninsular Malaysia with an MMI scale of IV) and the lower Zones (along the central and eastern belts of the Peninsula with MMI scales of III and II).

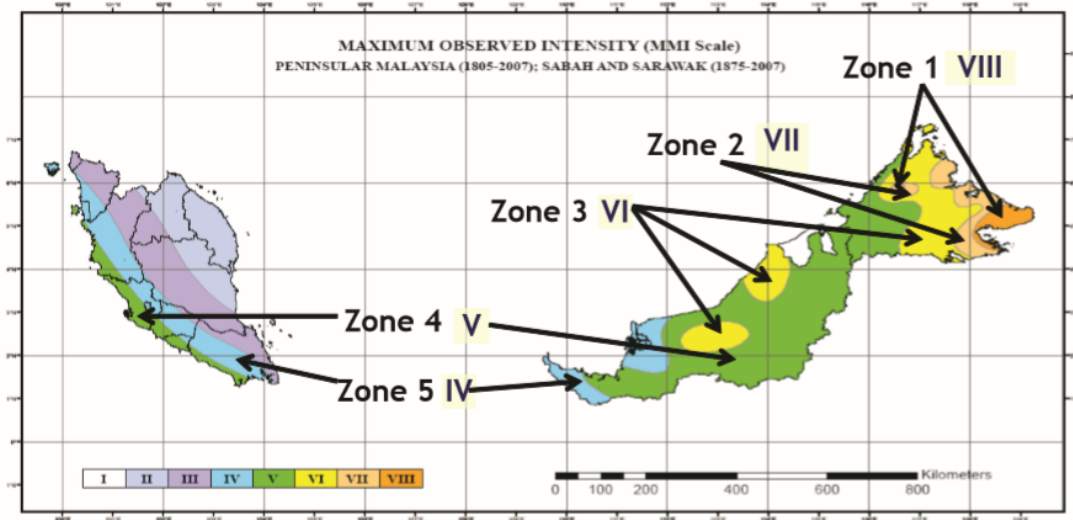


Figure 2.11 Earthquake hazard zonation

Sources: (Malaysian Meteorological Service, 2009)

In 2005, Jabatan Kerja Raya (JKR), in collaboration with IKRAM Structure Assessment Sdn. Bhd. (formerly known as IKRAM Research Centre Sdn Bhd) and Structural Earthquake Engineering Research (SEER), University Technology of Malaysia, conducted a study to assess the vulnerability to earthquakes of selected 65 public buildings at a total of thirteen locations including townships, cities, and districts in Peninsular Malaysia, Sabah, Sarawak, and Labuan. Five buildings were evaluated at each site. The selection of buildings was depend on the type of structure, design, building height, soil type, etc in order to determine a broad spectrum of the various types of buildings in Malaysia. The selected public buildings subjected to earthquake forces were checked by using established methodologies known as ATC 21 & ATC 22 and conducting linear and non-linear dynamic analysis on susceptible buildings.

In the study's findings, from the total of 65 buildings inspected, 60% are low-rise buildings, 15.4% medium-rise, and 24.6% are high-rise buildings. Based on the ATC-21 evaluation, it showed that more than 50% of the selected buildings on every site required for further investigation. 55% of evaluated buildings in Peninsular Malaysia needed detailed evaluation, while in Sabah and Sarawak, 56% and 60%

respectively of the evaluated buildings needed detailed evaluation. Due to the limited time and information on the building (drawing documents and construction data), only 80% of the critical buildings were evaluated in detail using the ATC22 procedure.

In short, the study showed that the buildings' structural system is not critical to earthquake load. Most of the buildings in Peninsular Malaysia were in good condition and at least 50% of the selected buildings in Sabah and Sarawak were found to suffer from concrete deterioration problems. The connections between subsystems were found to be adequate. Besides, the highest damage index of building at moderate earthquake level indicates that there no significant damage to the structure, but some non-structural damages can be expected.

## **2.5 Offshore Structure**

Offshore structure is built to manufacture the hydrocarbon oil and gas for development purposes that mostly used in every end-use sector such as residential, commercial, industrial in manufacturing and agriculture, transportation, and electric power. According to Mukhlas et al., (2016), the offshore structure can be classified into two types which are fixed and floating. There is five major areas of operation from exploration to transportation of oil: (i) exploration, (ii) exploration drilling, (iii) development drilling, (iv) production operations and (v) transportation. The lowest deck must keep a minimum distance at approximately 1.5m or more from the waves crest considering the maximum expected level of water from the combination of wave height and tides. After seismic field surveying, one or more exploration wells are drilled. Factors that are considered in the evaluation of the development plans are number of wells needed, type of production facilities, number of facilities, and pipeline or tanker off-loading.

There are three major categories of offshore structure: (i) fixed platform, (ii) compliant platforms, and (iii) floating platforms. The fixed platform consists of jacket platform, gravity platform, and jack-up rigs; compliant platform includes guyed tower, articulate tower, and tension leg platform, while floating platform comprises of semisubmersible, floating production unit (FPU), floating production, storage, and offloading (FPSO) and spar. Types of the offshore structure are shown in Figure 2.12.

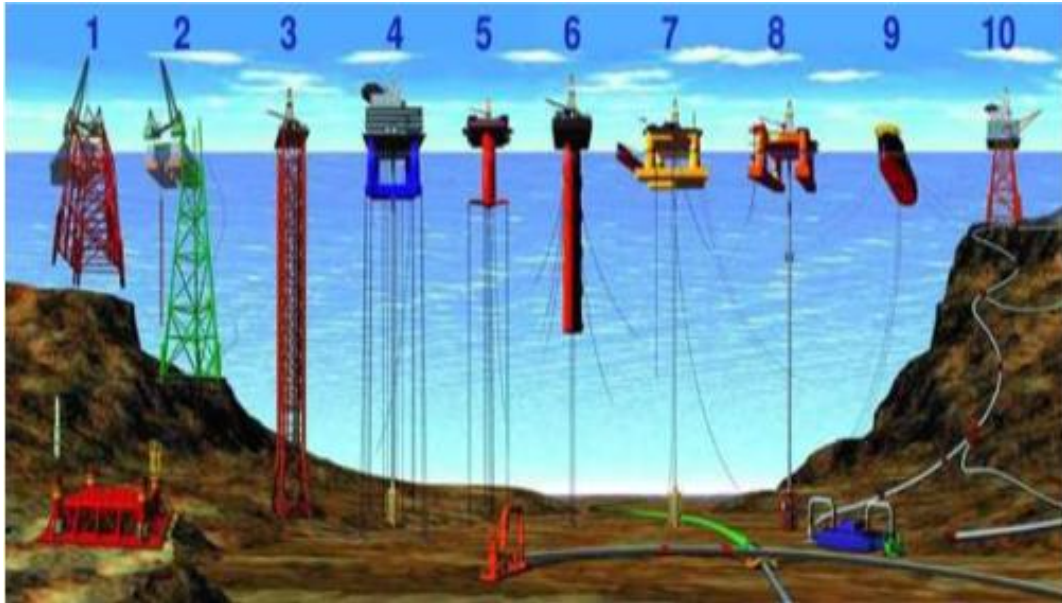


Figure 2.12 Type of offshore structure

Sources: (Maske, Maske, & Shiras, 2014)

### 2.5.1 Offshore Wellhead Platform Support Frame

Wellhead platform is used for drilling and supporting the wellhead equipment such as wellhead control panel and piping and helicopter landing structure for emergency evacuation. The majority part of wellhead platform is built in steel which is piled jacket or welded spaced frame with deck structures to support other operational activities.

There are two typical fixed platform concepts: the jacket based platform is applied to shallow water and the gravity based platform is used for deep water. For shallow water, the progress of design and construction of the topside are proportional to the drilling which products are allowed to start only after installed deck. For deep water, the drilling will start after the platform is built and completely installed, this causes the production will start in between 1 to 2 years after the platform installation.

Detailed of the structure is shown in figure 2.13. A major component of offshore platforms are:

- a) Superstructure: It consists of deck and equipment for the functioning of the platform
- b) Substructure: It supports the deck and transmits the load from the substructure to the foundation.

- c) Foundation: It supports both substructure and superstructure and transmits the load to the seabed.
- d) Mooring system: it is used to for station keeping of floating platform by the anchor.

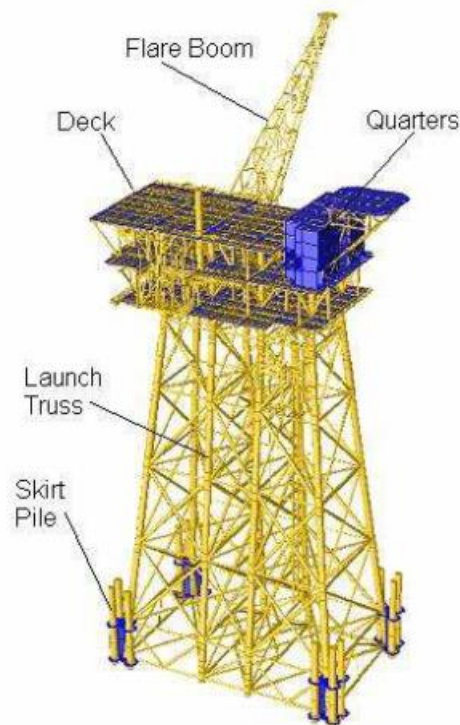


Figure 2.13 Fixed offshore platform

Source: (S. Nallayarasu, 1981)

## 2.6 Code of Practices for Offshore Structure

The offshore structures must be safely functioning with a design lifetime of 25 years or more. Potty, Akram, & Khamidi, (2012) stated that there are over 200 installations have been operating for more than 40 years. In Malaysia, there are 48% of the platforms have exceeded their 25 years design life where 28% of Sarawak, 12% of Sabah region and the remaining 8% of Peninsular, Malaysia (Zawawi, Liew, & Na, 2012). If the structures are not well designed and constructed with adequate strength, it will lead to the failure of the structures. To ensure the safety of the structures against seismic sufficiently, there are different types of design codes used to design offshore structure in different countries. Current practices code that used in Malaysia will be explained in the following.

## **2.6.1 Seismic Design Guideline**

There are three design codes used frequently in seismic design: API-RP2A, ISO 19901-2:2004 and Eurocode 8. API-RP2A provide detailed information about the considerations need to be taken during the design process of the offshore platform where ISO 19901-2 is mostly described more detailed about the seismic design procedure.

### **2.6.1.1 API-RP2A**

API-RP2A outlined specific guidelines that can be used in the planning, design, and construction of offshore platforms. The seismic design platform depends on the expected ground motion, risks involved and acceptable damage to the platform. To determine the seismic level, a first determination is exposure category intended for the platform. These are including the life safety consideration refer to the human life on the platform and failure consequence such as the expected damage to the operation and environment. Safety of life will involve three categories which are manned-nonevacuated, manned-evacuated, and unmanned. The consequences of failure involved high level, medium level, and low level.

According to Brown, 2003, design of the platform to resist earthquake forces is to fulfill two requirements, strength requirement and ductility requirement. Strength requirement is used to design for Strength Level Earthquake (SLE) to ensure platform has adequate strength to withstand an earthquake and not suffer any massive structural damage. Return interval of these earthquakes normally is in between 100 to 500 years. For ductility requirement, it is used to design Ductility Level Earthquake (DLE) for providing sufficient reserve capacity to the platform to prevent collapse. Probabilistic Seismic Hazard Assessment (PSHA) and Deterministic Seismic Hazard Assessment (DSHA) shall be addressed later.

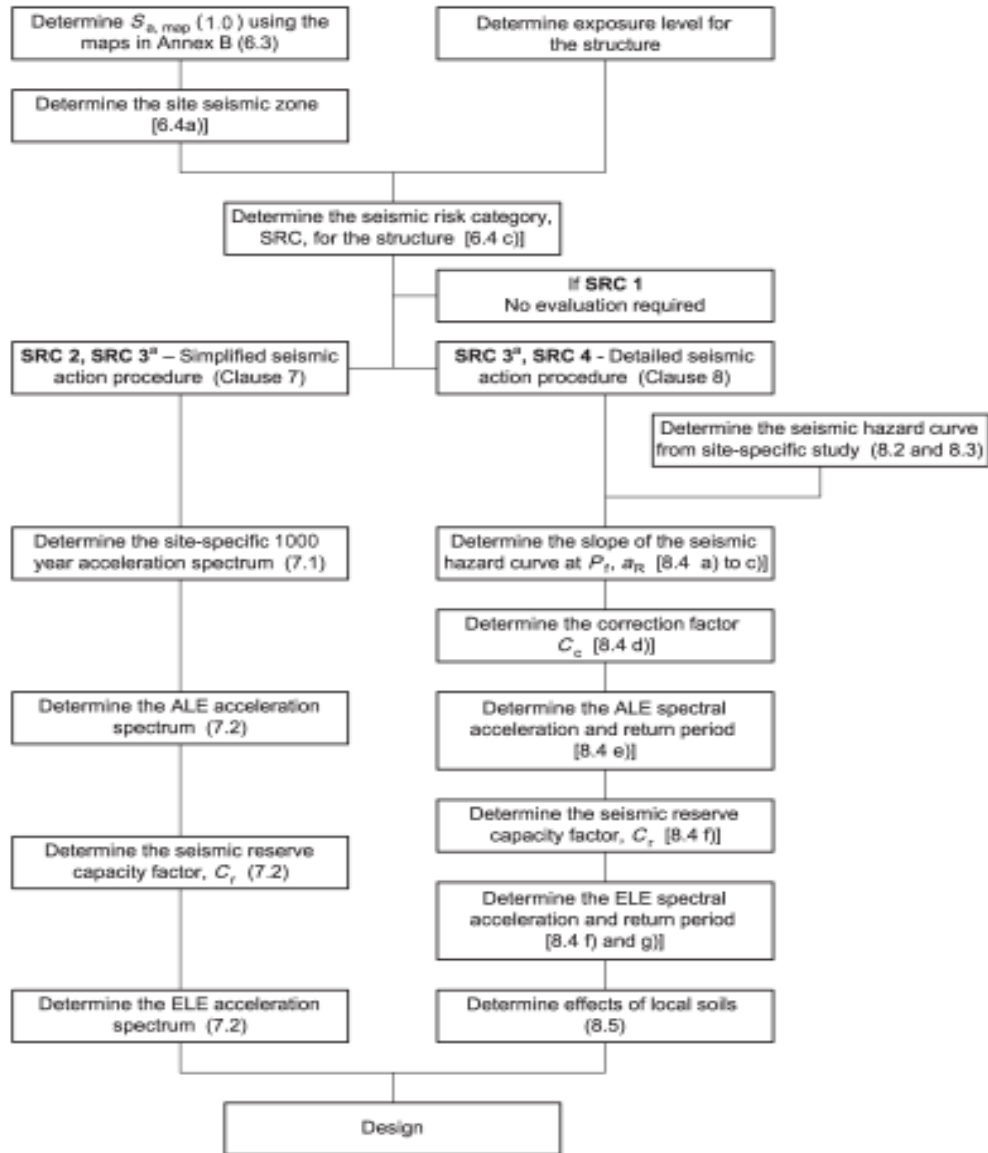
### **2.6.1.2 ISO 19901-2:2004**

ISO 19901-2:2004 outlined the design requirement and guidance of the procedure for the seismic design of offshore structure. The requirement is applicable to both steel structures and concrete structures. It also briefly explained the effect of seismic events on floating structure and partially buoyant structures. Another series of



similar design of codes are API-RP2A, Eurocode 8, Eurocode 5, International Organization for Standardization, ISO 19901-4:2003 and ISO 19902:2007. All of these are approved and incorporated under European Committee for Standardization (CEN). The study will be referred to as the ISO 19901-2:2004 for the determination of seismic design procedure as it has proven to provide a better outline of the seismic design procedure and more user friendly than API-RP2A (Trevon, 2009)

It identified two levels of earthquakes need to be considered in seismic design which are Extreme level Earthquake (ELE) and Abnormal Level Earthquake (ALE). ELE is used to design ultimate limit state (ULS) for strength and stiffness to ensure no major damages occur to the structure during design service life and ALE is to ensure that the structure has sufficient reserve strength and energy dissipation requirements without loss of integrity. There are two alternative procedures for seismic design: (i) simplified method and (ii) Detailed method. Simplified method is used when seismic consideration is unlikely to disturb the design of structure where detailed method is for seismic consideration that contributes great impact on the design. The selection of the appropriate procedure depends on the exposure level of structure and expected intensity and characteristics of seismic events (Joseph, 2009). Below figure showed the design procedure for seismic analysis.



\* SRC 3 structures may be designed using either a simplified or detailed seismic action procedure, see Table 4.

Figure 2.14 Seismic design procedure

Source: American Petroleum Institute, API-RP 2EQ, 2014

### 2.6.1.3 Eurocode 8

By 2002, there are 10 sets Eurocode have been developed and published, two cover the basis of structural design and actions, one covers geotechnical design and six cover aspects specific to concrete, steel, composite steel and concrete, timber, masonry and aluminium and last one cover all aspect of seismic design. Since it covered all aspect of seismic design, it gives the option to low seismicity countries not to apply it at all. Eurocode 8 has 6 parts: Part 1 (EN1998-1): “General rules, seismic actions, rules for buildings”; Part 2 (EN1998-2): Bridges; Part 3 (EN1998-3): “Assessment and

retrofitting of buildings”; Part 4 (EN1998-4): “Silos, tanks, pipelines”; Part 5 (EN1998-5): “Foundations, retaining structures, geotechnical aspects”; Part 6 (EN1998-6): “Towers, masts, chimneys” (Fardis, 2004).

In this study, we are only focused on Part 1 of the EN-Eurocode 8 includes also the general provisions such as performance demands, seismic loading, analysis procedures, general concepts and rules applicable to structures beyond buildings. It covers concrete, steel, a composite of steel and concrete, timber and masonry buildings, and buildings with base isolation in separate chapters. Analysis procedure is including for the design is linear modal response spectrum analysis and nonlinear dynamic which known as response time history.

Modal results in the response spectrum analysis are combined through the attentive application of the SRSS or CQC rule to determine displacement and internal forces at the level of the final seismic action effects. SRSS or CQC rule will combine and calculate lateral forces in that story for each mode from modal story acceleration for analyzing the structural system. The input for Response time history analysis in 3D should use at least 3 pairs of different records, the mean elastic spectrum of which should not fall below by more than 10% of the design seismic action. In all analysis methods, 5%-damped elastic response spectrum or the target displacement for nonlinear static analysis, or acceleration time-histories for nonlinear dynamic analysis represent seismic action. The spectrum depends on PGA chose for the analysis results corresponding to the hazard level, with multiplication by the suitable importance factor.

### **2.6.2 Environmental Load Design Guideline**

The worldwide leading structural code for the specific offshore structure is the API-RP2A. It provides the specific guidelines on the design requirement and characterization of environmental load that are to be used in planning, design, and construction of offshore platforms, including foundation and additional constructs. The consideration of environmental load is composed of wind, wave, and current loads. All the formulation of the environmental load is referred to API-RP2A.

### 2.6.3 Structural Design Guideline for Steel Structure

There are several design codes available for designing a safe structural building or other civil engineering works. Each country will have their own favorable design codes, as in Malaysia is moving toward implementation of Eurocode from British Standard practice (Suriati & Yusoff, 2015). It was approved by CEN on 16 April 2004 and comprises 20 documents dealing with different aspects of the steel structure. In the Civil Engineering courses in Malaysia's local universities, they implement Eurocode BS EN 1993-1-1:2005 in the learning syllabus for manual calculation of allowable stress of the structural member such as tension, compression, bending and shear to compare the result from software analysis.

### 2.7 Design Criteria for Offshore Structure

Some important design consideration must be taken including (i) water depth at location, (ii) soil at sea-bottom and in-depth, (iii) wind speed, (iv) waves, current, (v) ice (fixed, floes, icebergs), and (vi) earthquake. In this study, the analysis of offshore structure is only considered dead loads, live load, wind load, waves load, earthquake load, and current load. Basically, offshore structures are designed to resist various types of loading that are greater in magnitude and complexity than onshore structure. Types of loading applied to the structure are shown in Figure 2.15 and will be briefly explained in the following section.

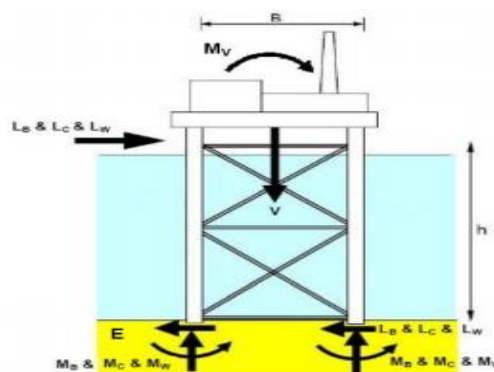


Figure 2.15 Loads on an offshore platform. ( $V$ , self-weight of topside;  $M_v$ , moment with eccentric loading of platform;  $L_b$ , lateral wind load;  $L_c$ , lateral current load;  $L_w$ , lateral wave load,  $M_b$  &  $M_c$  &  $M_w$ , moment related to lateral loadings, and  $E$ , seismic load)

Source: Dean, 2008

### **2.7.1 Dead Load**

The dead load will be divided into two types: structural dead loads and facility dead loads. Structural dead loads will include all fixed items such as primary steel structure, secondary structural items such as boat landing, stiffeners, handrails, deck plating and small access platform in the platform deck, jacket, and bridge.

The primary steel structure are calculated automatically in the computer program when used to analyze the structure; while the weight of secondary structural steel items needs to calculate and apply to the appropriate locations. Facility dead load is the weight of structure that built for drilling or wellhead type platform that supports several equipment and facilities. The weight of the items shall be calculated and applied at the appropriate location since they do not provide any stiffness to the integrity of the structure.

### **2.7.2 Live Load**

Live loads are a temporary movable load that could vary in magnitude, position, and direction applied to the structure. They will only apply to areas such as temporary or long-term storage, lay down area for material transfer to the boat, an open areas like walkways, access platform and helicopter loads in helipad. These loads shall be considered in the analysis of the offshore structures.

### **2.7.3 Wind Load**

Wind load shall be calculated according to API RP2A guidelines. Wind loads are a dynamic load that occurred in nature similar to wave loads. It only contributes loads less than 10 percent to global loads of a conventionally fixed steel template in relatively shallow water. In contrast, it can be significant loads to the structure in deeper water and for compliant design.

Forces on flat surfaces are assumed to act normal to the surface where the forces exerted on vertical cylindrical objects are assumed to act in the direction of the wind from all angle of wind approach to the structure. An appropriate formula should be used that take into account the direction of the wind in relation to the attitude of the object if the forces on objects whether in flat surfaces or cylindrical objects are not in vertical

attitude. The designer should consider the effect of local wind including the concentration of pressure and internal pressures in the design. Details of the formulation will be discussed in the following chapter.

#### 2.7.4 Waves Load

According to Reddy, D.V, and Swanmidas, 2014, winds are the cause to the generation of waves in the ocean by transferring different kinds of kinetic energy intensities to the ocean water over large areas. The forces on structures are caused by the motion of water due to the waves is higher than wind loadings. For deeper waters or where platforms tend to be more flexible, the static analysis may not appropriately explain the real dynamic loads exerted to the platform. Hence, the load analysis of such platforms requires involving the dynamic action of the structure.

The strength of the waves depends on its height which can be obtained from crest to trough (Figure 2.16). Besides that, it also imposed buoyant force and cyclic loading on offshore structure. The force exerted by waves can be determined by using Morison's equation. Morison's equation expresses the wave force as the sum of an inertia force that proportional to the particle acceleration and a non-linear drag force that proportional to the square of the particle velocity. As a result, it can only be applied when  $D/L < 0.2$ , where  $D$  is the diameter of the member and  $L$  is wavelength.

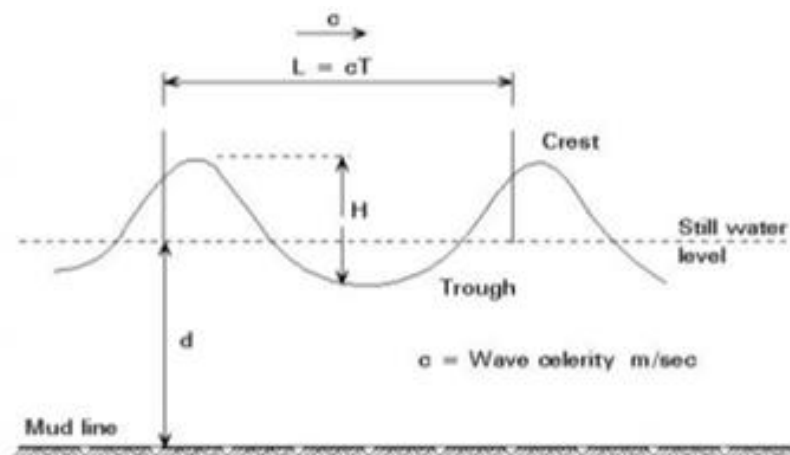


Figure 2.16 Waves characteristic

Source: (Afolalu, Ajayi, Ikumapayi, & Adejuyigbe, 2015)

### **2.7.5 Current Load**

As a result of wind blowing across the ocean surface, it creates a dynamic friction pressure on the ocean water. The equilibrium of the ocean water surface interrupted by the transference of kinetic and potential energies from air to the water and cause surface current and waves (Reddy, D.V, and Swanmidas, 2014). There are two types of ocean currents depend on their nature which is tidal current, and wind-driven current. Current created by wind-driven are small in nature and it varies linearly with depth whereas tidal currents vary nonlinearly with depth (S. Nallayarasu, 1981). The current forces that act on the structural member can be determined by neglect the wave's conditions in the Morison's equation. Briefly, discussion on the formula used will be discussed in next chapter.

### **2.7.6 Earthquake Load**

Earthquake loads are to be imposed as a separate environmental load and combined with other environmental loads like wind, waves, etc. Structures located in a seismic offshore region are generally analyzed and designed for two levels of earthquake intensities: (i) strength level earthquake intensity and (ii) ductility level earthquake intensity. For the strength-level earthquake, which is defined as having a mean recurrence interval equal to 200 to 500 years, the structure will be designed to respond in an elastic manner. For the ductility level earthquake, defined as the earthquake intensity close to the maximum possible earthquake intensity at the site, the structure will be designed for inelastic response; the structure should also have adequate reserve strength to prevent its total collapse.

If the expected earthquake strength is low, then the effects of an earthquake can be neglected in the design process; if the horizontal acceleration is small but greater than 0.05g, then the structure should be analyzed by spectral analysis method for determination of earthquake force demands (American, 2007). There are many modes need to be considered for response spectrum analysis to representing an appropriate response. It also needs to consider a minimum two modes that are the highest from the overall response for each of the three principal directions including significant torsional modes. The design response needs to be averagely calculated from the maximum values for each of the time histories considered. Ductility analysis of traditional jacket-type

structures is needed no acquired if the structure is located in the area where the intensity ratio is equal or less than 2 of rare and intense earthquake ground motion to strength level earthquake ground motion.

## 2.8 Seismic Response of the Structure

Study of the seismic response is required to design earthquake resistance structures that allow significant damages will not occur to the structure under strong earthquake. The response includes the magnitude, distribution of the resulting forces and displacement of the structure. A building will experience a complex series of oscillation due to the continuous shaking of the base during an earthquake where the inertia mass of the building is trying to resist this motion and cause distortion to the building. It can be 3 cases for the ground shaking motion: (1) when the ground shaking is slower than nature oscillation of the building, the period of structure will be approximately same as the displacement amplitude of ground; (2) if the ground motion period same as the structure, large dynamic amplification of the motion occurs; and (3) when the ground shaking is faster than the natural period of structure, the structure experiences less motion than the ground. There are three methods used in this study to determine the seismic response of the wellhead offshore platform that located in Kuala Terengganu: free vibration analysis, time history analysis, and response spectrum.

Free vibration analysis is used to determine the natural frequencies, natural periods and corresponding vibration modes of the structures. It is the simplest form of dynamic response that may exist from the structure without considering ground motion and damping. Whether the system is damped or undamped, the oscillation of frequency,  $\omega$  will be the same, amplitude changed only. For damped oscillation, the amplitude will be reduced to zero where undamped oscillation has a constant amplitude. The formula of natural frequencies,  $f$  and natural periods,  $T$  is as below:

$$f = \omega/2\pi = 1/T \quad 2.9$$

$$T = 2\pi/\omega = 1/f \quad 2.10$$

Where  $\omega$  = radians/second;  $f$  = number of vibration in time, Hertz or cycles/second;  $T$  = time required to complete one cycle of vibration.



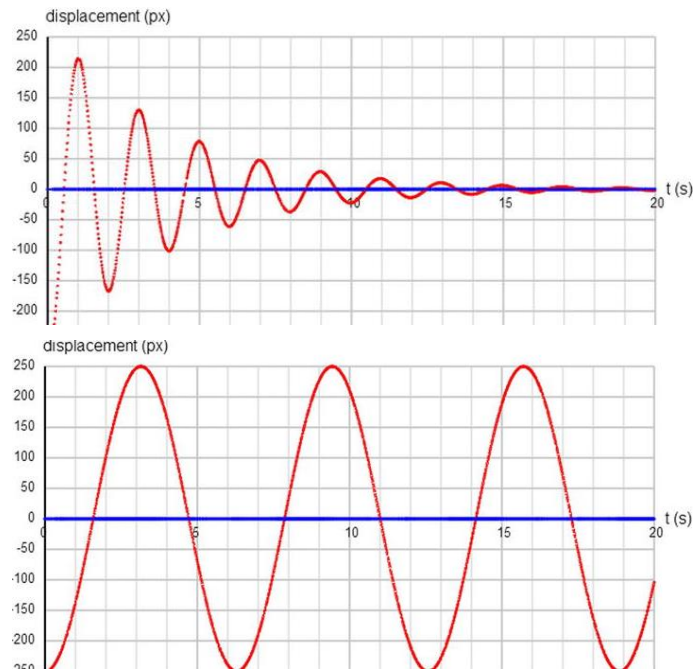


Figure 2.17 Damped and undamped oscillations

Source: (Ramtal D. & Dobre A., 2014)

According to Elshafey, Haddara, & Marzouk, (2009) the displacement will only have slight effect if the frequencies are far from the value of model's natural frequency. The peak frequencies become closer to the model's natural frequency will contribute to the major effect of aspects. Park, Koo, & Kawano, (2011) stated that maximum displacement will occur when the seismic motion's period is closer to the natural period of the model. Shreyasvi & Shivakumaraswamy, (2015) also stated the probability of undergoing damage of buildings that have lesser time periods due to high-frequency ground motion is higher as they are more susceptible to high-frequency ground motions which create resonance effect. According to Gerhard W. Leo, (1991), buildings in excess of 7 stories usually have a natural frequency less than 0.6 Hz. Building from three-to-seven stories resonates at 0.6 to 2.5 Hz. One-to-two story buildings resonate at 2.5 Hz or more. Larger earthquakes are known to have a greater proportion of their energy concentrated in lower frequency ranges and are, thus, relatively more hazardous to taller buildings

Time history analysis is the most complicated method of dynamic analysis for building and the most accurate means of representing earthquake actions. It used the mathematical model of the building that subjected to accelerations from earthquake records to represent as the expected earthquake at the base of the building. Each

earthquake record is unique having different peaks, duration and dominant period. It is applicable to both elastic and inelastic analysis. Inelastic analysis, the stiffness is assumed to be constant along the whole duration of an earthquake; wherein the inelastic analysis, the stiffness is only constant along the incremental time.

A response spectrum is used to find the peak response of a structure during an earthquake from the seismic response spectrum. It is the most famous tool in the seismic analysis of structures as the response of the structure is according to the frequency content of ground motion and its own dynamic properties. It is a plot of the maximum response of displacement, acceleration or spring force against the period of vibration, the natural frequency of vibration or the circular frequency of vibration. There are computational advantages in using the response spectrum method of seismic analysis for the assumption of displacements and member forces in structural systems. Response spectra also able to determine the maximum structural responses under linear range, for obtaining lateral forces developed in structure due to the earthquake and facilitating in earthquake-resistant design of structures. When earthquake ground motion data is available, response spectra is very useful in understanding and allow engineers to visually imagine how buildings will perform and to determine deficiencies and potential damage during a major damaging earthquake.

It can divide into two systems which are elastic and inelastic. The elastic system assumes a linear relationship between structural force and displacement and the response spectra only represent maximum responses. The inelastic system is for economical design use of ductility of the structure to reduce the force demands as an elastic system for strong ground motion will be uneconomical due to large force demands. Multiple modes of response of a building are considered based on their modal frequency and modal mass to provide an estimate of the overall response of the structure.

After conducting dynamic analysis, there are several results could be obtained related to the dynamic response of the structure. Below table showed the result obtained by other researchers with using different inputs in the dynamic analysis.

Table 2.4 Result of dynamic response from different input in the analysis

Author	Input	Output
Ahmad, Adnan, Nazir, Ramli.N, Ali, Ramli.M, 2017	Dynamic analysis of fixed offshore platform by using SAP2000. Load considerations are Aceh earthquake loading, wind and wave load. Free vibration analysis, Response spectrum analysis, and Time history analysis are carried out.	Design interaction ratios vary but less than 1.0s and the maximum is 0.888. From the free vibration analysis, The maximum value of natural period for free vibration analysis is 0.577s. The maximum displacement is 17.708m.
Li-Jeng, Hong-Jie, 2014	To determine the displacement, velocities, acceleration of typical node of Tower Crane by using SAP 2000 considering 2 kinds of earthquake ground acceleration.	The maximal displacement, velocity, and accelerations obtained from the nodal point located at the highest position. The maximal displacements of the typical tower crane due to earthquake excitations can be large to more than 1 meter and the associated maximal velocity and acceleration can be greater than 4 m/s and 40 m/ s <sup>2</sup> , respectively
Park, Koo, Kawano, 2011	Dynamic response analysis of offshore platform due to seismic motion with various maximum seismic accelerations and shear wave velocities of soil.	Period of seismic motion that close to the natural period of the structure will tend to provide a maximum response.
Bargi, Hosseini, H.Tadayon, 2011	Using simultaneously wave and earthquake loading to analyze the seismic response of fixed jacket offshore platform.	The highest model period is 2.02s. It concluded the maximum response of displacement under a combination of earthquake and wave loads are more than maximum displacement response of earthquake load alone.
Elshafey, Haddara, Marzouk, 2009	Dynamic analysis of four-legged jacket with a combination of diagonal and k-bracings.	The maximal displacement, velocity, and accelerations obtained from the nodal point located at the highest position. The maximal displacements of the typical tower crane due to earthquake excitations can be large to more than 1 meter and the associated maximal velocity and acceleration can be greater than 4 m/s and 40 m/ s <sup>2</sup> , respectively

Source: Elshafey et al., 2009; Ahmad et al., 2017; Bargi, Khosro; Hosseini, S.Reza; H.Tadayon, Mohammad; Sharifian, 2011; Li-Jeng & Hong-Jie, 2014; Park et al., 2011

## **CHAPTER 3**

### **METHODOLOGY**

#### **3.1 Planning of Study**

The whole process of the study will be briefly discussed in this chapter. To ensure the efficiency of the project work, planning and scheduling have been conducted in the initial stage before starting the work. In this study, the modal used in the dynamic analysis is wellhead offshore platform and the purpose of the study is to determine the critical member of the structure under seismic excitation. The software used for computational analysis and structural modeling of the structure is SAP2000 version 18. After the modeling has been done, the response spectrum, time history, and free vibration analyses will be performed.

For the response spectrum analysis, it will be analyzed by using the curve of response spectra in Eurocode 8 (EC8). Time history analysis will be conducted by referring to time history of the earthquake in Aceh 2004. For the free vibration analysis, it is obtained by SAP2000 to provide the natural frequency, natural period and the mode shape of the structure. All the responses from the wellhead offshore platform structure due to surrounding earthquake will be determined. The result obtained by response spectrum and time history analysis will be compared and discussed in details.

For the load combinations, it involved a dead load of the structure, live load, environmental loads and earthquake load. The environmental loads such as current load, wave load and wind load for the wellhead offshore platform will be governed by the location of the structure in the Malaysia region and will be determined all the loads by using API design criteria standard. Moreover, manual calculation of allowable stress of the structural member will be performed and implemented Eurocode 3 for comparing the result obtained from software.

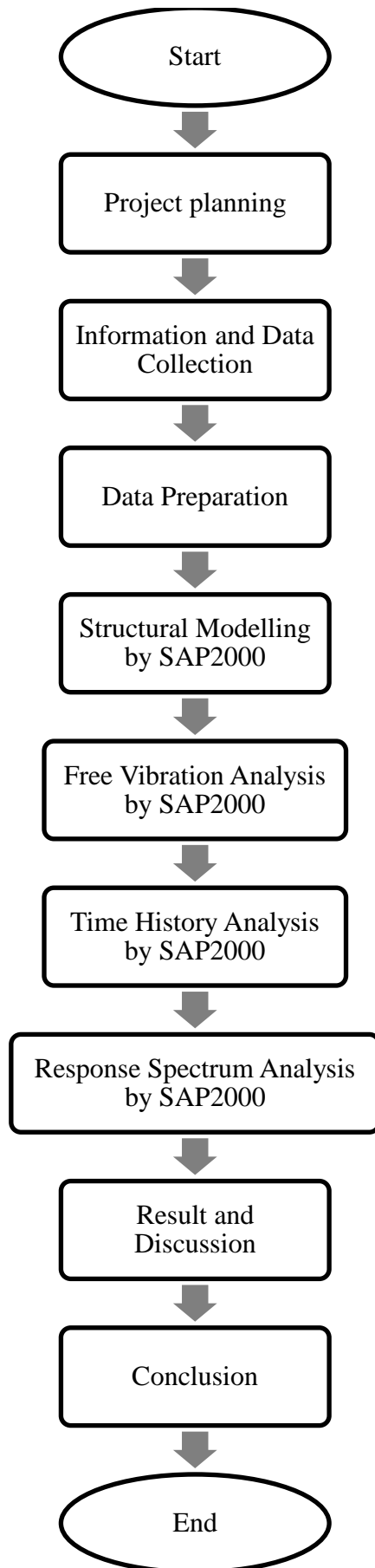


Figure 3.1 Flow Chart of Methodology

## **3.2 Information and Data Collection**

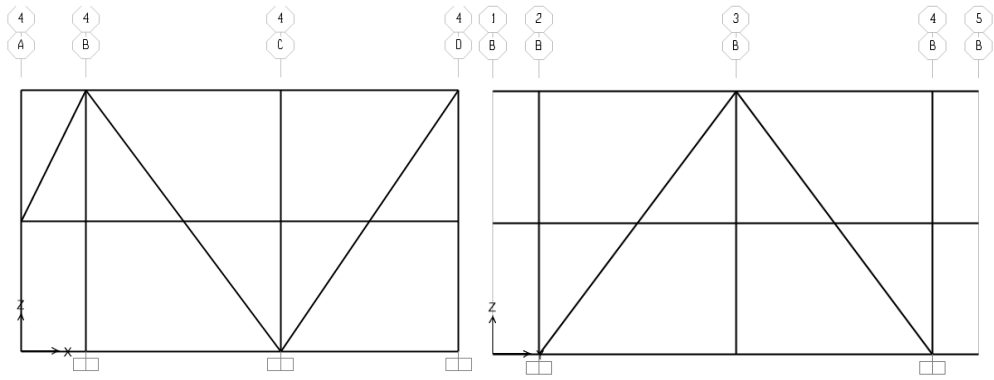
The information and data needed for the conduct the modeling and analysis including:

- I. Structural drawing of wellhead support frame to show the layout, dimension, and details of the structure.
- II. Location, material, size and section used of the offshore structure.
- III. Environmental data from the site location including wind speed, maximum wave height, wave period, current velocity, maximum tide, storm surge.
- IV. El Centro, 1940 ground motion data from PEER Center.

### **3.2.1 Detailing Description**

The type of offshore structure used in this analysis is wellhead support frame which is known as deck framing or topside, the upper part of wellhead offshore structure that located at Terengganu, Malaysia. The support frame consists of three floors: main deck, mezzanine deck, and weather deck. Figure 3.2 and 3.3 clearly showed the side view and plan view of wellhead frame. The total height of the structure is about 8 m tall and the elevation of each floor is 4 m height. The dimension of the platform is 14.725m x 13.366m.

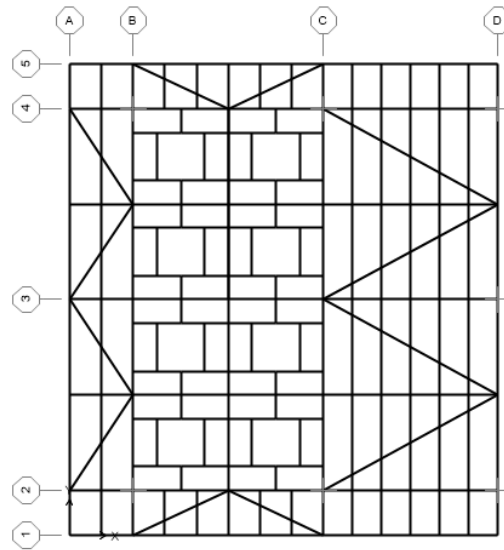
The primary structural steel used in the framing is seamless tubular with diameter 406 mm times wall thickness (W.T) 25.40 mm and the material used is high strength steel with a yield strength of 355 MPa. Usually, the primary structural steel is used as a bracing member and the main frame of the structure. For the secondary structural steel, it has two different diameters and wall thicknesses which are 273 Ø x 25.4 mm W.T and 168 Ø x 21.95 W.T. Both secondary structural steel is also using S355 high strength seamless tubular and functioned as an internal member. The design of this structure complies with America Institute of Steel Construction, Manual of Steel Design, Allowable Stress Design, 9<sup>th</sup> edition and American Petroleum Institute API RP-2A.



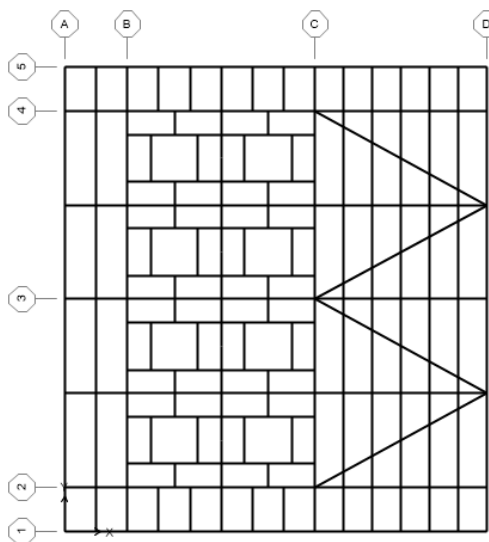
a) Side view X-Z

b) Side view Y-Z

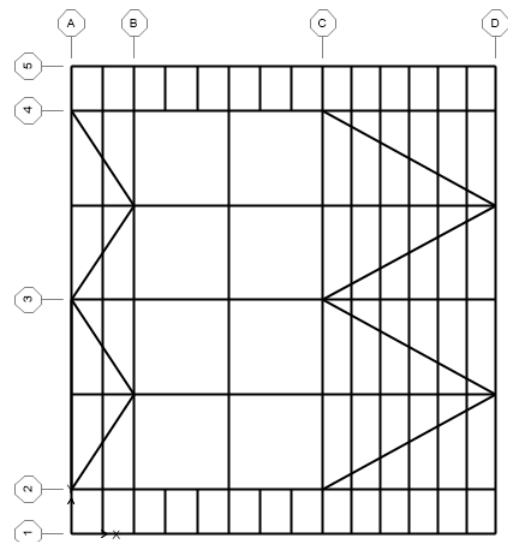
Figure 3.2 Side view of wellhead support frame



a) Main deck frame



b) Mezzanine deck frame



c) Weathered deck frame

Figure 3.3 Plan view of wellhead support frame

### 3.2.2 Material Description

Before we define the section properties of tubular used in the SAP 2000 analysis, we need to define the material used first. In this analysis, we implement S355 high strength steel that minimum yield strength,  $f_y$  is equal to  $355 \text{ N/mm}^2$  and ultimate tensile strength,  $f_u$  is  $430 \text{ N/mm}^2$ . The modulus elasticity,  $E$  of high strength steel used is  $210\,000 \text{ N/mm}^2$ , where shear modulus,  $G$  of  $81\,000 \text{ N/mm}^2$  and Poisson's ratio,  $\nu$  of 3.0. After complete define of material, we can proceed to section properties of steel. There is total three types size of tubular utilized which are  $406 \text{ } \varnothing \times 25.4 \text{ W.T}$  (main structural steel),  $273 \text{ } \varnothing \times 25.4 \text{ mm W.T}$  (internal member),  $168 \text{ } \varnothing \times 21.95 \text{ W.T}$  (internal member).

Section	Property	Value
General Data	Material Name and Display Color	S355
	Material Type	Steel
	Material Notes	Modify/Show Notes...
Weight and Mass	Weight per Unit Volume	76.9729
	Mass per Unit Volume	7.849
Isotropic Property Data	Modulus of Elasticity, E	2.100E+08
	Poisson, U	0.3
	Coefficient of Thermal Expansion, A	1.170E-05
	Shear Modulus, G	80769231.
Other Properties for Steel Materials	Minimum Yield Stress, Fy	355000.
	Minimum Tensile Stress, Fu	510000.
	Effective Yield Stress, Fye	390500.
	Effective Tensile Stress, Fue	561000.

Figure 3.4 Data of material properties

### 3.2.3 Loads Description

In this sub-chapter, detailed information regarding the load combination of dead loads, live loads, wind load, wave load, current load, and earthquake load will be briefly discussed.



### 3.2.3.1 Dead and Live Loads

The computational software SAP2000 will automatically calculate the self-weight of the wellhead platform offshore. Hence, dead loads other than self-weight of the structure and live loads are required to search and collect. The table below listed out the dead loads and live loads will be applied to the structure:

Table 3.1 Dead loads and live load description

No.	Load description	Weight (MN)
1	Jacket appurtenances weight	0.339
2	Topside dead loads	0.393
3	Topside live loads	1.150
4	Piping & equipment weights	0.400
TOTAL		2.282

### 3.2.3.2 Environmental Loads

Environmental loads were obtained from the data of MeteOcean. It is direct response and depending on the location and is not a permanent value that can be used in all places. Environmental criteria used for wellhead offshore platform will be based on the location in Terengganu and is clearly showed in Table 3.2. Environmental loads such as wind, wave, and current load will be determined by referring to the provided criteria in Table 3.2 and formulation that obtained from API-RP2A.

Table 3.2 Environmental criteria used at Terengganu

MSL	Types of data	Unit	Design condition
47.629 m	Wave height	m	10.79
	Wave period	s	10.90
	Current velocity	m/s	0.75
	Wind speed	m/s	21.80
	Maximum tide	m	2.00
	Storm surge	m	0.40

### 3.2.3.3 Wind Load

Wind load is one of the environmental loads and it is subjecting to elevations and duration. In this study, wind profile and gust and wind drag force will be considered for the design of wellhead platform offshore according to API-RP2A.

Wind profile and gust considered the design wind speed,  $u(z, t)$  (m/s) at height  $z$  (ft) above sea level and corresponding to an averaging time period  $t(s)$ , where  $t \leq t_o = 3600$  sec during strong wind condition. The formula is given by:

$$U(z, t) = U(z) \times [1 - 0.41 \times I_u(z) \times \ln(\frac{t}{t_o})] \quad 3.1$$

Where the 1 hour mean wind speed  $U(z)$  (ft/s) at level  $z$  (ft) is given by:

$$U(z) = U_o \times [1 + C \times \ln(\frac{z}{32.8})] \quad 3.2$$

$$C = 5.73 \times 10^{-2} \times [1 + 0.0457 \times U_o]^{1/2} \quad 3.3$$

Where the turbulence intensity,  $I_u(z)$  at level  $z$  is given by:

$$I_u(z) = 0.06 \times [1 + 0.0131 \times U_o] \times (\frac{z}{32.8})^{-0.22} \quad 3.4$$

Where  $U_o$  (ft/s) is the 1 hour mean wind speed at 32.8 ft or approximately to 10m.

The wind drag force for an object caused by the wind speed is determined as:

$$F = (\rho/2) \times u^2 C_s A \quad 3.5$$

Where

$F$  = wind force [N],

$\rho$  = density of air [1.22 kg/m<sup>3</sup>],

$U$  = wind speed [m/s],

$C_s$  = shape coefficient [Table 3.3],

$A$  = area of object [m<sup>2</sup>]

Table 3.3 Shape Coefficient,  $C_s$

Projected Area by perpendicular wind	Shape Coefficient, $C_s$
Beams	1.5
Sides of buildings	1.5
Cylinder sections	0.5
Overall projected area of the platform	1.0

### 3.2.3.4 Wave Load

Wave loads on a member of the structure can be determined by the total of a drag force and an inertia force by using Morison equation 3.6 as below. For typical design conditions, global platform wave forces of unshielded circular cylinders can be computed according to Table 3.4. These values are a suitable to use for the case of a steady current where waves are neglected or the case of large waves with  $U_{mo} T_{app}/D > 30$ .  $U_{mo}$  represented the highest velocity of the horizontal particle at storm mean water level under the wave crest from the two-dimensional wave kinematics theory;  $T_{app}$  represented the period of the apparent wave, and  $D$  represents the diameter of platform leg at storm mean water level. Furthermore, circular cross-sections element need to group as either “smooth” or “rough” based on the expected amount of marine growth for accumulating at the time of the loading event.

$$F = F_D + F_I = C_D \frac{w}{2g} A U|U| + C_m \frac{w}{g} V \left( \frac{\delta U}{\delta t} \right) \quad 3.6$$

Where

$F$  = hydrodynamic force vector per unit length acting normal to the axis of the member [N/m],

$F_D$  = drag force per unit length acting to the axis of the member [N/m],

$F_I$  = inertia force vector per unit length acting normal to the axis of the member [N/m],

$C_d$  = drag coefficient [Table 3.4],

$C_m$  = inertia coefficient [Table 3.4],

$w$  = density of water [N/m<sup>3</sup>],

$g$  = gravity acceleration, [m/s<sup>2</sup>],

$A$  = projected area normal to the cylinder axis per unit length (=  $D$  for circular cylinders), [m],

$V$  = displaced volume of the cylinder per unit length (=  $\pi D^2/4$  for circular cylinders), [m<sup>2</sup>],

$D$  = effective diameter of the circular cylindrical member including marine growth [m],

$U$  = component of the velocity vector (due to wave or current or both) of the water normal to the axis of the member [m/s],

$|U|$  = absolute value of  $U$  [m/s],

$\frac{\delta U}{\delta t}$  = component of the local acceleration vector of the water normal to the axis of the member [m/s<sup>2</sup>]

Table 3.4 Drag coefficient,  $C_d$  and Inertia Coefficient,  $C_m$

Marine Growth	Drag Coefficient, $C_d$	Shape Coefficient, $C_s$
Smooth	0.65	1.6
Rough	1.05	1.2

According to API-RP2A, it stated that the Morison equation neglect the component's convective acceleration in the calculation of inertia force. Lift forces, slam forces, and axial Froude-Krylov forces also neglected.

### 3.2.3.5 Current Load

The current force that exerted on the wellhead structure can be calculated by Morison's equation with  $\frac{\delta U}{\delta t} = 0$  where no wave condition is applied. The formula is generated from equation 3.6:

$$F = F_D + F_I = C_D \frac{w}{2g} A U|U| + C_m \frac{w}{g} V \left( \frac{\delta U}{\delta t} \right) \quad 3.6$$

$$F = F_D = C_D \frac{w}{2g} A U|U| \quad 3.7$$

### 3.2.3.6 Earthquake Load

To determine the seismic load, the seismic analysis is being done using the SAP2000 version 18 by response spectra curve under Eurocode 8, 2004 for the response spectrum analysis. Time history will be utilized the collected earthquake data that

obtained from Pacific Earthquake Engineering Research Center and also analyzed through SAP2000. The data used is of El Centro earthquake May 19<sup>th</sup>, 1940.

The earthquake data collected is in North (N) direction as it the most critical vibration compared to other direction. All the data is in a notepad document and need to be transferring the data into Microsoft Excel file for data filtering and graph plotting purposes. From the graph, we would be able to determine the maximum critical acceleration and compare the data easily. Figure 3.5 showed the earthquake data from East direction has been transferred to MS Excel file.

Al-Centro	
Time (sec)	A (g)
0	0.0063
0.02	0.00364
0.04	0.00099
0.06	0.00428
0.08	0.00758
0.1	0.01087
0.12	0.00682
0.14	0.00277
0.16	-0.00128
0.18	0.00368
0.2	0.00864
0.22	0.0136
0.24	0.00727
0.26	0.00094
0.28	0.0042
0.3	0.00221
0.32	0.00021

Figure 3.5 Transferring earthquake data from East direction in MS Excel

In the data, there are some values which are in positive and negative values. Hence, formula code of =MAX (-MIN (Range); MAX (Range)) is implemented to determine the maximum data among the data. The maximum values of acceleration obtained for N direction are 0.32g at time 2.006 seconds. The graph of time (s) versus acceleration (g) has plotted and the result is shown as below:

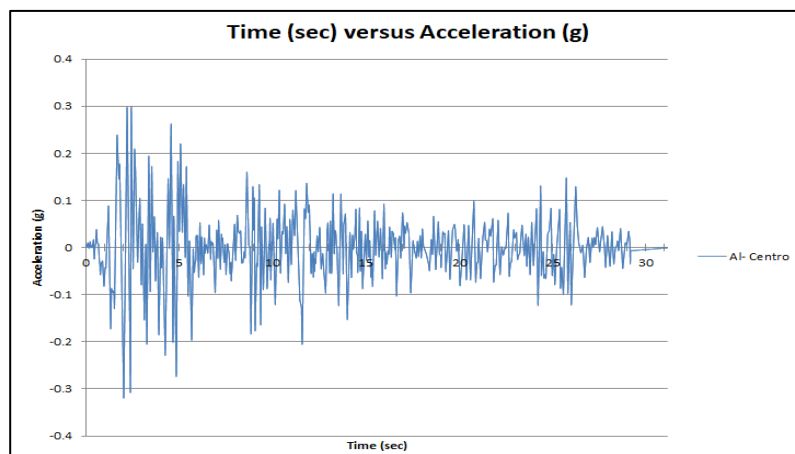


Figure 3.6 Time (s) vs Acceleration (g) in E-direction

### **3.3 Load Combination**

Wellhead offshore platform has been modeled by SAP2000 version 18. Free vibration analysis can be performed at the initial stage since it does not including any loads on the structure but by the linear elastic material behavior (modal load) of the structure. Since Time history and Response spectrum are analyzed in the study, the loads considering in the analysis including dead loads, live loads, modal load, environmental load consists of wind, wave and current, time history load and response spectrum load. Several combinations of load cases are implementing the analysis as below:

- I. Free Vibration analysis (FVA)
- II. Dead load (DL) + Live load (LL)
- III. Environmental load (EL)
- IV. Dead load (DL) + Live load (LL) + Environmental load (EL) + Time history load (TH)
- V. Response spectrum (RS)

Furthermore, the results that are expected to acquire from SAP2000 are as:

- I. The modal shape of the wellhead offshore platform
- II. Natural period and natural frequency of wellhead offshore platform
- III. Maximum unity check of all structural member
- IV. Maximum shear and bending stress in the member under various load cases
- V. Joint displacement, velocity, and acceleration under different types of load combination

### **3.4 Resistance Capacity for Structural member**

The following sub-section will show the formula of member's resistance that will be used for purpose of manual calculation checking according to Eurocode BS EN 1993-1-1:2005.

### 3.4.1 The resistance of Cross Sections

The resistance of cross section is the maximum design value that can be supported by the member. It considered in tension, compression, bending, and shear.

#### 3.4.1.1 Tension

For sections with holes (bolt), the design tension resistance,  $N_{t, Rd}$  should be taken as smaller of design plastic resistance of gross section,  $N_{pl, Rd}$  and design ultimate resistance of the net cross section at the hole,  $N_{u, Rd}$ :

$$N_{pl, Rd} = \frac{Af_y}{\gamma_{M0}} \quad 3.8$$

$$N_{u, Rd} = \frac{0.9A_{net}f_u}{\gamma_{M2}} \quad 3.9$$

Where

$A$  = area of cross section [ $m^2$ ],

$f_y$  = yield strength [ $N/mm^2$ ],

$f_u$  = ultimate strength [ $N/mm^2$ ],

$\gamma_{M0}$  = partial factor for resistance of cross section what class is [1.0],

$\gamma_{M2}$  = partial factor for resistance of cross section in tension to fracture [1.25]

#### 3.4.1.2 Compression

The design resistance of the cross section for uniform compression should be determined as below:

For Class 1, 2, 3 cross sections:

$$N_{c, Rd} = \frac{Af_y}{\gamma_{M0}} \quad 3.10$$

Where

$A$  = area of cross-section [ $m^2$ ],

$f_y$  = yield strength [ $N/mm^2$ ],

$\gamma_{M0}$  = partial factor for resistance of cross section what class is [1.0]

### 3.4.1.3 Bending moment

The design resistance for bending about one principal axis of a cross-section is determined as follows:

For Class 1 or 2 cross sections:

$$M_{c,Rd} = M_{pl,Rd} = \frac{W_{pl} f_y}{\gamma_{M0}} \quad 3.11$$

Where

$W_{pl}$  = plastic section modulus [ $\text{cm}^3$ ]

$f_y$  = yield strength [ $\text{N}/\text{mm}^2$ ],

$\gamma_{M0}$  = partial factor for resistance of cross section what class is [1.0]

### 3.4.1.4 Shear

For plastic design, design shear resistance,  $V_{c, Rd}$  is the design of plastic shear resistance,  $V_{pl, Rd}$ . In the absence of torsion, the design of plastic shear resistance,  $V_{pl, Rd}$  is given by:

$$V_{c,Rd} = V_{pl,Rd} = \frac{A_v (f_y / \sqrt{3})}{\gamma_{M0}} \quad 3.11$$

Where

$A_v$  = shear area (circular hollow sections and tubes of uniform thickness,  $2A/\pi$ ), [ $\text{m}^2$ ],

$A$  = cross-sectional area [ $\text{m}^2$ ]

## 3.4.2 Buckling Resistance of Members

### 3.4.2.1 Uniform Members in Compression

A compression member should be verified against the buckling as follows:



For Class 1, 2 and 3 cross sections:

$$N_{b,Rd} = \frac{\chi A f_y}{\gamma_{M1}} \quad 3.12$$

$$\lambda_1 = \pi \sqrt{\frac{E}{f_y}} = 93.9 \varepsilon \quad 3.13$$

$$\lambda = \frac{L_{cr}}{i} \frac{1}{\lambda_1} \quad 3.14$$

$$\Phi = 0.5[1 + \alpha(\lambda - 0.2) + \lambda^2] \quad 3.15$$

$$\chi = \frac{1}{\Phi + \sqrt{\Phi^2 - \lambda^2}} (\leq 1.0) \quad 3.16$$

Where

$\chi$  = reduction factor for buckling mode,

$\Phi$  = value to determine reduction factor,  $\chi$ ,

$\lambda$  = non-dimensional slenderness,

$\lambda_1$  = slenderness value to determine relative slenderness,

$\varepsilon$  = strain,

$A$  = Cross sectional area [m<sup>2</sup>],

$f_y$  = Yield strength [N/mm<sup>2</sup>],

$L_{cr}$  = buckling length [mm],

$i$  = radius of gyration [cm],

$\alpha$  = imperfection factor,

$\gamma_{M1}$  = partial factor for resistance of members to instability [1.0]


Cross section	Limits	Buckling about axis	Buckling curve	
			S 235 S 275 S 355 S 420	S 460
	hot finished	any	a	a <sub>0</sub>
	cold formed	any	c	c

Figure 3.7 Selection of buckling curve for a cross section

Sources: Eurocode 3, 2005

Table 3.5 Imperfection factors fro buckling factors,  $\alpha$

Buckling curve	Imperfection factor, $\alpha$
a <sub>0</sub>	0.13
a	0.21
b	0.34
c	0.49
d	0.76

Sources: Eurocode 3, 2005

### 3.5 SAP2000 Computational Program

SAP2000 is the most integrated, productive and practical engineering software for structural analysis and design of any type of structural system, ranging from 2D to 3D. Integrated modeling templates, code-based loading assignments, advanced analysis options, design-optimization procedures, and customizable output reports all coordinate across a powerful platform which makes SAP2000 very useful for practicing professionals. It is object-based program where a complex model can be generated and meshed with powerful built-in template including simple beams, 3D truss, 3D frame, pipe etc and integrated design code features that can automatically generate wind, wave, and seismic load with comprehensive steel and concrete design code such as AASHTO, Eurocode, British Standard, American Petroleum Institute, Hong Kong Codes of Practices, Singapore Code of Practice etc.

It also possesses standard and sophisticated analysis process which makes SAP2000 more practical and productivity for any analysis such as simple static, linear elastic, dynamic and nonlinear – inelastic. For instance, engineers are able to quickly obtain the result of bending moments, shear force, axial force, and deflection of the structural members of the building that is modeled with different elements such as

beams, column, slabs with different loading and support restraints according to a different code of practice used. SAP2000 can easily handle large multi-story projects with ease and provide desired specific result including the area of steel, concrete quantity, and size of an element required for the safety of the structure.

The output of SAP-2000 is available in the form of 3D perspectives of deformed and un-deformed shape. Besides that, it also allows animation of different mode shapes and deformed shapes where can be seen in different output parameters by multiple windows. Moreover, the size of beam, column, and area of steel are directly displayed on the frame members in concrete structure whereas, for steel structure, the section size and shape are directly displayed on each member of a structure. Lastly, the output design results in SAP-2000 will automatically revise the change input parameter without re-analysis.

### **3.5.1 Checklist of SAP2000 Modelling and Analysis**

To ensure the efficiency of the overall analysis in SAP2000, below are the checklist to show the steps in modelling and analysis of wellhead platform:

- I. Define the type of model
- II. Create, define, and coordinate the grid system for the model
- III. Define material and frame section properties
- IV. Construct the frame geometry by assigning the member
- V. Assign the restraints at the base of the structure
- VI. Define all load patterns and load combination
- VII. Assign the loads at specific frame element or joint
- VIII. Define function of Time History and Response Spectrum
- IX. Run the analysis of model
- X. Review analysis result and output table
- XI. Check the structural design

### **3.5.2 Steps in SAP2000 Modelling and Analysis**

Step 1: Define the type of model

First, click the **File Menu > New Model** command, select the unit of the project in “kN, m, C” and template of 3D Frame for wellhead offshore platform.

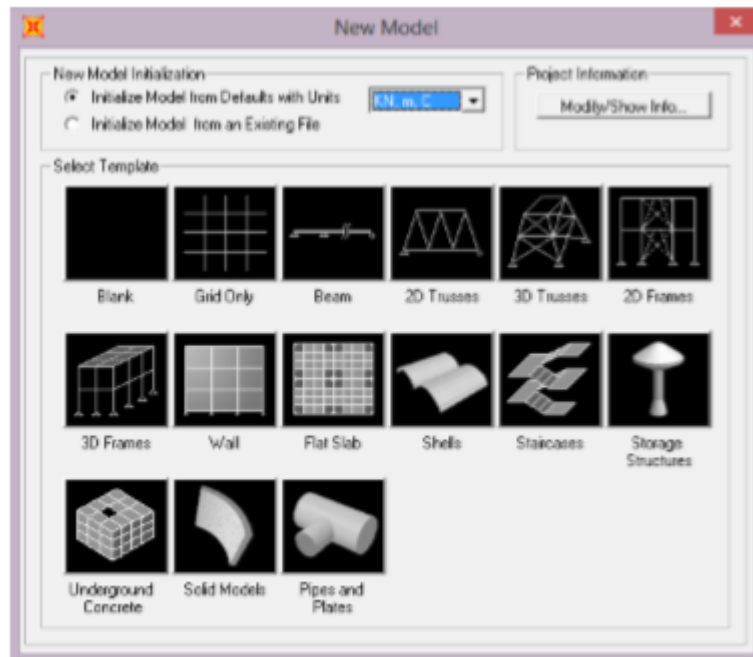


Figure 3.8 Select the modal type and unit

Step 2: Setting up the coordinate of grid line

Click the **Define menu > Coordinate System/Grids** command to display the Coordinate/Grid system form shown in Figure 3.9, then insert the grid value of the structure accordingly to the drawing for easily modelling the structure in next stage.

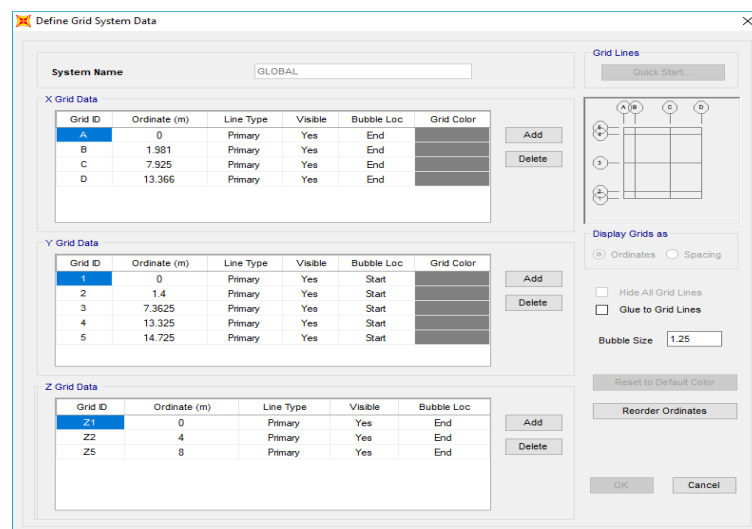


Figure 3.9 Define grid system data

Step 3: Define material and frame section properties

Click the **Define menu > Materials** command to display the Define material form shown in Figure 3.10. Click the **Add New Material Quick** for insert new material S355. Next is to define frame section, click the **Define menu > Section properties > Frame properties > Import New Property**. For our case, select the Circular Hollow Sections (CHS) from the steel list.

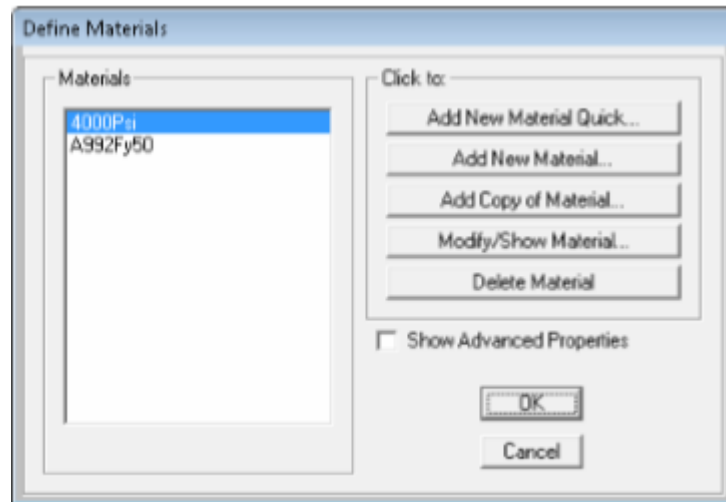


Figure 3.10 Define material types

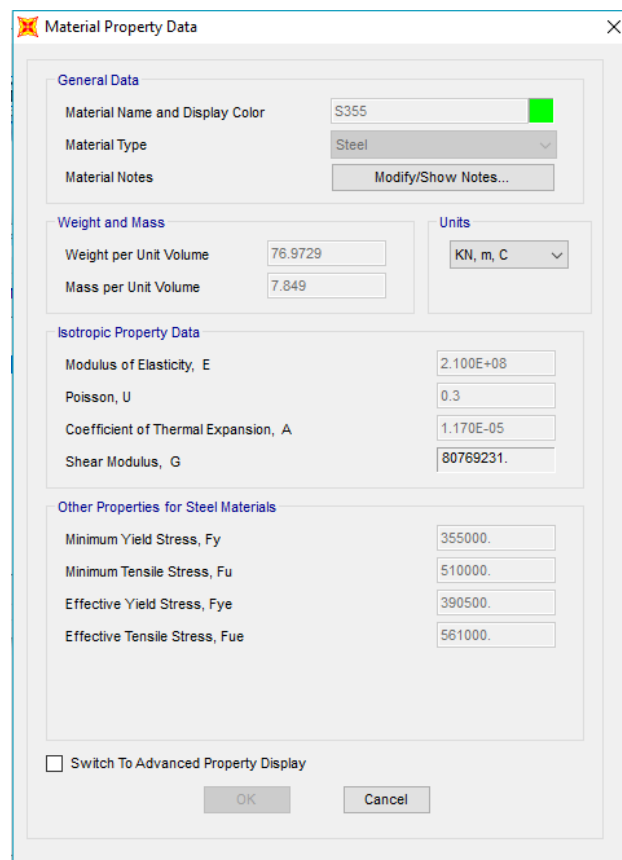


Figure 3.11 Material properties data

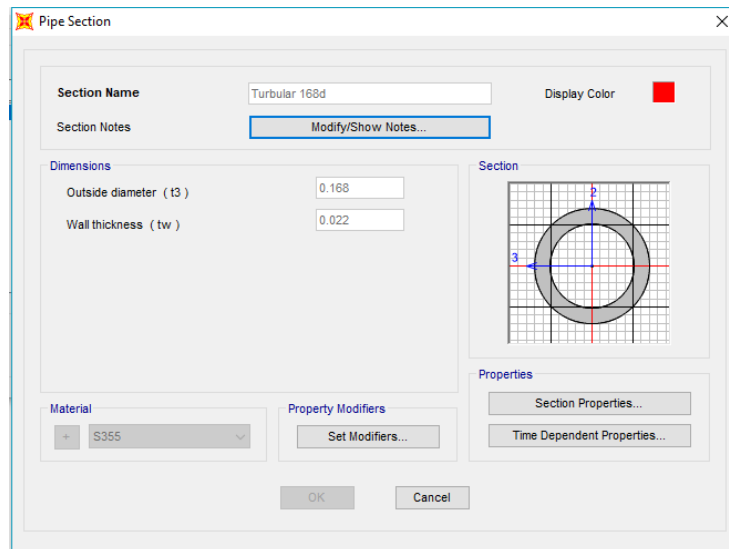


Figure 3.12 Define pipe section

#### Step 4: Draw the frame geometry by assigning member section properties

Wellhead offshore structure is modeled by assigning the frame element according to the sizing of the member based on the architectural drawing. After assigning all the frame geometry, added the slab on the structure and makes the slab and the frame connected with each other by using “Auto-mesh” function. In meshing tool, try to increase the mesh size instead of using default mesh size for obtaining an accurate result. Lastly, assigning and add the restraints of the structure as fixed support at the base.

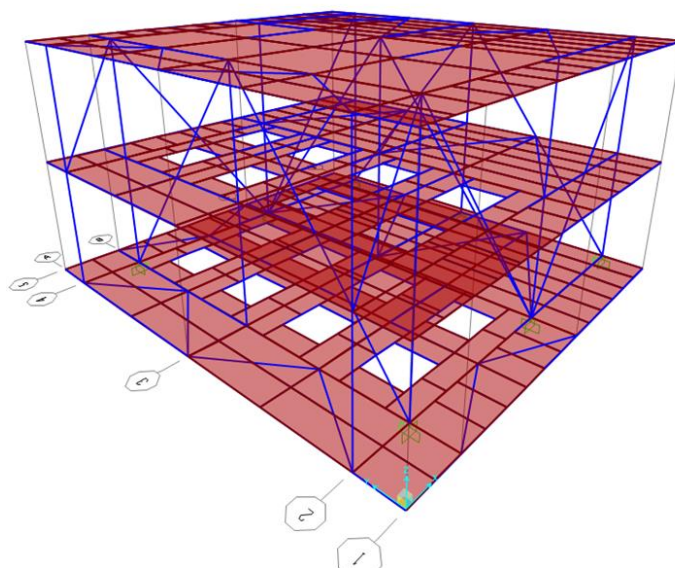


Figure 3.13 3D modeling of the structure

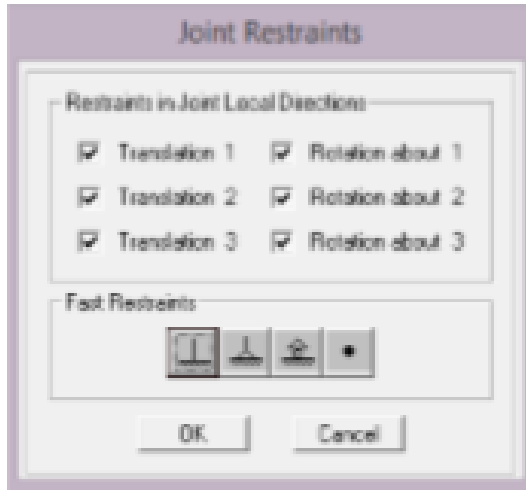


Figure 3.14 Restraint at the base

Step 5: Define load cases

Define all the load cases that will be applied to the structure. Load cases including dead load, live load, environmental load and earthquake loading. First is to define load pattern for each loading. After calculating the dead load and live load, then applied to the structure as gravity load. Click the button **Define > Load cases**, set the load case as Linear Static analysis type. Next is environmental load data. The load patterns of each of the environmental load have been defined. API 4F 2008 design codes have been implemented in the wind load case for both X and Y direction. While wave and current load have been implemented API WSD 2000 as the design code. In load cases, wind load is set to Linear Static analysis and wave load is set to multi-step static.

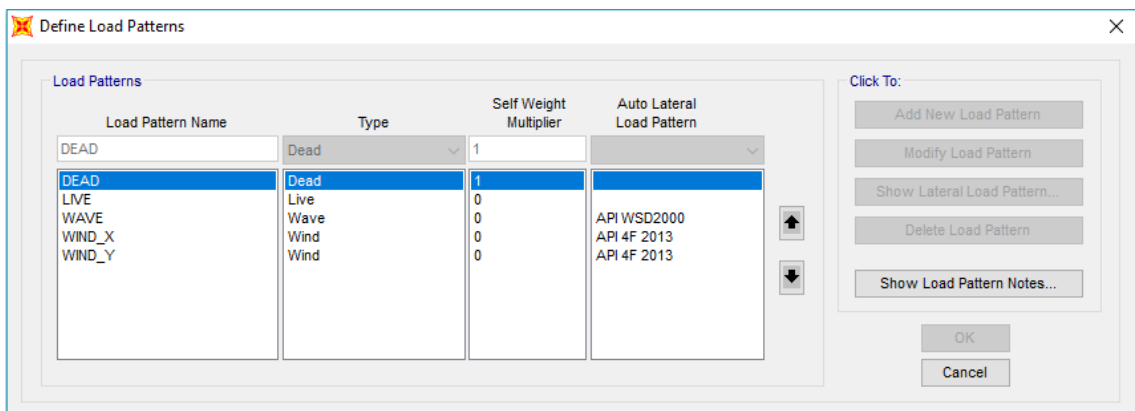


Figure 3.15 Define load pattern for each loading

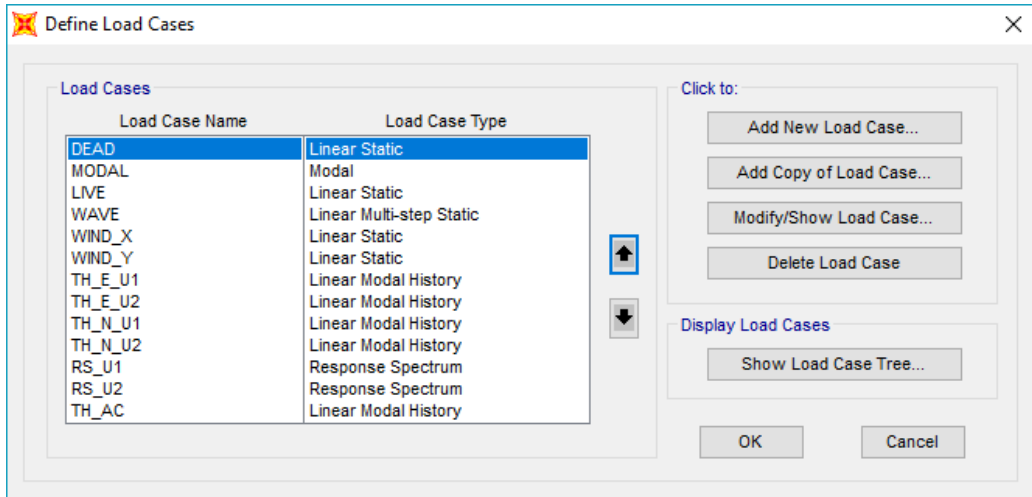


Figure 3.16 Define all load cases

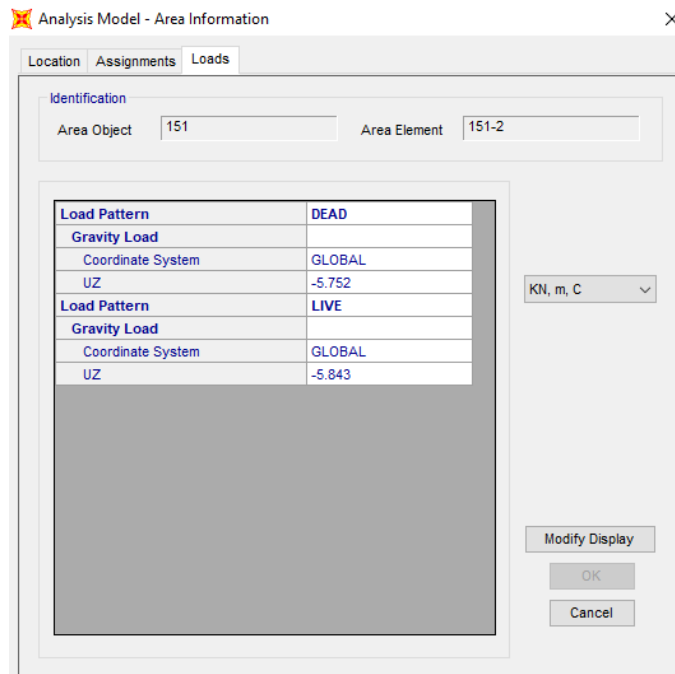


Figure 3.17 Dead load & live load

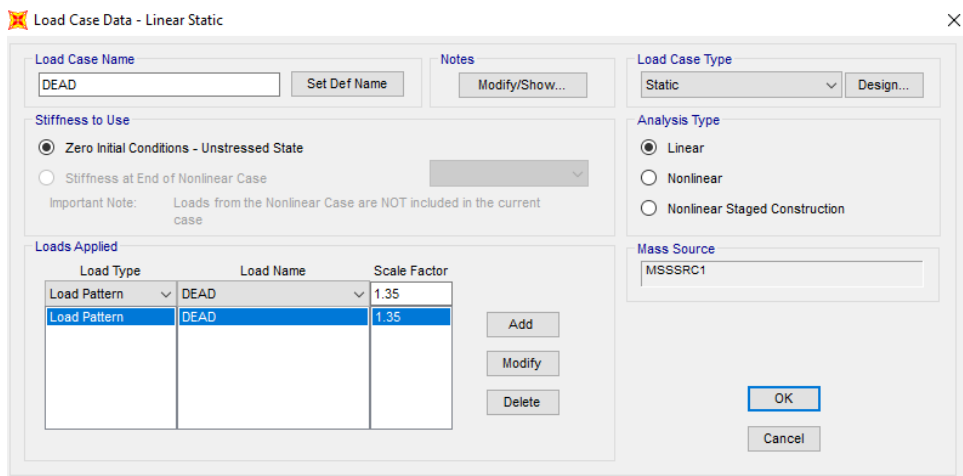


Figure 3.18 Dead load case data



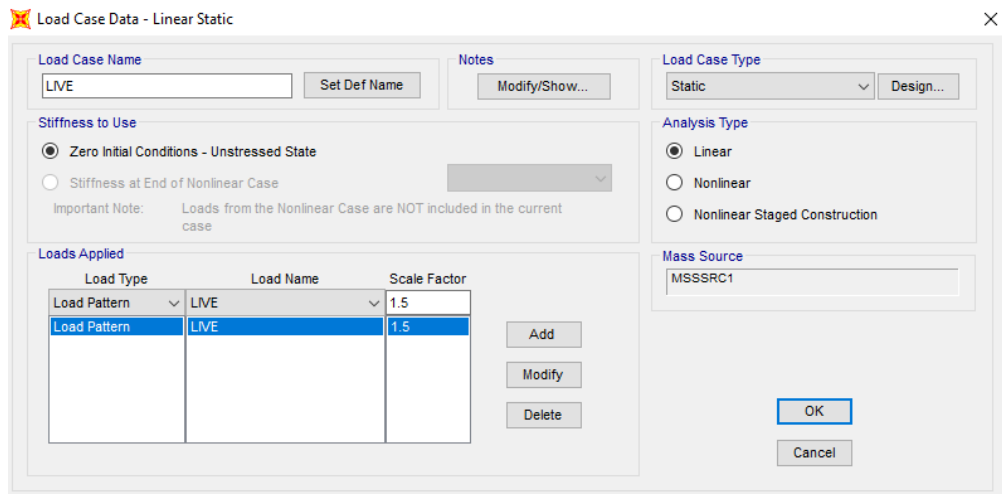


Figure 3.19 Live load case data

For wind load case, the data on wind coefficients, exposure height, and wind exposure parameters were inserted as showed at below.

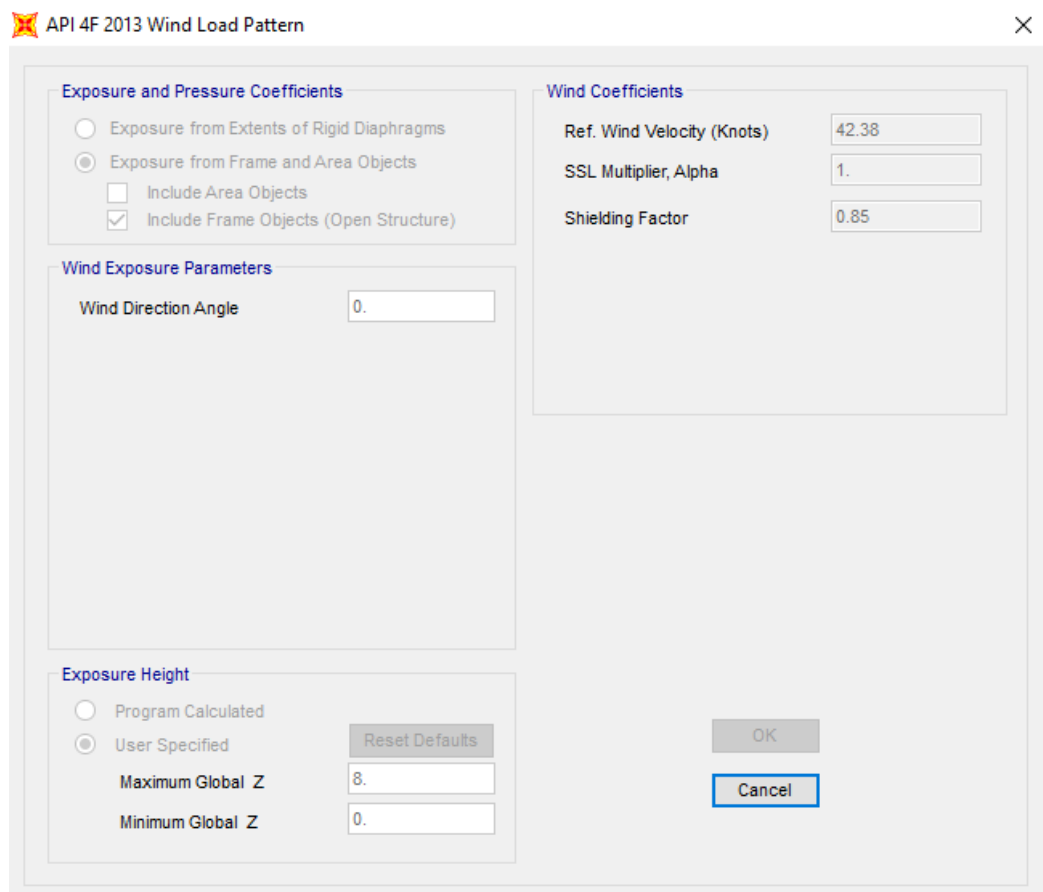


Figure 3.20 Wind load pattern data

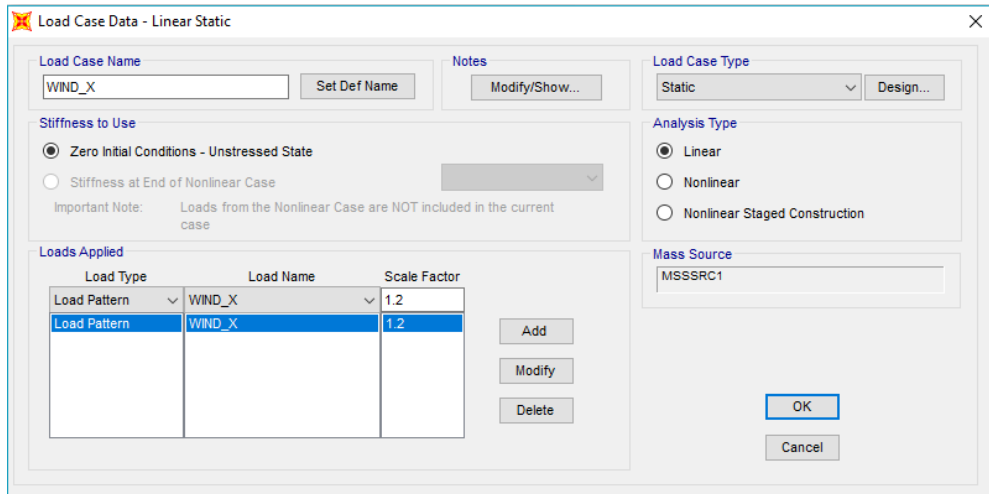


Figure 3.21 Wind load case data

The wave and current load part, the wave and current data have been inserted accordingly based on the environment data criteria at Terengganu.

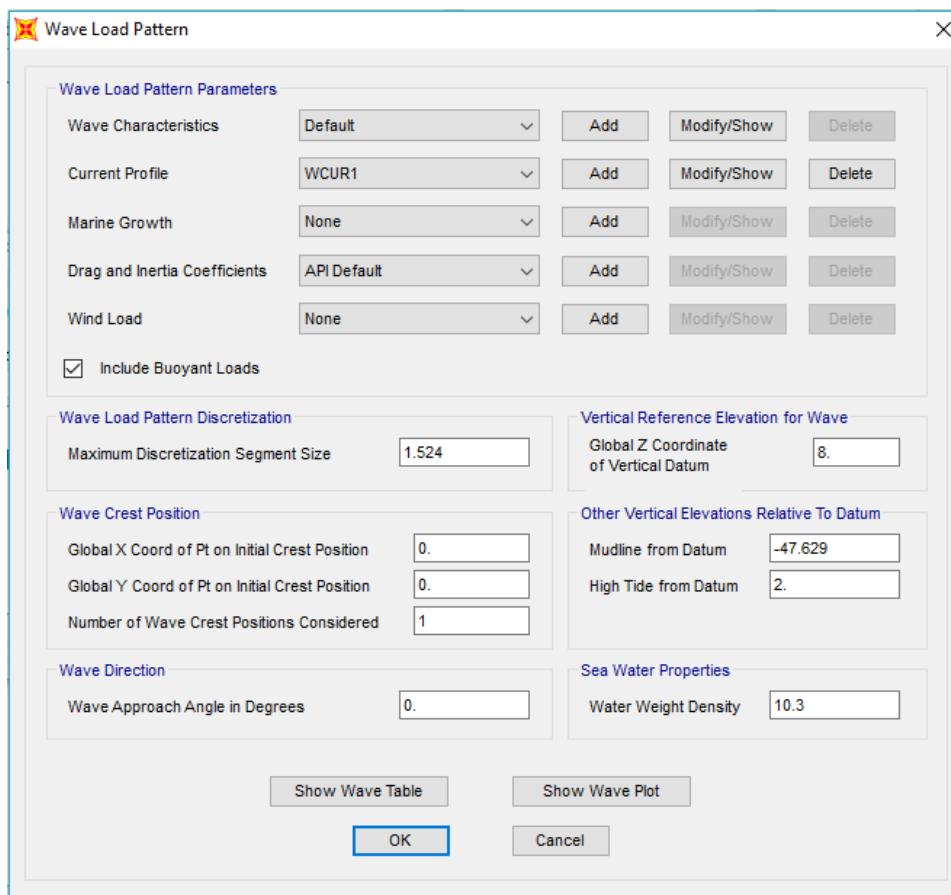


Figure 3.22 Wave load pattern

**Wave Characteristics**

Edit

**Wave Characteristic Name** Default

**Wave Factors**

Wave Kinematics Factor 1.

Storm Water Depth 47.629

**Wave Data**

Wave Height 10.79

Wave Period 10.9

**Wave Type**

From Selected Wave Theory

User Defined

**Wave Theory**

Airy Wave Theory (Linear)

Stokes Wave Theory Order

Cnoidal Wave Theory Order

OK Cancel

Figure 3.23 Wave characteristics

**Current Profile Data**

Edit

**Current Profile Name** WCUR1

**Current Profile Factors**

Current Blockage Factor 0.9

Current Profile Stretching Option Linear

**Data Is Specified at This Number of Elevations**

Number of Elevations 1

**Current Profile Data**

	Vert from Datum	Current Velocity	Current Direction
1	0.	0.75	90.

Order Rows

OK

Cancel

Figure 3.24 Current profile data

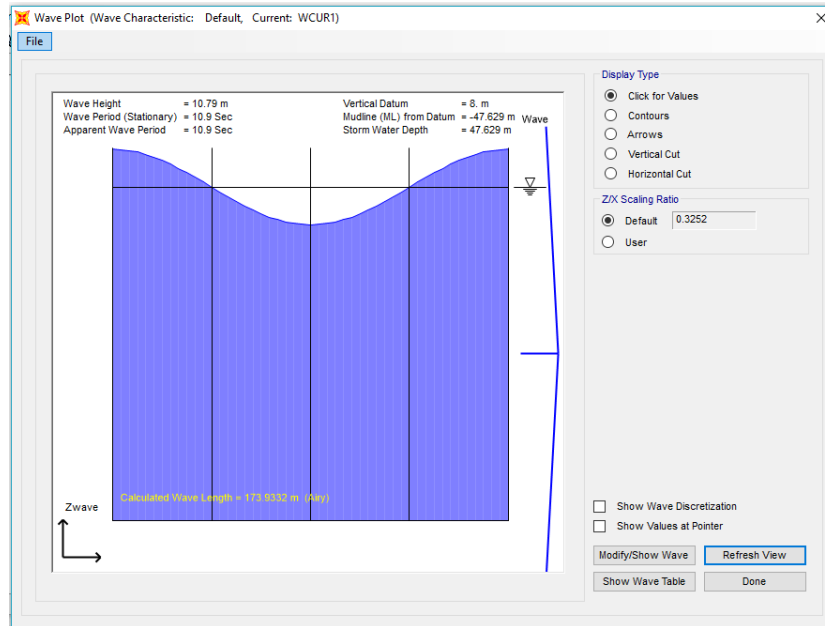


Figure 3.25 Wave plot

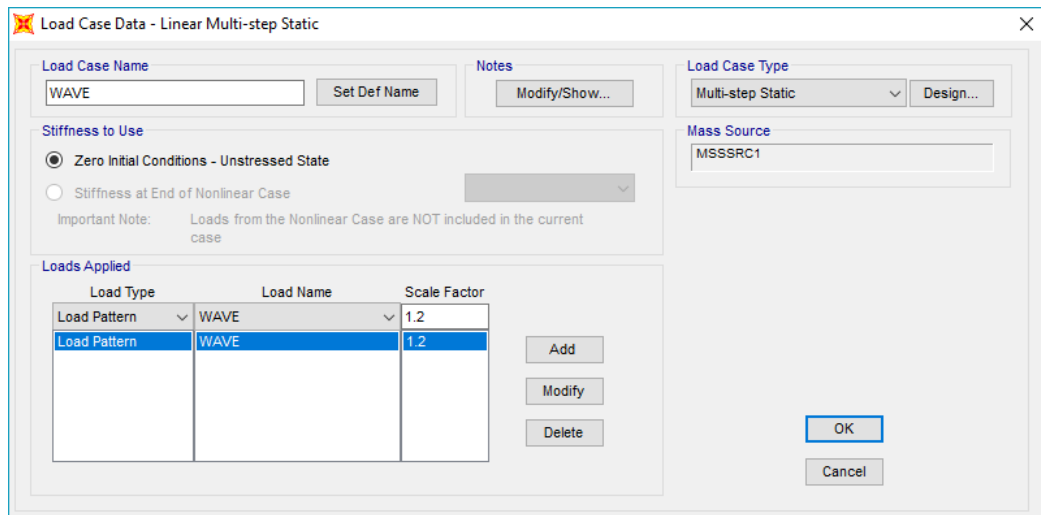


Figure 3.26 Wave load case data

### Step 6: Define function of Time History and Response Spectrum

Define the functions of Time History by attached the ground motion which in the notepad file and adjusting time interval based on the seismic data. In our case, we only have N direction of Time History function; hence we applied in U1 direction only. If there are different directions then we applied seismic data in a different direction. Moreover, load applied at U1 and U2 in each direction are determined. For Response Spectrum, load applied for both U1 and U2 are considered in the analysis. Therefore, total of two response spectrum load cases is performed. Moreover, the modal load case is set at maximum 12 numbers of modes shape in this study.

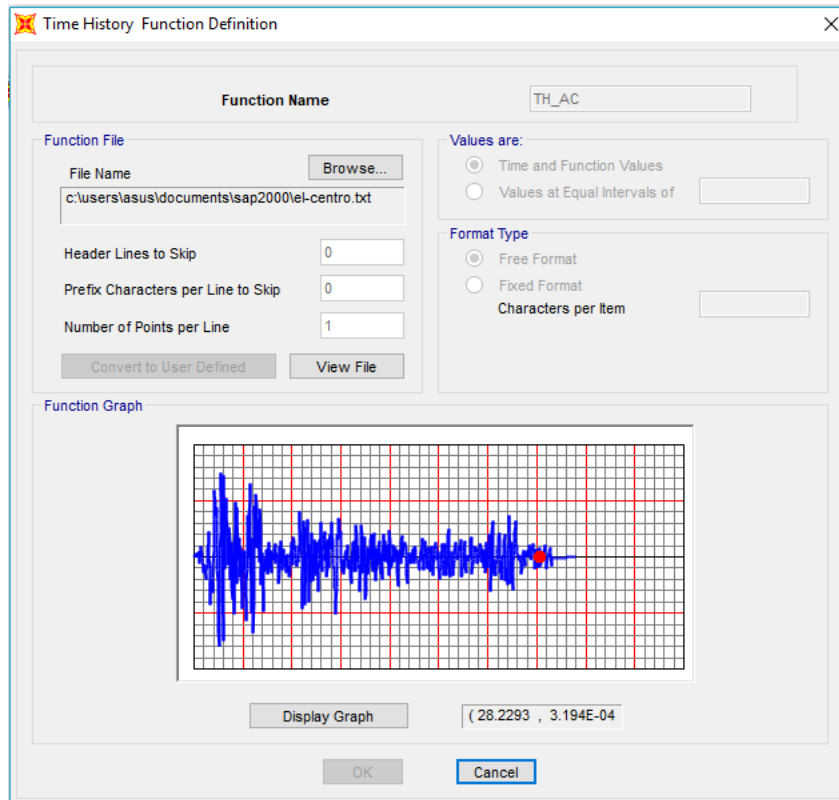


Figure 3.27 Define time history function

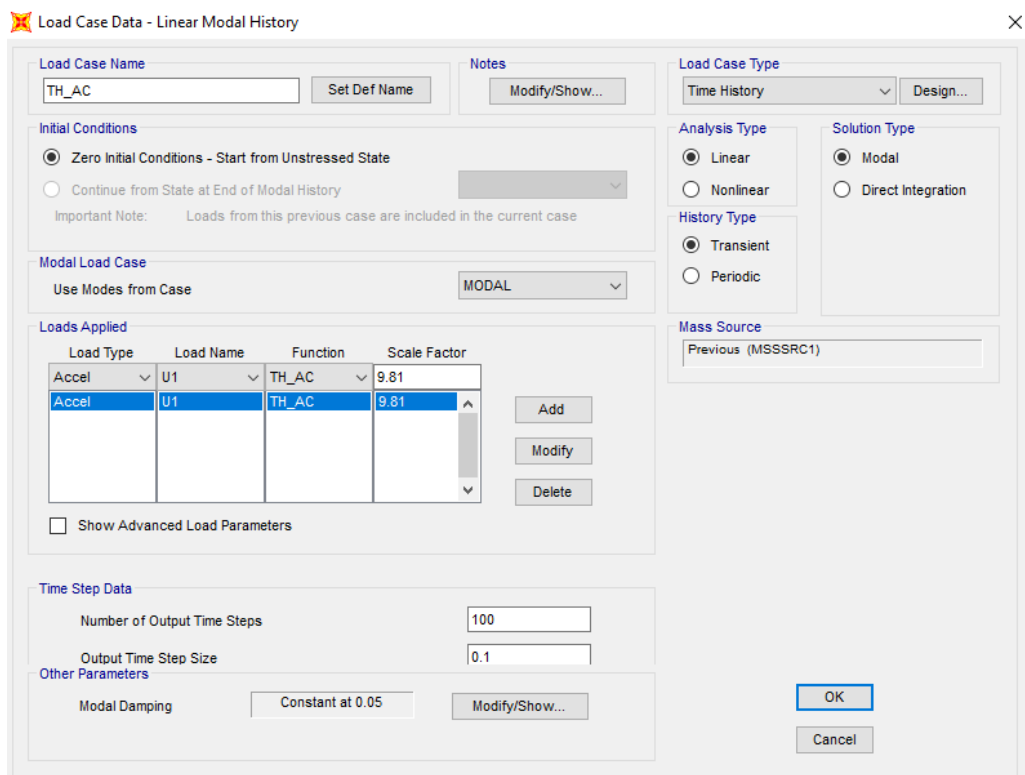


Figure 3.28 Linear modal history case data

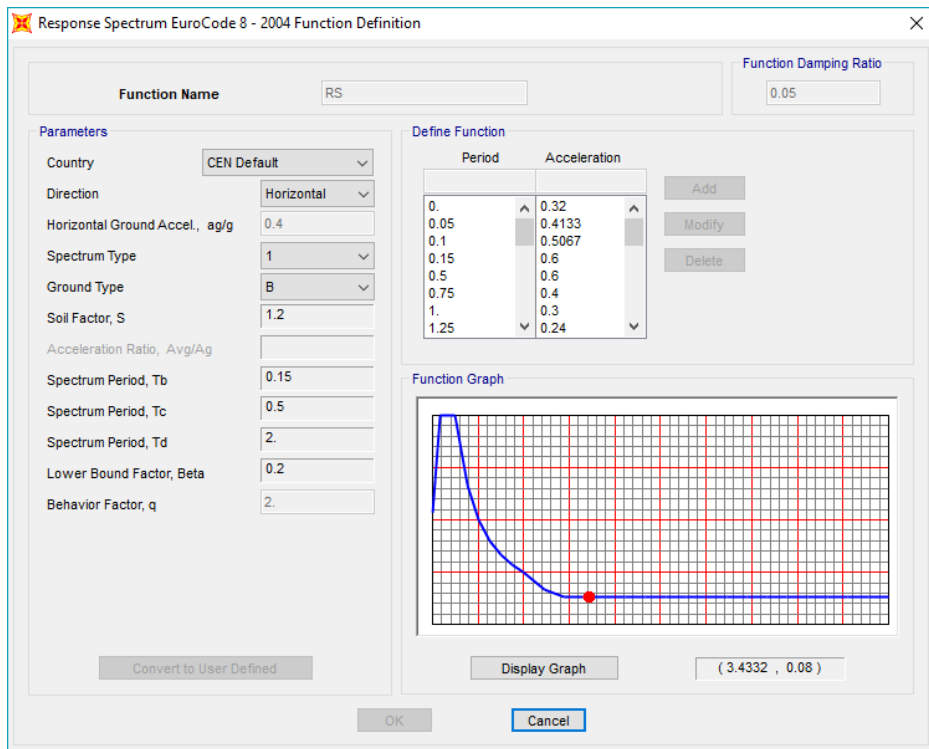


Figure 3.29 Response spectrum Eurocode 8 function

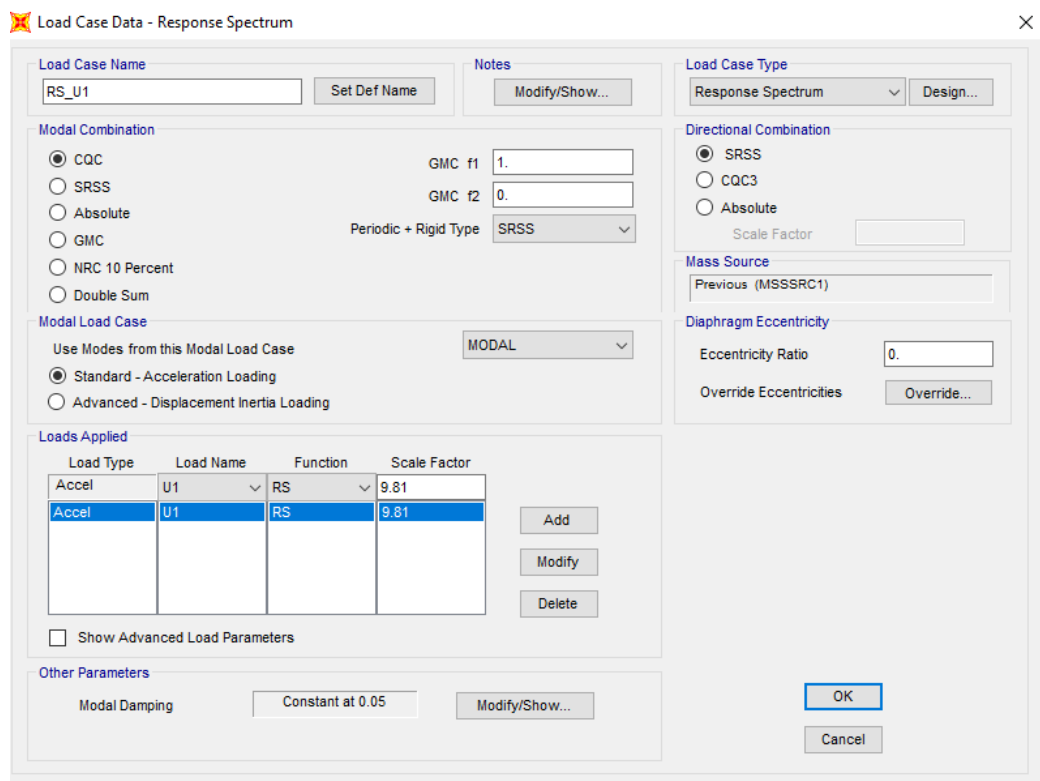


Figure 3.30 Response spectrum load case data

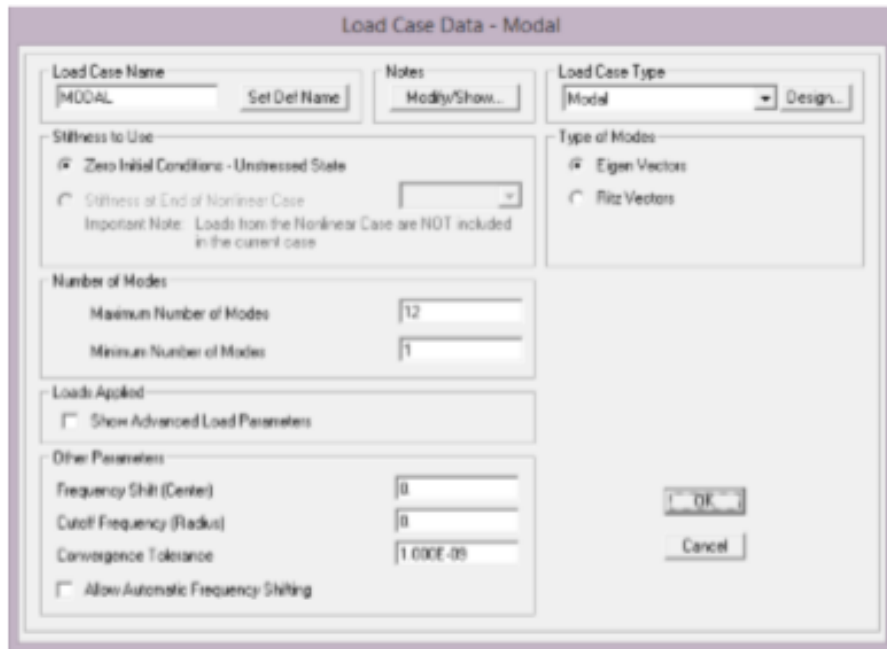


Figure 3.31 Modal load case

#### Step 7: Analysis the Model

Define the load combination will be used in the analysis as shown in Figure xx. Then start to run the analysis. After running the load cases analysis, check the steel structure accordance to EuroCode3, the critical member and maximum unity check of the entire structures member are determined.

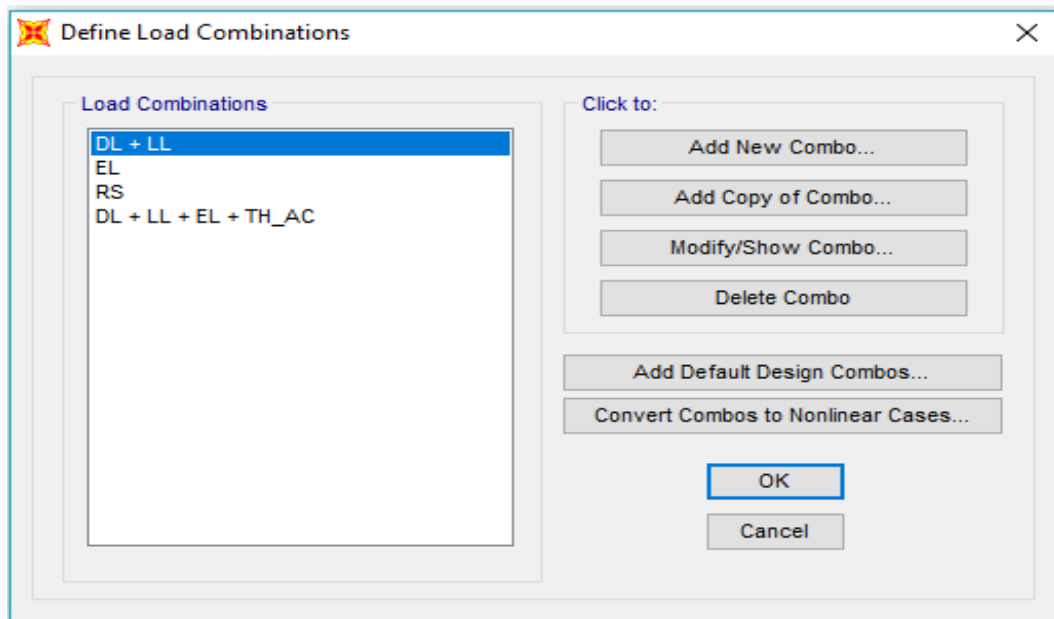


Figure 3.32 Define load combination

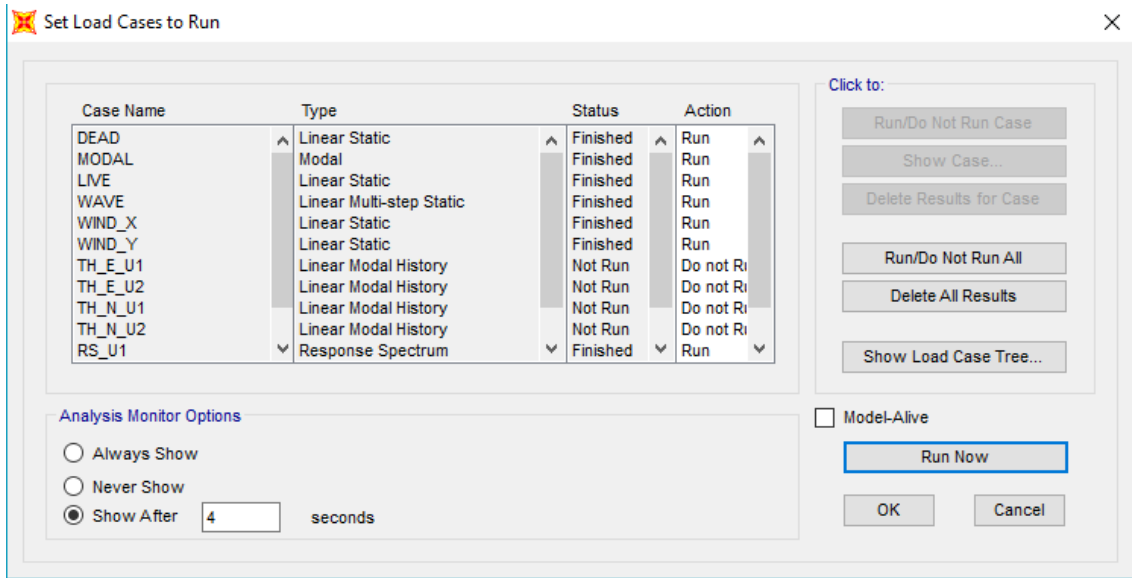


Figure 3.33 Set load case to run

Step 8: Display result and output table

After performed all the analysis, the result can be obtained from **Display** tab in the menu and used for report purposes.

Joint Text	Mass Source	U1 KN-s2/m	U2 KN-s2/m	U3 KN-s2/m	R1 KN-m-s2	R2 KN-m-s2	R3 KN-m-s2	CenterX m	CenterY m	CenterZ m
1	MSSSRC1	0.59	0.59	0.59	0	0	0	0	14.725	0
2	MSSSRC1	0.88	0.88	0.88	0	0	0	1.981	14.725	0
3	MSSSRC1	0.88	0.88	0.88	0	0	0	7.925	14.725	0
4	MSSSRC1	0.59	0.59	0.59	0	0	0	13.366	14.725	0
5	MSSSRC1	1.06	1.06	1.06	0	0	0	0	13.325	0
6	MSSSRC1	1.43	1.43	1.43	0	0	0	1.981	13.325	0
7	MSSSRC1	2.96	2.96	2.96	0	0	0	7.925	13.325	0
8	MSSSRC1	1.43	1.43	1.43	0	0	0	13.366	13.325	0
9	MSSSRC1	1.42	1.42	1.42	0	0	0	0	7.3625	0
10	MSSSRC1	0.85	0.85	0.85	0	0	0	1.981	7.3625	0
11	MSSSRC1	1.58	1.58	1.58	0	0	0	7.925	7.3625	0
12	MSSSRC1	0.98	0.98	0.98	0	0	0	13.366	7.3625	0
13	MSSSRC1	1.06	1.06	1.06	0	0	0	0	1.4	0
14	MSSSRC1	1.43	1.43	1.43	0	0	0	1.981	1.4	0
15	MSSSRC1	2.96	2.96	2.96	0	0	0	7.925	1.4	0
16	MSSSRC1	1.43	1.43	1.43	0	0	0	13.366	1.4	0

Figure 3.34 Result output table



## CHAPTER 4

### RESULTS AND DISCUSSION

#### 4.1 Summary of Analysis

Wellhead offshore platform has been modelled by SAP2000 version 18. Free vibration analysis is performed at the early stage since it does not including any loads on the structure but by the linear elastic material behaviour (modal load) of the structure. Earthquake analysis such as Time history and Response spectrum are analysed in the study, the loads considering in the analysis including dead loads, live loads, modal load, environmental load consists of wind, wave and current, time history load and response spectrum load. Several combinations of load cases are implementing to the analysis as below:

- I. Free Vibration analysis (FVA)
- II. Dead load (DL) + Live load (LL)
- III. Environmental load (EL)
- IV. Dead load (DL) + Live load (LL) + Environmental load (EL) + Time history load (TH)
- V. Response spectrum (RS)

Furthermore, the results that are expected to acquire from SAP2000 are as:

- I. Modal shape of the wellhead offshore platform
- II. Natural period and natural frequency of wellhead offshore platform
- III. Maximum unity check of all structural member
- IV. Maximum shear and bending moment in the member under various load cases
- V. Joint displacement, velocity, and acceleration under different types of load combination

## 4.2 Wellhead Offshore Modelling

The model of wellhead offshore platform has been performed by using SAP 2000 version 18 shown in Figure 4.1. There are some assumptions and linear properties have been made and used to model the structure:

- I. The geometry, dimension and details of the structure are according to actual structural drawing of wellhead support frame.
- II. Location, material, size, and section used of the offshore structure are represented similarly to the actual structure.
- III. Environmental data from the site location including wind speed, maximum wave height, wave period, current velocity, maximum tide, storm surge.
- IV. The ground motion of Al- Centro Earthquake, 1940.
- V. The support of the structure is assumed to be fixed on the ground instead of piled.

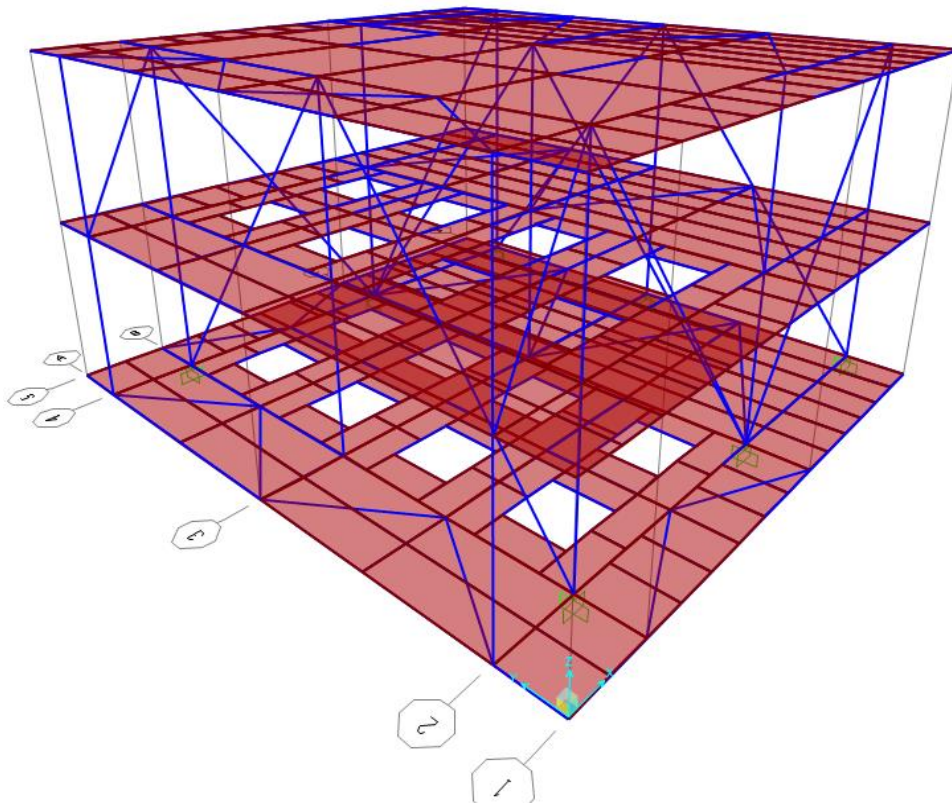


Figure 4.1 3D model of the wellhead support frame

### 4.3 Free Vibration Analysis

Free vibration analysis of the frame has been carried out by only considered the modal in SAP2000 software. It is about the deformed shape of the frame that has set in an initial input for motion and allowed it to vibrate freely. The mode is a standing wave that will affect all the components of the system under a constant frequency. This mode concept is only taken as a general characterization of specific states of oscillation as there is no real system that can perfectly fit under the standing wave framework.

In the analysis, the model number we applied to the frame is up to twelve (12) types of mode shape. The natural frequency, natural period and deformed shape of each modal of the wellhead support frame have been acquired. The summary of the results has been tabulated in Table 4.1 and graph plotted in Figure 4.2. Generally, the mode shape represents the shape that the structure will vibrate in free motion and the same shape tends to dominate the motion of the structure during an earthquake. The first three modes of vibration are the most interest because they usually have the largest contribution to the structure's motion. The natural period of the first mode is the longest and follows by the second mode and third mode. The first three mode shapes are shown in Figure 4.3 (a), (b) and (c) respectively. The grey color lines showed the original shape of the wellhead offshore frame, where the blue color lines showed the deflected shape of the frame. Generally, the result is quite acceptable and logical as the structure is a two story building and its natural frequency should not lesser than 2.5 Hz.

Table 4.1 Modal period and frequencies

<b>Mode</b>	<b>Natural Period, T (sec)</b>	<b>Natural Frequency, f (Hz)</b>
1	0.1060	9.4344
2	0.0878	11.3889
3	0.0776	12.8815
4	0.0767	13.0347
5	0.0752	13.2988
6	0.0720	13.8862
7	0.0717	13.9418
8	0.0652	15.3343
9	0.0607	16.4723
10	0.0605	16.5394
11	0.0596	16.7784
12	0.0593	16.8748

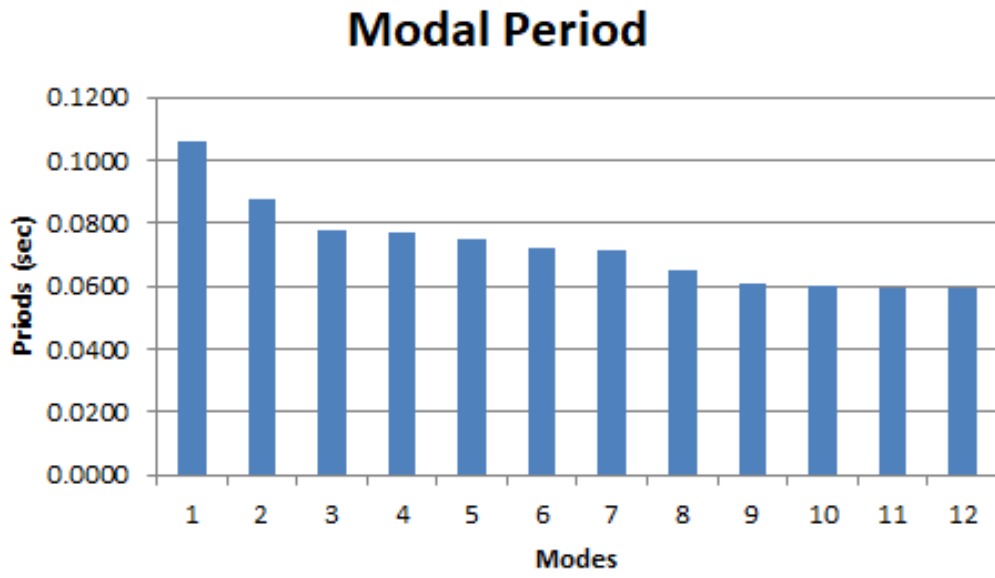
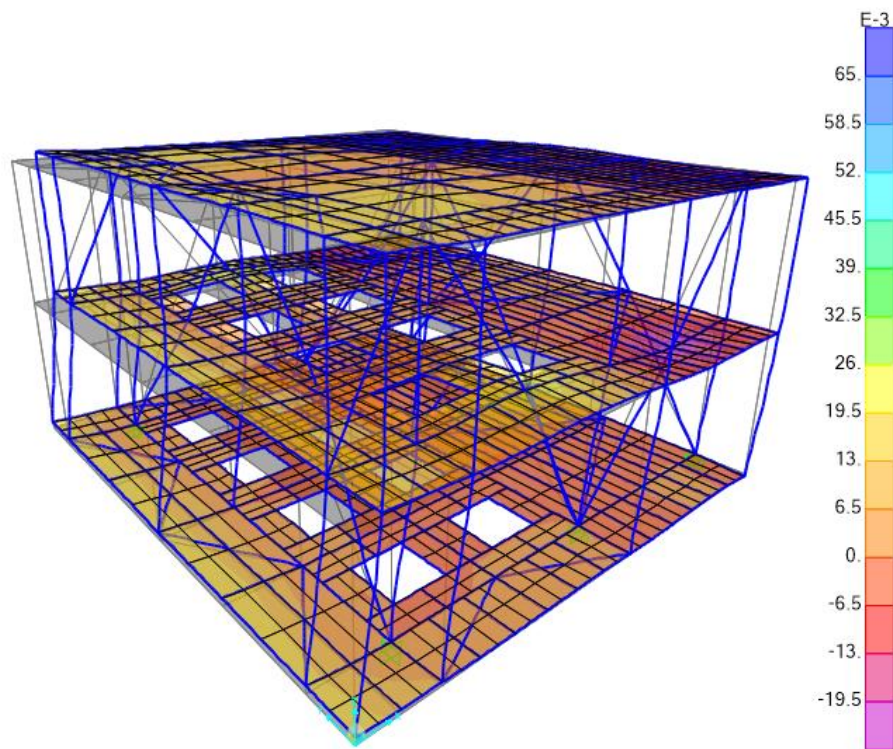
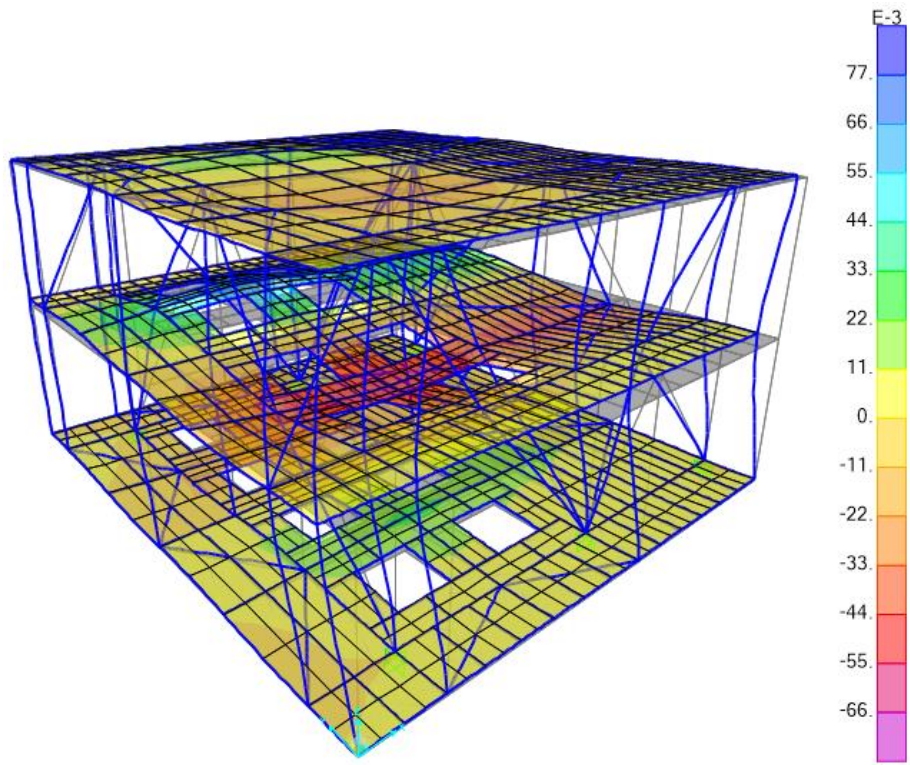


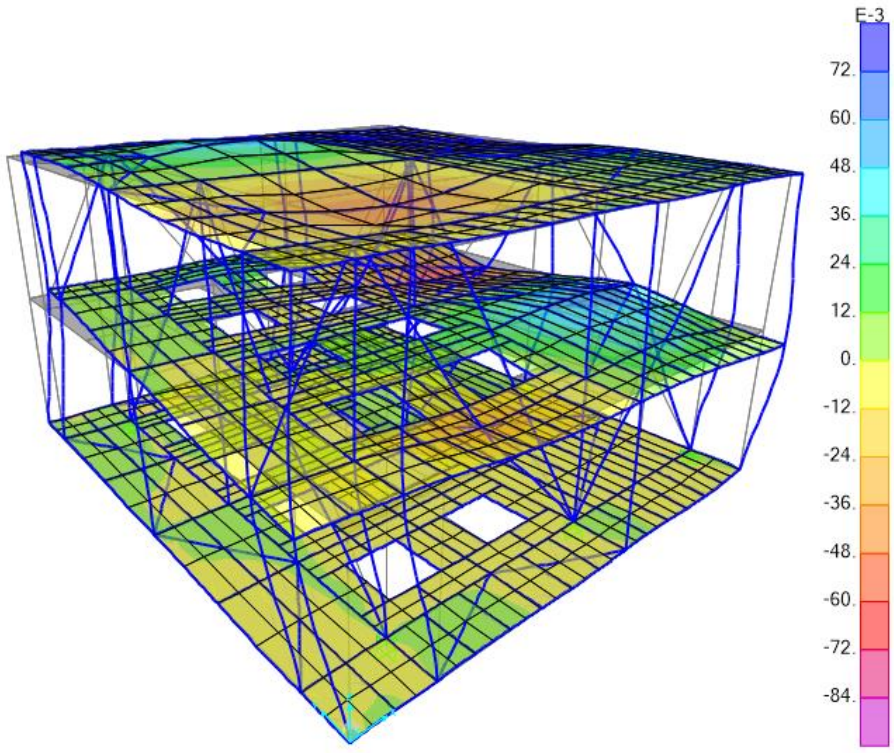
Figure 4.2 Modal periods



(a)



(b)



(c)

Figure 4.3 Three modes of vibration (a) mode shape 1 (0.1060 sec) (b) mode shape 2 (0.0878 sec) (c) mode shape 3 (0.0776 sec)

#### 4.4 Time History Analysis

Time history earthquake analysis has been performed on the wellhead offshore structure by referring to the ground motion of El Centro obtained from the PEER Center. El- Centro Earthquake occurred on May 18, 1941, at Imperial Valley with magnitude 6.9 on the Richter Scale or 0.32g of ground acceleration. Figure 4.3 presented plotted graph of time versus acceleration.

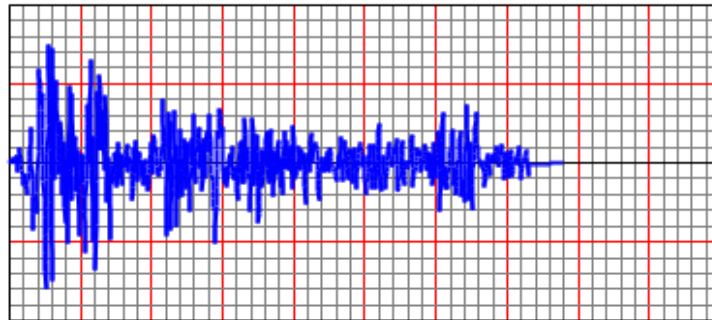
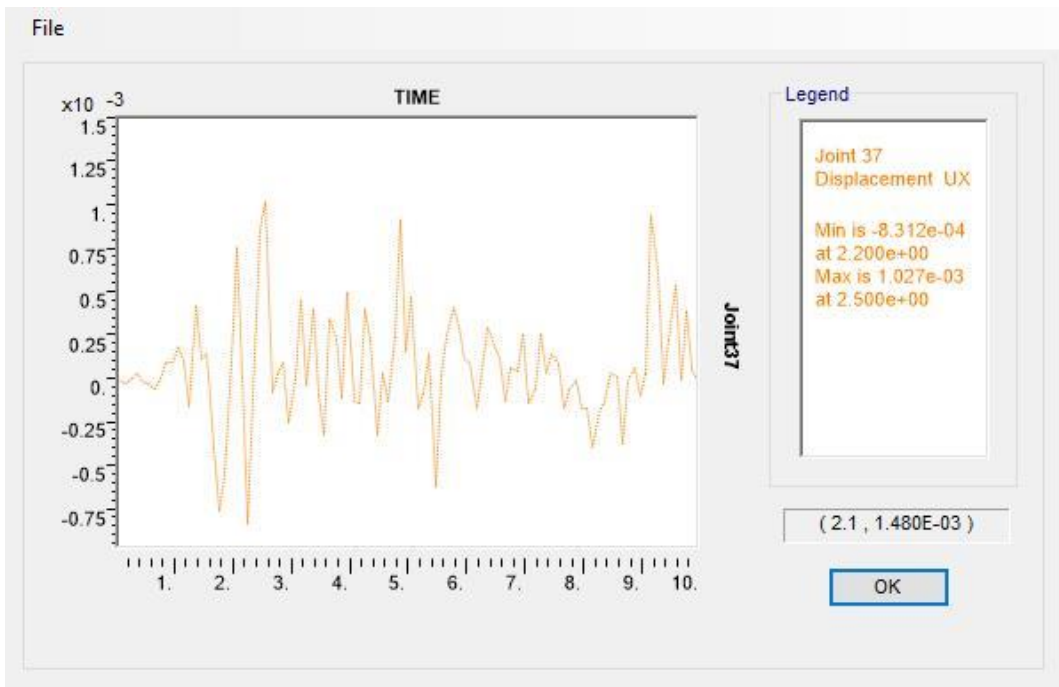


Figure 4.4 Time (sec) versus Acceleration (g)

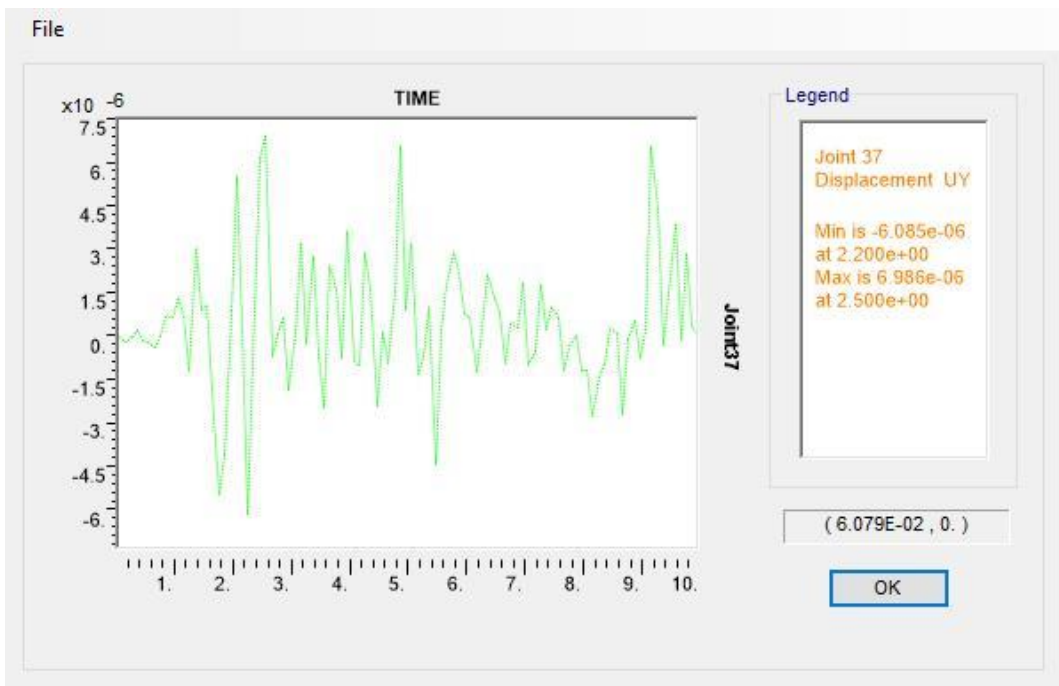
It is used to determine the dynamic response of a structure under the action of any general time-dependent loads. The results obtained from this analysis are time-varying displacements, velocities, and accelerations of the wellhead offshore structure in x, y and z directions under El- Centro Earthquake loading. The most critical part of joint of the structure is joint 37 after analyzed by computational software, SAP2000. The analysis of time history results in different directions are presented in Table 4.2 and graph plotted showed in Figure 4.5 to 4.7. The table presented only the maximum response of the investigated model to the seismic excitation. Basically, all the peak responses occur in x-direction among other directions. The maximum displacement of 0.0010 m occurs at 2.5s; for velocity, the maximum value is 0.028 m/s occurred at 4.9s, and maximum acceleration happened at 2.5s with 1.1220 m/s<sup>2</sup>.

Table 4.2 Time History Displacement, Velocities, and Acceleration of Joint 37 in 3 directions

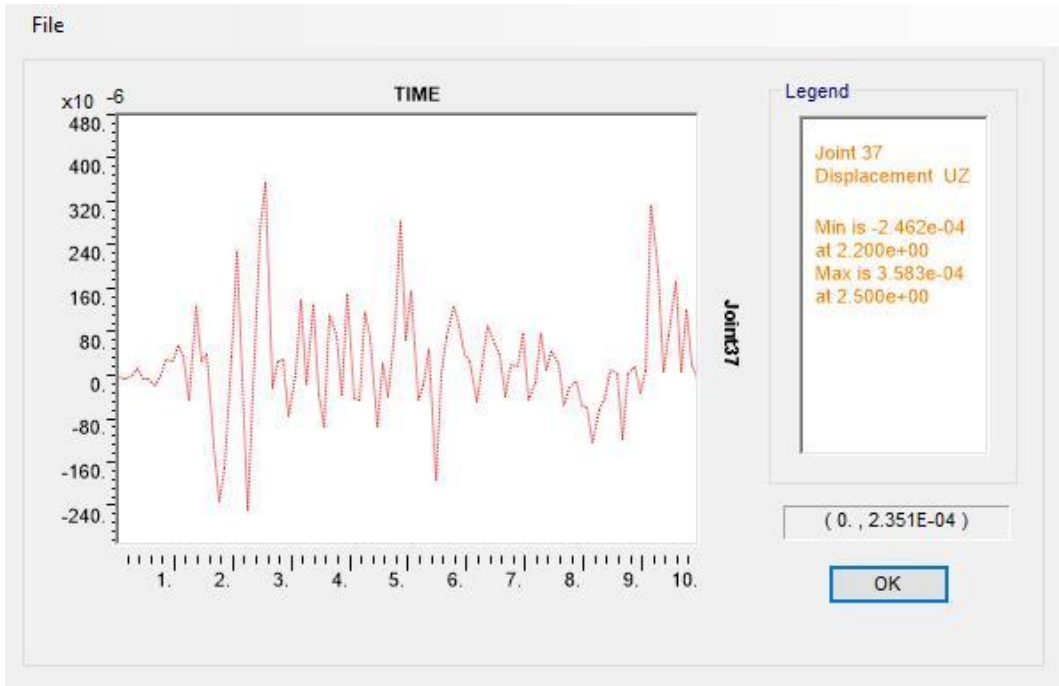
Joint	Direction	Displacement, m		Velocities, m/sec		Accelerations, m/sec <sup>2</sup>	
		Min	Max	Min	Max	Min	Max
37	X	-0.0008	0.0010	-0.0385	0.028	-3.9020	1.1220
37	Y	0.0000	0.0000	-0.0003	0.0002	-0.0259	0.0081
37	Z	-0.0002	0.0004	-0.0122	0.0088	-1.4460	0.3469



(a) x-direction

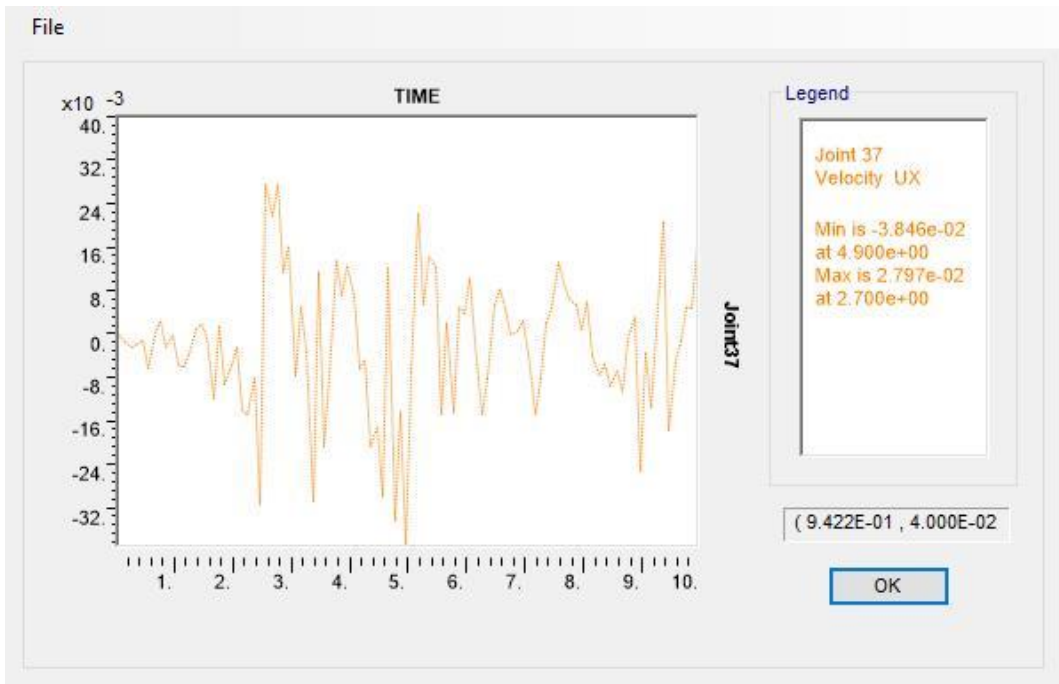


(b) y-direction



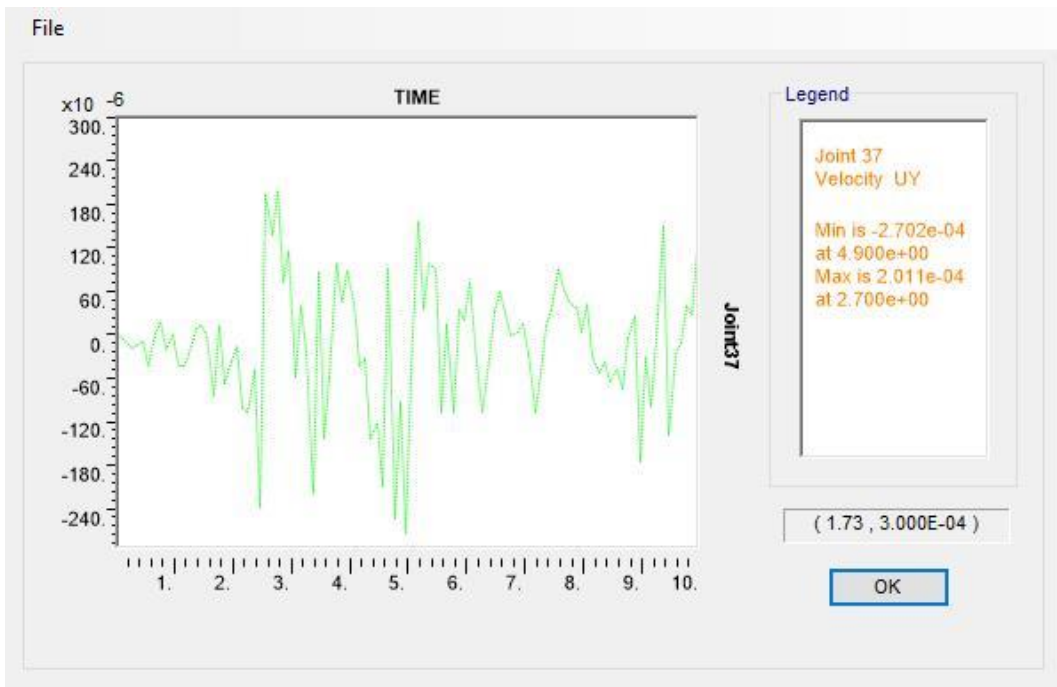
(c) z-direction

Figure 4.5 Comparison of displacement history in x, y and z direction at Joint 37

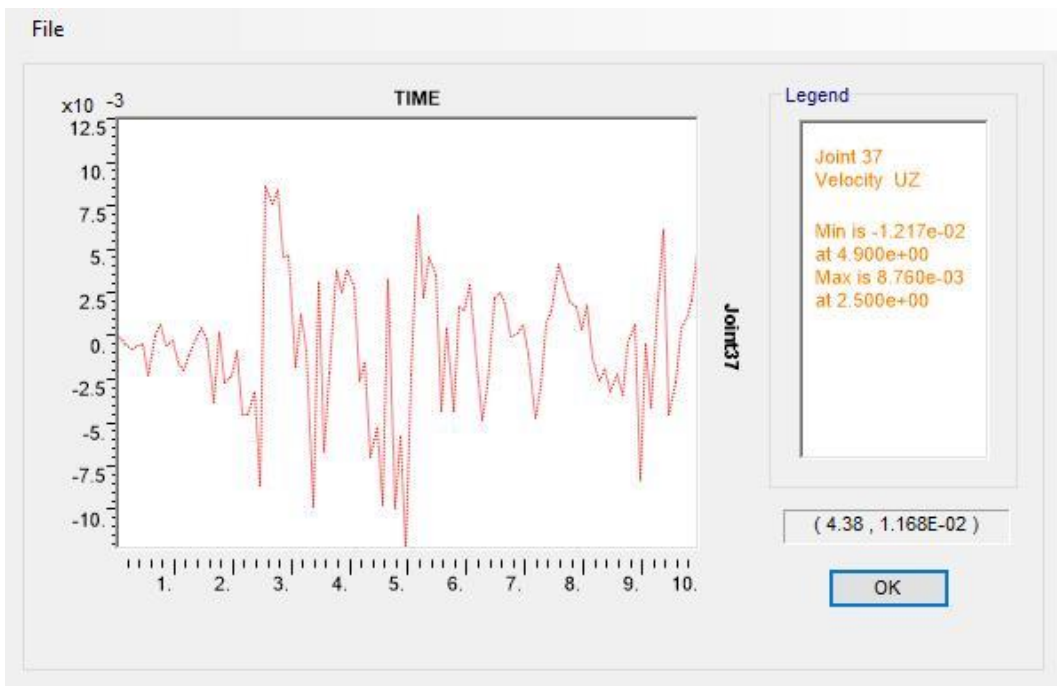


(a) x-direction



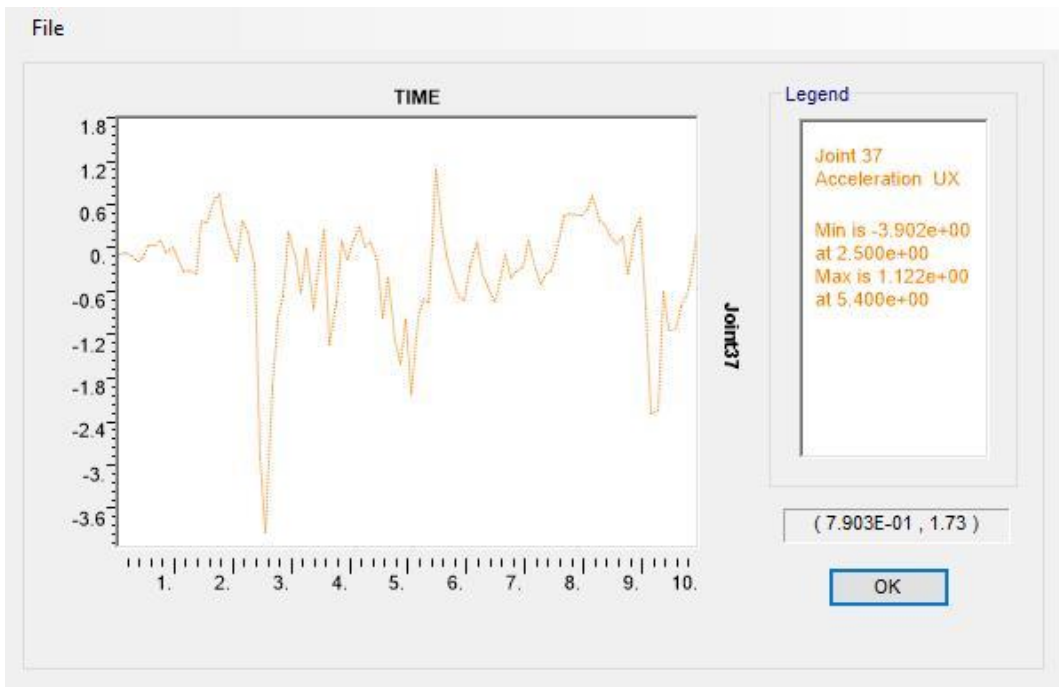


(b) y-direction

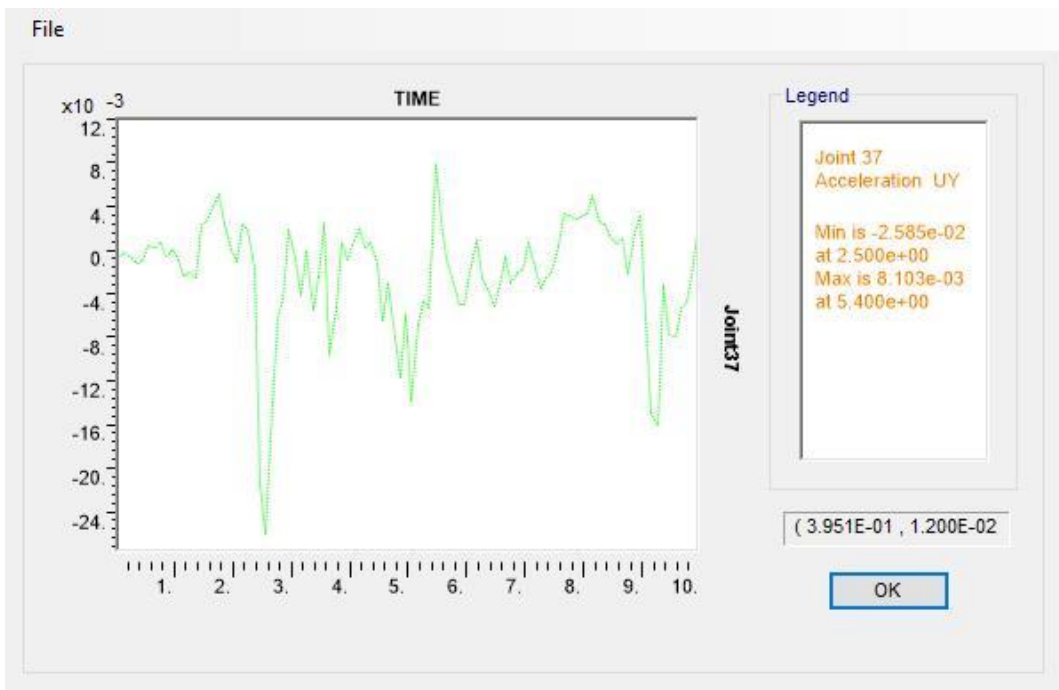


(c) z-direction

Figure 4.6 Comparison of velocity history in x, y and z-direction at Joint 37



(a) x-direction



(b) y-direction



(c) z-direction

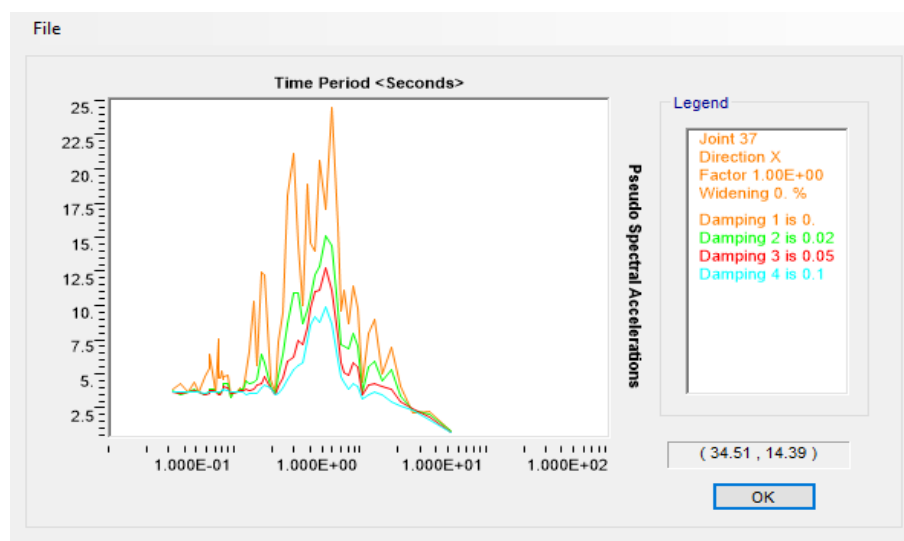
Figure 4.7 Comparison of acceleration history in x, y and z-direction at Joint 37

#### 4.5 Response Spectrum Analysis

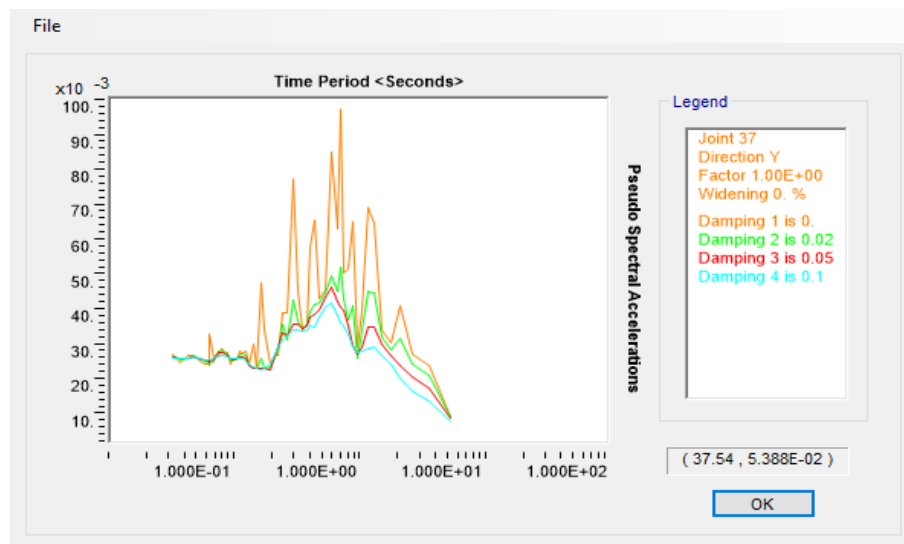
In order to perform the dynamic analysis and design of a structure to be built at a particular location, the actual time history record is required. However, it is not possible to have such records at each and every location. Furthermore, the seismic analysis of structures cannot be simply conducted based on the peak value of the ground acceleration as the response of the structure depends upon the frequency content of ground motion and its own dynamic properties. To solve all these difficulties, earthquake response spectrum is the most famous instrument in the seismic analysis of structures. There are computational advantages in using the response spectrum method of seismic analysis for prediction of displacements and member forces in structural systems. However, the calculation only considered the maximum values of the displacements and member forces in each mode of vibration by using smooth design spectra that are the average of several earthquake motions.

Response spectrum analysis has been performed according to Eurocode 8 2004. The overall response of the system is calculated by combining maximum modal responses specified by one of the mode combination methods (SRSS, CQC, GRP, etc.). Based on results from the modal analysis, Complete Quadratic Combination (CQC)

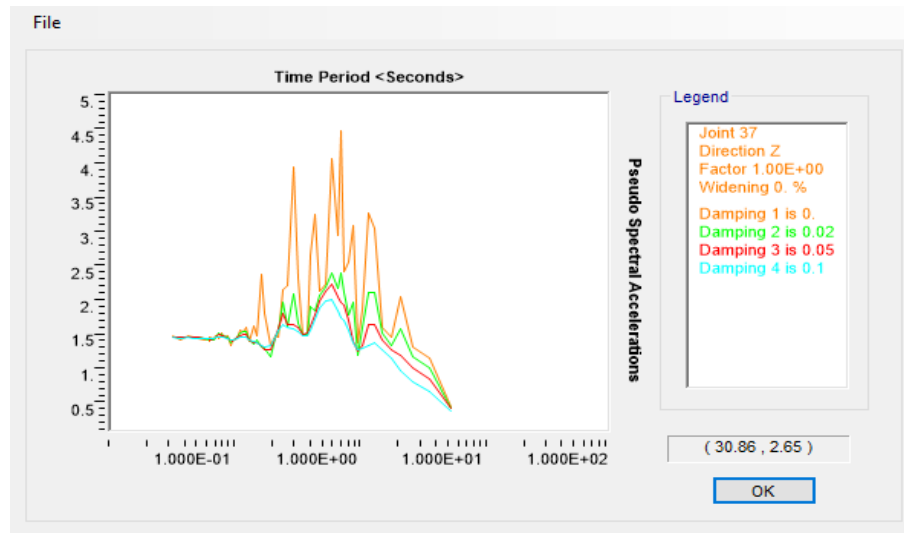
method is applied for the combination of maximum modal responses. CQC method is proposed as it will provide a more accurate result compared to SRSS. According to Xi-Yuan ZHOU, (2004), SRSS method has good accuracy only when the modal frequencies are well separated; while CQC is good in closely spaced modes of oscillation. For directional combination type option, Square Root of Sum of Square (SRSS) option is applied due to horizontal (U1 and U2) are having similar scale factor. The response spectrums with 0%, 2%, 5 % and 10% damping ratio used in spectrum analysis at joint 37 wins three directions are presented in Figure 4.8. Figure 4.8a presented the maximum response of the model to the correspondent response spectrum.



(a) x-direction



(b) y-direction



(c) z-direction

Figure 4.8 Pseudo-Spectral Acceleration in x, y and z-direction at Joint 37

#### 4.6 Linear Analysis

There are several combinations of load cases that been applied in this linear analysis, these consist of combination of dead load (DL) + live load (LL), environmental load (EL), dead load (DL) + live load (LL) + environmental load (EL) + time history load (TH) and response spectrum load (RS). The most critical frame element in this offshore structure has been determined which is frame element 25 with 0.51 unity ratio. Moreover, the results of the various combinations of load case of this frame element have been determined and presented in the table and diagram form. The result and output obtained consist of the shear force diagram and bending moment diagram

Table 4.3 showed the shear force diagrams of four (4) types of different combination of load cases that was applied in this linear analysis. The result of the shear force diagram for the combination of dead load (DL) + live load (LL) linear analysis is shown as below. From the shear force diagram, the maximum shear force is  $-449.44 \text{ kN}$  which happen at the frame element 25. From the maximum shear stress result, shear stress and allowable capacity check have been calculated and tabulated in the table 4.4, which is  $-14\,796.77 \text{ kN/m}^2$  and  $130\,464.21 \text{ kN/m}^2$  respectively.

Moreover, the result of the shear force diagram for the combination of environmental load (EL) also showed as below. Wind load, wave load, and current load

are the load that comprised in this environmental load analysis. From the shear force diagram, the maximum shear force for environmental load analysis is 22.86 *kN* which happen at the frame element 25. From the maximum shear stress result, shear stress and althe lowable capacity check has been calculated and tabulated in the table 4.3, which is 752.64 *kN/m<sup>2</sup>* and 130 464.21 *kN/m<sup>2</sup>* respectively.

For the result of combined load cases of dead load (DL) + live load (LL) + environmental load (EL) + time history load from El Centro (TH) are determined, the shear force diagram has obtained as showed in table 4.2. The maximum shear force of this analysis which happens at the frame element 25 is -427.38 *kN*. From the maximum shear stress result, shear stress and althe lowable capacity check has been calculated and tabulated in the table 4.3, which is -14 070.47 *kN/m<sup>2</sup>* and 130 464.21 *kN/m<sup>2</sup>* respectively.

Lastly, the response spectrum (RS) analysis have been performed, the shear force diagram has been obtained as showed in table 4.2, the maximum shear force of this analysis which happens at the frame element 25 is 9.45 *kN*. From the maximum shear stress result, shear stress and allowable capacity check have been calculated and tabulated in the table 4.3, which is 311.18 *kN/m<sup>2</sup>* and 130 464.21 *kN/m<sup>2</sup>* respectively.

Among all the load combination cases, the biggest shear force and shear stress obtained from the analysis is the load combination with dead loads and live loads (DL+LL) which are -499.44 *kN* and -14 796.77 *kN/m<sup>2</sup>* from SAP2000 respectively. The smallest moment and bending stress are belonging to fourth cases: Response Spectrum, which has only 9.45 *kNm* and 311.18 *kN/m<sup>2</sup>* respectively.

Table 4.3 Shear force diagram for several load combination at element 25

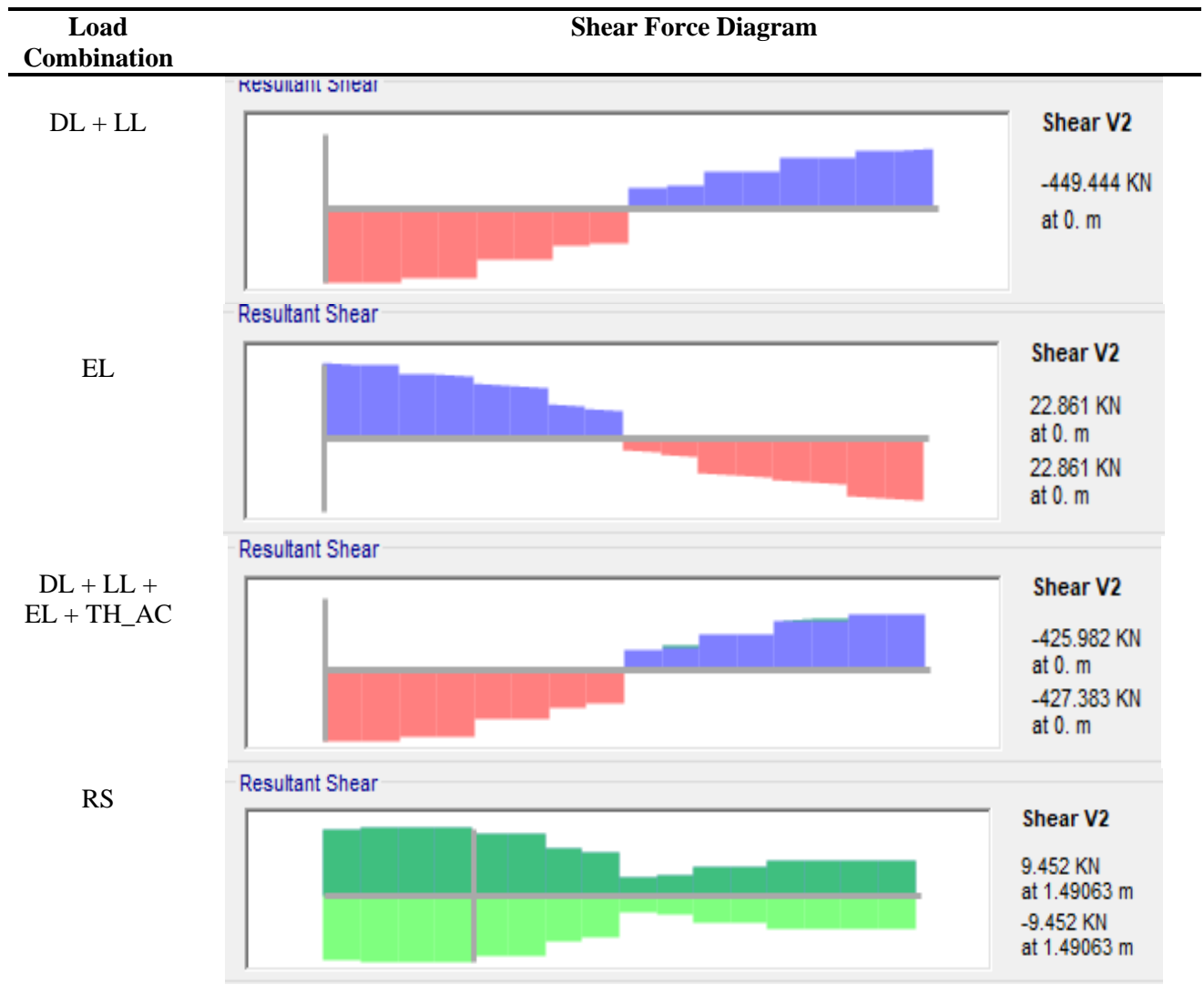


Table 4.4 Shear stress and allowable capacity check for several load combination at element 25

Load Combination	Design shear force, $V_{Ed}$ (kN)	Shear stress, $f_{ive}$ (kN/m <sup>2</sup> )	Allowable shear force, $V_{b, RD}$ (kN)	Allowable shear stress, $F_v$ (kN/m <sup>2</sup> )
DL + LL	-449.44	-14 796.77	3 962.78	130 464.21
EL	22.86	752.64	3 962.78	130 464.21
DL + LL + EL + TH_AC	-427.38	-14 070.47	3 962.78	130 464.21
RS	9.45	311.18	3 962.78	130 464.21

Table 4.4 showed the bending moment diagrams of several combinations of load cases that was applied in this linear analysis. The result of bending moment diagram for the combination of dead load (DL) + live load (LL) linear analysis is shown as below. From the bending moment diagram, the maximum bending moment is -667.58 kNm

which happen at the frame element 25. From the maximum bending moment result, bending stress and the allowable capacity check has been calculated and tabulated in the table 4.5, which are  $-245\,307.52\text{ kN/m}^2$  and  $480\,677.45\text{ kN/m}^2$  respectively.

Moreover, the result of bending moment diagram for the combination of environmental load (EL) also showed as below. Wind load, wave load, and current load are the load that comprises in this environmental load analysis. From the bending moment diagram, the maximum bending moment for environmental load analysis is  $31.93\text{ kNm}$  which happen at the frame element 25. From the maximum bending moment result, bending stress and the allowable capacity check has been calculated and tabulated in the table 4.5, which are  $11\,733.58\text{ kN/m}^2$  and  $480\,677.45\text{ kN/m}^2$  respectively.

For the result of combined load cases of dead load (DL) + live load (LL) + environmental load (EL) + time history load (TH) are determined, the bending moment diagram has obtained as showed in table 4.4. The maximum bending moment of this analysis which happens at the frame element 25 is  $-636.77\text{ kNm}$ . From the maximum bending moment result, bending stress and the allowable capacity check has been calculated and tabulated in the table 4.5, which are  $-233\,986.45\text{ kN/m}^2$  and  $480\,677.45\text{ kN/m}^2$  respectively.

The response spectrum (RS) analysis have been performed, the bending moment diagram has been obtained as showed in table 4.5, the maximum bending moment of this analysis which happens at the frame element 25 is  $14.83\text{ kNm}$ . From the maximum bending moment result, bending stress and the allowable capacity check has been calculated and tabulated in the table 4.6, which are  $5\,448.14\text{ kN/m}^2$  and  $480\,677.45\text{ kN/m}^2$  respectively.

Among all the load combination cases, the biggest bending moment and bending stress obtained from the analysis is the load combination with dead loads and live loads (DL+ LL) which are  $-667.58\text{ kNm}$  and  $-245\,307.52\text{ kN/m}^2$  from SAP2000 respectively. The smallest moment and bending stress are belonging to fourth cases: Response Spectrum, which has only  $14.83\text{ kNm}$  and  $5\,448.14\text{ kN/m}^2$  respectively.



Table 4.5 Bending moment diagram for several load combination at element 25

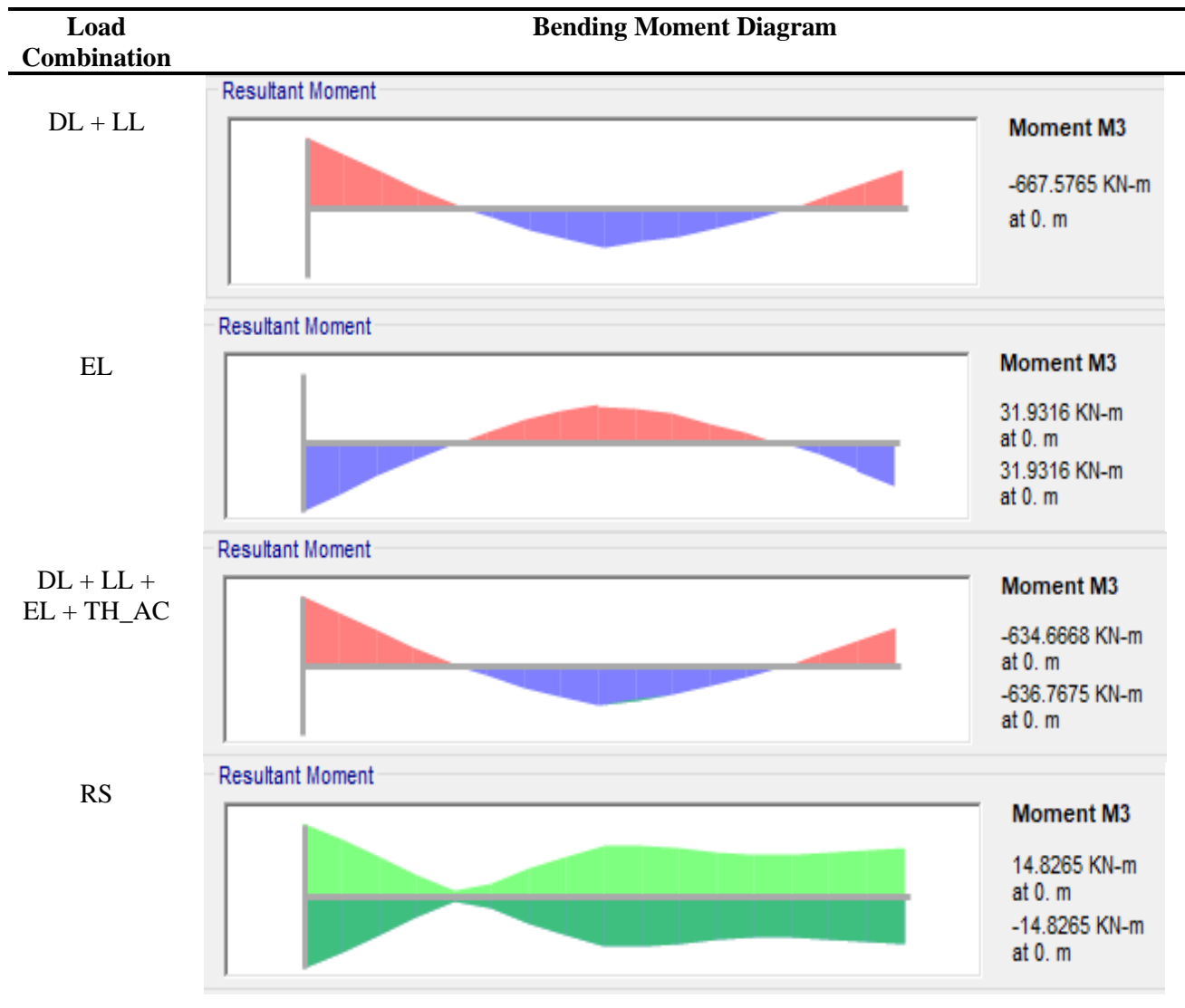


Table 4.6 Bending stress and allowable capacity check for several load combination at element 25

Load Combination	Design moment, $M_{Ed}$ (kNm)	Bending stress, $f_b$ (kN/m <sup>2</sup> )	Allowable bending moment, $M_{b, RD}$ (kNm)	Allowable bending stress, $F_b$ , (kN/m <sup>2</sup> )
DL + LL	-667.58	-245 307.52	1 308.11	480 677.45
EL	31.93	11 733.58	1 308.11	480 677.45
DL + LL + EL + TH_AC	-636.77	-233 986.45	1 308.11	480 677.45
RS	14.83	5 448.14	1 308.11	480 677.45

#### 4.7 Result Comparison of SAP 2000 and Manual Calculation

In order to determine the safest design for our structure, a variety of design analysis options has been considered including manual calculation or computational software calculation. Then, both calculations were compared to indicate that our design is safe and sound and to check if there are any differences between the calculations. For the manual calculations, we only analysed for element 25 (beam) as it is the most critical member in the structure with 4 types of load combination cases including dead load plus live loads (DL + LL), environmental loads (EL), time history loads with dead loads, live loads and environmental loads (DL + LL + EL + TH\_AC), and response spectrum (RS).

Below shown is the comparison of manual calculations and design calculation using SAP2000 ver18. We have checked and compared the final PMM demand/capacity ratios obtained from both manual calculation and SAP2000 calculation. All steel frames are showing passed the stress/ capacity check as the ratio is less than 1 for all load combinations cases as shown in the table below. In the calculation of SAP2000, the most critical ratio of the element in this offshore model is a beam member 25 with 0.51 ratios under the load combination of dead loads and live loads. Compared with manual calculation, the most critical ratio of the member in this offshore model is 0.52 ratios for the same element. The percentages difference is only 1.96% which is the second smallest differences in the comparison. For environmental loads cases, it is the maximum percentages differences between the manual and SAP2000, 25% where 0.025 ratios are from manual calculations and 0.020 for SAP2000. Moreover, both demand/capacity ratios calculations are same for time history combination load which is 0.49. In the end, for response spectrum cases, the differences between both ratio calculations are about 10%.

Based on the comparison between manual calculations and software analysis, the differences might be explained by rounding error made during calculations. For instances, SAP2000 has rounded off the value of plastic modulus,  $W_{pl}$ , and elastic modulus,  $W_{el}$  to 3 decimal places only, while manual calculation is using exact value in the table properties of section based on BS EN 1993-1-1: 2005, which lead to the slightly difference of bending moment resistance, hence ratio will difference a little.

Among all the load combination cases, the biggest ratio obtained from the analysis is the load combination with dead loads and live loads (DL+ LL) which is 0.51 from SAP2000. In short, we are blessed to obtain a safe and stable design for our structure and the results are shown below.

Table 4.7 PMM Demand/Capacity Ratio between manual calculation and SAP2000

Load Combination	Element Design	Frame number	PMM Demand/ Capacity ratio		Percentage Difference, %
			Manual Calculations	SAP2000	
DL + LL	Beam	25	0.520	0.510	1.96
EL	Beam	25	0.025	0.020	25.00
DL + LL + EL + TH_AC	Beam	25	0.490	0.490	0.00
RS	Beam	25	0.011	0.010	10.00

#### 4.8 Summary of Analysis

At the end of the analysis, all elements' unity check has been executed; the final P-M demand/capacity ratios are obtained and displayed in figure 4.8 below. All the analysis and design sections matched for all steel frames and all steel frames passed the stress/capacity check as the maximum ratio is only 0.51 which is less than 1.0. The most critical frame member in this wellhead offshore platform is beam element 25 showed in table 4.8. Deformed shape of the structures for each load case combination also shown in this summary of the analysis.

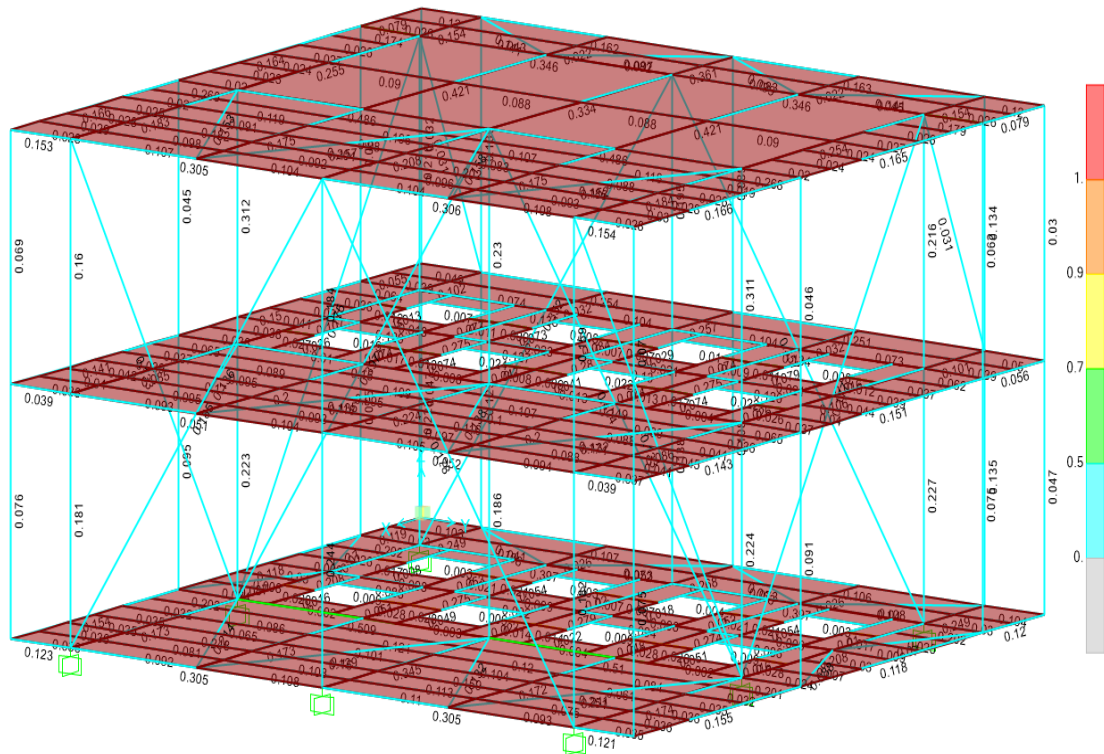


Figure 4.9 PMM Demand/Capacity Ratio of Wellhead Offshore Structure

Table 4.8 Unity Ratio of Structure Member

Frame Number	Design Section	Design Type	Maximum Unity Check	Load Combination
1	Turbular 273d	Beam	0.12	DL + LL + EL + TH_AC
2	Turbular 273d	Beam	0.12	DL + LL + EL + TH_AC
3	Turbular 273d	Beam	0.15	DL + LL
4	Turbular 406d	Beam	0.25	DL + LL
5	Turbular 406d	Beam	0.21	DL + LL
6	Turbular 406d	Beam	0.17	DL + LL
7	Turbular 406d	Beam	0.27	DL + LL
8	Turbular 406d	Beam	0.28	DL + LL
9	Turbular 406d	Beam	0.34	DL + LL
10	Turbular 406d	Beam	0.25	DL + LL
11	Turbular 406d	Beam	0.21	DL + LL
12	Turbular 406d	Beam	0.17	DL + LL
13	Turbular 273d	Beam	0.12	DL + LL + EL + TH_AC
14	Turbular 273d	Beam	0.12	DL + LL + EL + TH_AC
15	Turbular 273d	Beam	0.15	DL + LL
16	Turbular 273d	Beam	0.10	DL + LL
17	Turbular 406d	Beam	0.11	DL + LL
18	Turbular 406d	Beam	0.11	DL + LL
19	Turbular 273d	Beam	0.10	DL + LL
20	Turbular 406d	Beam	0.20	DL + LL
21	Turbular 406d	Beam	0.40	DL + LL
22	Turbular 406d	Beam	0.40	DL + LL
23	Turbular 406d	Beam	0.20	DL + LL

24	Turbular 406d	Beam	0.20	DL + LL
25	Turbular 406d	Beam	0.51	DL + LL
26	Turbular 406d	Beam	0.51	DL + LL
27	Turbular 406d	Beam	0.20	DL + LL
28	Turbular 273d	Beam	0.12	DL + LL + EL + TH_AC
30	Turbular 406d	Beam	0.31	DL + LL
31	Turbular 406d	Beam	0.30	DL + LL
32	Turbular 273d	Beam	0.12	DL + LL + EL + TH_AC
29	Turbular 273d	Beam	0.06	DL + LL + EL + TH_AC
33	Turbular 273d	Beam	0.15	DL + LL
34	Turbular 273d	Beam	0.14	DL + LL + EL + TH_AC
35	Turbular 406d	Beam	0.10	DL + LL
37	Turbular 406d	Beam	0.09	DL + LL + EL + TH_AC
38	Turbular 406d	Beam	0.26	DL + LL
39	Turbular 406d	Beam	0.28	DL + LL
40	Turbular 406d	Beam	0.22	DL + LL + EL + TH_AC
41	Turbular 406d	Beam	0.10	DL + LL
42	Turbular 406d	Beam	0.11	DL + LL + EL + TH_AC
43	Turbular 406d	Beam	0.09	DL + LL + EL + TH_AC
44	Turbular 273d	Beam	0.06	DL + LL + EL + TH_AC
45	Turbular 273d	Beam	0.15	DL + LL
46	Turbular 273d	Beam	0.14	DL + LL + EL + TH_AC
47	Turbular 273d	Beam	0.05	DL + LL + EL + TH_AC
48	Turbular 273d	Beam	0.25	DL + LL
49	Turbular 273d	Beam	0.25	DL + LL
50	Turbular 273d	Beam	0.05	DL + LL + EL + TH_AC
51	Turbular 406d	Beam	0.06	DL + LL
52	Turbular 406d	Beam	0.13	DL + LL
53	Turbular 406d	Beam	0.13	DL + LL
54	Turbular 406d	Beam	0.06	DL + LL + EL + TH_AC
55	Turbular 406d	Beam	0.06	DL + LL
56	Turbular 406d	Beam	0.15	DL + LL
57	Turbular 406d	Beam	0.15	DL + LL
58	Turbular 406d	Beam	0.06	DL + LL
59	Turbular 406d	Beam	0.04	DL + LL
60	Turbular 406d	Beam	0.05	DL + LL
61	Turbular 406d	Beam	0.05	DL + LL
62	Turbular 406d	Beam	0.04	DL + LL
63	Turbular 273d	Beam	0.08	DL + LL
64	Turbular 273d	Beam	0.16	DL + LL
65	Turbular 273d	Beam	0.17	DL + LL + EL + TH_AC
66	Turbular 406d	Beam	0.15	DL + LL
67	Turbular 406d	Beam	0.25	DL + LL
68	Turbular 406d	Beam	0.18	DL + LL + EL + TH_AC
69	Turbular 406d	Beam	0.36	DL + LL
70	Turbular 406d	Beam	0.33	DL + LL
71	Turbular 406d	Beam	0.21	DL + LL
72	Turbular 406d	Beam	0.15	DL + LL
73	Turbular 406d	Beam	0.25	DL + LL
74	Turbular 406d	Beam	0.18	DL + LL + EL + TH_AC
75	Turbular 273d	Beam	0.08	DL + LL
76	Turbular 273d	Beam	0.16	DL + LL
77	Turbular 273d	Beam	0.17	DL + LL + EL + TH_AC
78	Turbular 273d	Beam	0.12	DL + LL
79	Turbular 273d	Beam	0.16	DL + LL

80	Turbular 273d	Beam	0.16	DL + LL
81	Turbular 273d	Beam	0.12	DL + LL
82	Turbular 406d	Beam	0.18	DL + LL + EL + TH_AC
83	Turbular 406d	Beam	0.35	DL + LL
84	Turbular 406d	Beam	0.35	DL + LL
85	Turbular 406d	Beam	0.17	DL + LL + EL + TH_AC
86	Turbular 406d	Beam	0.27	DL + LL
87	Turbular 406d	Beam	0.49	DL + LL
88	Turbular 406d	Beam	0.49	DL + LL
89	Turbular 406d	Beam	0.27	DL + LL
90	Turbular 406d	Beam	0.15	DL + LL
91	Turbular 406d	Beam	0.31	DL + LL
92	Turbular 406d	Beam	0.31	DL + LL
93	Turbular 406d	Beam	0.15	DL + LL
94	Turbular 406d	Column	0.03	DL + LL + EL + TH_AC
95	Turbular 406d	Column	0.06	DL + LL + EL + TH_AC
96	Turbular 406d	Column	0.07	DL + LL
97	Turbular 406d	Column	0.04	DL + LL + EL + TH_AC
98	Turbular 406d	Column	0.08	DL + LL + EL + TH_AC
99	Turbular 406d	Column	0.09	DL + LL + EL + TH_AC
100	Turbular 406d	Column	0.07	DL + LL
101	Turbular 406d	Column	0.05	DL + LL + EL + TH_AC
102	Turbular 406d	Column	0.14	DL + LL + EL + TH_AC
103	Turbular 406d	Column	0.22	DL + LL
104	Turbular 406d	Column	0.16	DL + LL + EL + TH_AC
105	Turbular 406d	Column	0.31	DL + LL
106	Turbular 406d	Column	0.18	DL + LL + EL + TH_AC
107	Turbular 406d	Column	0.22	DL + LL + EL + TH_AC
108	Turbular 406d	Column	0.23	DL + LL + EL + TH_AC
109	Turbular 406d	Column	0.13	DL + LL + EL + TH_AC
118	Turbular 406d	Column	0.09	DL + LL
119	Turbular 406d	Column	0.19	DL + LL + EL + TH_AC
120	Turbular 406d	Column	0.18	DL + LL
121	Turbular 406d	Column	0.23	DL + LL
122	Turbular 406d	Column	0.24	DL + LL + EL + TH_AC
123	Turbular 406d	Column	0.19	DL + LL + EL + TH_AC
124	Turbular 406d	Column	0.14	DL + LL + EL + TH_AC
125	Turbular 406d	Column	0.11	DL + LL + EL + TH_AC
126	Turbular 406d	Column	0.13	DL + LL
127	Turbular 406d	Column	0.22	DL + LL
128	Turbular 406d	Column	0.16	DL + LL + EL + TH_AC
129	Turbular 406d	Column	0.31	DL + LL
130	Turbular 406d	Column	0.18	DL + LL + EL + TH_AC
131	Turbular 406d	Column	0.22	DL + LL + EL + TH_AC
132	Turbular 406d	Column	0.23	DL + LL + EL + TH_AC
133	Turbular 406d	Column	0.13	DL + LL + EL + TH_AC
134	Turbular 406d	Column	0.03	DL + LL + EL + TH_AC
135	Turbular 406d	Column	0.06	DL + LL + EL + TH_AC
136	Turbular 406d	Column	0.07	DL + LL
137	Turbular 406d	Column	0.05	DL + LL + EL + TH_AC
138	Turbular 406d	Column	0.07	DL + LL + EL + TH_AC
139	Turbular 406d	Column	0.09	DL + LL + EL + TH_AC
140	Turbular 406d	Column	0.07	DL + LL
141	Turbular 406d	Column	0.05	DL + LL + EL + TH_AC
156	Turbular 406d	Beam	0.11	DL + LL + EL + TH_AC

163	Turbular 406d	Brace	0.03	DL + LL + EL + TH_AC
164	Turbular 406d	Brace	0.17	DL + LL + EL + TH_AC
165	Turbular 406d	Brace	0.13	DL + LL + EL + TH_AC
166	Turbular 406d	Brace	0.03	DL + LL + EL + TH_AC
167	Turbular 406d	Brace	0.18	DL + LL + EL + TH_AC
168	Turbular 406d	Brace	0.13	DL + LL + EL + TH_AC
173	Turbular 406d	Brace	0.35	DL + LL
174	Turbular 406d	Brace	0.36	DL + LL + EL + TH_AC
175	Turbular 406d	Brace	0.40	DL + LL
176	Turbular 406d	Brace	0.40	DL + LL
177	Turbular 406d	Brace	0.18	DL + LL + EL + TH_AC
178	Turbular 406d	Brace	0.18	DL + LL + EL + TH_AC
36	Turbular 406d	Beam	0.03	DL + LL + EL + TH_AC
110	Turbular 406d	Beam	0.27	DL + LL
111	Turbular 406d	Beam	0.17	DL + LL
112	Turbular 406d	Beam	0.17	DL + LL
113	Turbular 406d	Beam	0.28	DL + LL
114	Turbular 406d	Beam	0.03	DL + LL + EL + TH_AC
115	Turbular 168d	Beam	0.03	DL + LL + EL + TH_AC
116	Turbular 168d	Beam	0.03	DL + LL + EL + TH_AC
117	Turbular 168d	Beam	0.04	DL + LL
142	Turbular 168d	Beam	0.07	DL + LL
143	Turbular 168d	Beam	0.07	DL + LL
144	Turbular 168d	Beam	0.04	DL + LL
145	Turbular 168d	Beam	0.02	DL + LL + EL + TH_AC
146	Turbular 168d	Beam	0.01	DL + LL + EL + TH_AC
147	Turbular 168d	Beam	0.03	DL + LL + EL + TH_AC
148	Turbular 168d	Beam	0.01	DL + LL + EL + TH_AC
149	Turbular 168d	Beam	0.02	DL + LL
150	Turbular 168d	Beam	0.03	DL + LL + EL + TH_AC
151	Turbular 168d	Beam	0.03	DL + LL + EL + TH_AC
152	Turbular 168d	Beam	0.04	DL + LL + EL + TH_AC
153	Turbular 168d	Beam	0.04	DL + LL
154	Turbular 168d	Beam	0.04	DL + LL
155	Turbular 168d	Beam	0.08	DL + LL + EL + TH_AC
157	Turbular 168d	Beam	0.06	DL + LL + EL + TH_AC
158	Turbular 168d	Beam	0.25	DL + LL
159	Turbular 168d	Beam	0.08	DL + LL
160	Turbular 168d	Beam	0.09	DL + LL
161	Turbular 168d	Beam	0.12	DL + LL
162	Turbular 168d	Beam	0.10	DL + LL
169	Turbular 168d	Beam	0.16	DL + LL
170	Turbular 168d	Beam	0.11	DL + LL
171	Turbular 168d	Beam	0.11	DL + LL
172	Turbular 168d	Beam	0.12	DL + LL
179	Turbular 168d	Beam	0.10	DL + LL
180	Turbular 168d	Beam	0.16	DL + LL
181	Turbular 168d	Beam	0.11	DL + LL
182	Turbular 168d	Beam	0.11	DL + LL
183	Turbular 168d	Beam	0.09	DL + LL + EL + TH_AC
184	Turbular 168d	Beam	0.06	DL + LL + EL + TH_AC
185	Turbular 168d	Beam	0.25	DL + LL
186	Turbular 168d	Beam	0.08	DL + LL
187	Turbular 168d	Beam	0.09	DL + LL
188	Turbular 168d	Beam	0.03	DL + LL + EL + TH_AC

189	Turbular 168d	Beam	0.03	DL + LL + EL + TH_AC
190	Turbular 168d	Beam	0.04	DL + LL + EL + TH_AC
191	Turbular 168d	Beam	0.04	DL + LL + EL + TH_AC
192	Turbular 168d	Beam	0.04	DL + LL + EL + TH_AC
193	Turbular 168d	Beam	0.03	DL + LL + EL + TH_AC
194	Turbular 168d	Beam	0.01	DL + LL + EL + TH_AC
195	Turbular 168d	Beam	0.03	DL + LL + EL + TH_AC
196	Turbular 168d	Beam	0.01	DL + LL + EL + TH_AC
197	Turbular 168d	Beam	0.02	DL + LL
198	Turbular 406d	Beam	0.21	DL + LL
199	Turbular 406d	Beam	0.13	DL + LL
200	Turbular 406d	Beam	0.13	DL + LL
201	Turbular 406d	Beam	0.21	DL + LL
202	Turbular 406d	Beam	0.09	DL + LL
203	Turbular 406d	Beam	0.09	DL + LL
204	Turbular 406d	Beam	0.09	DL + LL
205	Turbular 406d	Beam	0.09	DL + LL
206	Turbular 406d	Beam	0.03	DL + LL
207	Turbular 406d	Beam	0.27	DL + LL
208	Turbular 406d	Beam	0.20	DL + LL
209	Turbular 406d	Beam	0.20	DL + LL
210	Turbular 406d	Beam	0.27	DL + LL
211	Turbular 406d	Beam	0.03	DL + LL
212	Turbular 168d	Beam	0.04	DL + LL
213	Turbular 168d	Beam	0.04	DL + LL
214	Turbular 168d	Beam	0.07	DL + LL + EL + TH_AC
215	Turbular 168d	Beam	0.10	DL + LL + EL + TH_AC
216	Turbular 168d	Beam	0.10	DL + LL + EL + TH_AC
217	Turbular 168d	Beam	0.07	DL + LL + EL + TH_AC
218	Turbular 168d	Beam	0.04	DL + LL
219	Turbular 168d	Beam	0.04	DL + LL + EL + TH_AC
220	Turbular 168d	Beam	0.04	DL + LL + EL + TH_AC
221	Turbular 168d	Beam	0.04	DL + LL + EL + TH_AC
222	Turbular 168d	Beam	0.04	DL + LL + EL + TH_AC
223	Turbular 168d	Beam	0.04	DL + LL + EL + TH_AC
224	Turbular 168d	Beam	0.04	DL + LL + EL + TH_AC
225	Turbular 168d	Beam	0.05	DL + LL
226	Turbular 168d	Beam	0.04	DL + LL
227	Turbular 168d	Beam	0.04	DL + LL + EL + TH_AC
228	Turbular 168d	Beam	0.09	DL + LL + EL + TH_AC
229	Turbular 168d	Beam	0.09	DL + LL
230	Turbular 168d	Beam	0.17	DL + LL
231	Turbular 168d	Beam	0.09	DL + LL
232	Turbular 168d	Beam	0.09	DL + LL
233	Turbular 168d	Beam	0.11	DL + LL + EL + TH_AC
234	Turbular 168d	Beam	0.10	DL + LL
235	Turbular 168d	Beam	0.12	DL + LL + EL + TH_AC
236	Turbular 168d	Beam	0.10	DL + LL
237	Turbular 168d	Beam	0.11	DL + LL
238	Turbular 168d	Beam	0.11	DL + LL + EL + TH_AC
239	Turbular 168d	Beam	0.10	DL + LL
240	Turbular 168d	Beam	0.12	DL + LL + EL + TH_AC
241	Turbular 168d	Beam	0.09	DL + LL
242	Turbular 168d	Beam	0.10	DL + LL
243	Turbular 168d	Beam	0.09	DL + LL + EL + TH_AC



244	Turbular 168d	Beam	0.09	DL + LL
245	Turbular 168d	Beam	0.17	DL + LL
246	Turbular 168d	Beam	0.10	DL + LL
247	Turbular 168d	Beam	0.09	DL + LL
248	Turbular 168d	Beam	0.04	DL + LL + EL + TH_AC
249	Turbular 168d	Beam	0.04	DL + LL + EL + TH_AC
250	Turbular 168d	Beam	0.04	DL + LL
251	Turbular 168d	Beam	0.04	DL + LL + EL + TH_AC
252	Turbular 168d	Beam	0.04	DL + LL + EL + TH_AC
253	Turbular 168d	Beam	0.04	DL + LL
254	Turbular 168d	Beam	0.04	DL + LL + EL + TH_AC
255	Turbular 168d	Beam	0.04	DL + LL + EL + TH_AC
256	Turbular 168d	Beam	0.04	DL + LL + EL + TH_AC
257	Turbular 168d	Beam	0.04	DL + LL
258	Turbular 406d	Beam	0.13	DL + LL
259	Turbular 406d	Beam	0.14	DL + LL
260	Turbular 406d	Beam	0.13	DL + LL
261	Turbular 406d	Beam	0.14	DL + LL
262	Turbular 273d	Beam	0.13	DL + LL
263	Turbular 273d	Beam	0.13	DL + LL
264	Turbular 273d	Beam	0.13	DL + LL
265	Turbular 273d	Beam	0.13	DL + LL
266	Turbular 406d	Beam	0.02	DL + LL
267	Turbular 406d	Beam	0.42	DL + LL
268	Turbular 406d	Beam	0.18	DL + LL
269	Turbular 406d	Beam	0.18	DL + LL
270	Turbular 406d	Beam	0.42	DL + LL
271	Turbular 406d	Beam	0.02	DL + LL
272	Turbular 168d	Beam	0.03	DL + LL + EL + TH_AC
273	Turbular 168d	Beam	0.03	DL + LL + EL + TH_AC
274	Turbular 168d	Beam	0.04	DL + LL + EL + TH_AC
275	Turbular 168d	Beam	0.08	DL + LL
276	Turbular 168d	Beam	0.08	DL + LL
277	Turbular 168d	Beam	0.04	DL + LL
278	Turbular 168d	Beam	0.03	DL + LL + EL + TH_AC
279	Turbular 168d	Beam	0.03	DL + LL + EL + TH_AC
280	Turbular 168d	Beam	0.02	DL + LL + EL + TH_AC
281	Turbular 168d	Beam	0.02	DL + LL + EL + TH_AC
282	Turbular 168d	Beam	0.02	DL + LL + EL + TH_AC
283	Turbular 168d	Beam	0.02	DL + LL + EL + TH_AC
284	Turbular 168d	Beam	0.03	DL + LL + EL + TH_AC
285	Turbular 168d	Beam	0.03	DL + LL + EL + TH_AC
286	Turbular 168d	Beam	0.03	DL + LL + EL + TH_AC
287	Turbular 168d	Beam	0.03	DL + LL + EL + TH_AC
288	Turbular 168d	Beam	0.12	DL + LL
289	Turbular 168d	Beam	0.09	DL + LL
290	Turbular 168d	Beam	0.18	DL + LL
291	Turbular 168d	Beam	0.09	DL + LL
292	Turbular 168d	Beam	0.11	DL + LL + EL + TH_AC
293	Turbular 168d	Beam	0.11	DL + LL
294	Turbular 168d	Beam	0.08	DL + LL
295	Turbular 168d	Beam	0.20	DL + LL
296	Turbular 168d	Beam	0.10	DL + LL
297	Turbular 168d	Beam	0.10	DL + LL
298	Turbular 168d	Beam	0.11	DL + LL

299	Turbular 168d	Beam	0.08	DL + LL
300	Turbular 168d	Beam	0.20	DL + LL
301	Turbular 168d	Beam	0.09	DL + LL
302	Turbular 168d	Beam	0.10	DL + LL
303	Turbular 168d	Beam	0.12	DL + LL
304	Turbular 168d	Beam	0.09	DL + LL
305	Turbular 168d	Beam	0.18	DL + LL
306	Turbular 168d	Beam	0.10	DL + LL
307	Turbular 168d	Beam	0.11	DL + LL + EL + TH_AC
308	Turbular 168d	Beam	0.02	DL + LL + EL + TH_AC
309	Turbular 168d	Beam	0.03	DL + LL + EL + TH_AC
310	Turbular 168d	Beam	0.03	DL + LL + EL + TH_AC
311	Turbular 168d	Beam	0.03	DL + LL + EL + TH_AC
312	Turbular 168d	Beam	0.03	DL + LL + EL + TH_AC
313	Turbular 168d	Beam	0.03	DL + LL + EL + TH_AC
314	Turbular 168d	Beam	0.03	DL + LL + EL + TH_AC
315	Turbular 168d	Beam	0.02	DL + LL + EL + TH_AC
316	Turbular 168d	Beam	0.02	DL + LL + EL + TH_AC
317	Turbular 168d	Beam	0.02	DL + LL + EL + TH_AC
318	Turbular 406d	Beam	0.15	DL + LL
319	Turbular 406d	Beam	0.16	DL + LL
320	Turbular 406d	Beam	0.16	DL + LL
321	Turbular 406d	Beam	0.15	DL + LL
322	Turbular 406d	Beam	0.09	DL + LL
323	Turbular 406d	Beam	0.09	DL + LL
324	Turbular 406d	Beam	0.09	DL + LL
325	Turbular 406d	Beam	0.09	DL + LL
326	Turbular 406d	Beam	0.11	DL + LL
327	Turbular 406d	Beam	0.05	DL + LL
328	Turbular 406d	Beam	0.05	DL + LL
329	Turbular 406d	Beam	0.11	DL + LL
330	Turbular 406d	Beam	0.14	DL + LL
331	Turbular 406d	Beam	0.10	DL + LL + EL + TH_AC
332	Turbular 406d	Beam	0.10	DL + LL + EL + TH_AC
333	Turbular 406d	Beam	0.14	DL + LL
411	Turbular 406d	Beam	0.07	DL + LL
412	Turbular 406d	Beam	0.09	DL + LL + EL + TH_AC
413	Turbular 406d	Beam	0.07	DL + LL
414	Turbular 406d	Beam	0.09	DL + LL + EL + TH_AC
340	Turbular 406d	Beam	0.05	DL + LL
342	Turbular 406d	Beam	0.01	DL + LL
343	Turbular 406d	Beam	0.05	DL + LL
345	Turbular 406d	Beam	0.02	DL + LL
346	Turbular 406d	Beam	0.02	DL + LL + EL + TH_AC
348	Turbular 406d	Beam	0.05	DL + LL
349	Turbular 406d	Beam	0.02	DL + LL
351	Turbular 406d	Beam	0.05	DL + LL
352	Turbular 406d	Beam	0.05	DL + LL
354	Turbular 406d	Beam	0.02	DL + LL + EL + TH_AC
355	Turbular 406d	Beam	0.05	DL + LL
357	Turbular 406d	Beam	0.02	DL + LL
358	Turbular 406d	Beam	0.01	DL + LL
360	Turbular 406d	Beam	0.05	DL + LL
364	Turbular 406d	Beam	0.02	DL + LL
366	Turbular 406d	Beam	0.05	DL + LL

367	Turbular 406d	Beam	0.02	DL + LL + EL + TH_AC
368	Turbular 406d	Beam	0.03	DL + LL + EL + TH_AC
369	Turbular 406d	Beam	0.02	DL + LL + EL + TH_AC
370	Turbular 406d	Beam	0.03	DL + LL + EL + TH_AC
371	Turbular 406d	Beam	0.02	DL + LL + EL + TH_AC
372	Turbular 406d	Beam	0.03	DL + LL + EL + TH_AC
373	Turbular 406d	Beam	0.01	DL + LL + EL + TH_AC
374	Turbular 406d	Beam	0.01	DL + LL + EL + TH_AC
375	Turbular 406d	Beam	0.01	DL + LL + EL + TH_AC
376	Turbular 406d	Beam	0.01	DL + LL + EL + TH_AC
377	Turbular 406d	Beam	0.02	DL + LL + EL + TH_AC
378	Turbular 406d	Beam	0.03	DL + LL + EL + TH_AC
379	Turbular 406d	Beam	0.02	DL + LL + EL + TH_AC
380	Turbular 406d	Beam	0.03	DL + LL + EL + TH_AC
383	Turbular 406d	Beam	0.02	DL + LL + EL + TH_AC
384	Turbular 406d	Beam	0.03	DL + LL + EL + TH_AC
385	Turbular 406d	Beam	0.00	DL + LL + EL + TH_AC
387	Turbular 406d	Beam	0.01	DL + LL + EL + TH_AC
388	Turbular 406d	Beam	0.01	DL + LL + EL + TH_AC
390	Turbular 406d	Beam	0.00	DL + LL + EL + TH_AC
391	Turbular 406d	Beam	0.00	DL + LL + EL + TH_AC
393	Turbular 406d	Beam	0.01	DL + LL + EL + TH_AC
394	Turbular 406d	Beam	0.01	DL + LL + EL + TH_AC
396	Turbular 406d	Beam	0.00	DL + LL + EL + TH_AC
397	Turbular 406d	Beam	0.00	DL + LL + EL + TH_AC
399	Turbular 406d	Beam	0.01	DL + LL + EL + TH_AC
400	Turbular 406d	Beam	0.01	DL + LL + EL + TH_AC
402	Turbular 406d	Beam	0.00	DL + LL + EL + TH_AC
403	Turbular 406d	Beam	0.00	DL + LL + EL + TH_AC
405	Turbular 406d	Beam	0.01	DL + LL + EL + TH_AC
406	Turbular 406d	Beam	0.01	DL + LL + EL + TH_AC
408	Turbular 406d	Beam	0.00	DL + LL + EL + TH_AC
409	Turbular 273d	Beam	0.08	DL + LL
415	Turbular 273d	Beam	0.02	DL + LL + EL + TH_AC
416	Turbular 273d	Beam	0.07	DL + LL
418	Turbular 273d	Beam	0.03	DL + LL
419	Turbular 273d	Beam	0.03	DL + LL + EL + TH_AC
421	Turbular 273d	Beam	0.07	DL + LL
422	Turbular 273d	Beam	0.04	DL + LL
424	Turbular 273d	Beam	0.07	DL + LL
428	Turbular 273d	Beam	0.07	DL + LL
430	Turbular 273d	Beam	0.03	DL + LL + EL + TH_AC
431	Turbular 273d	Beam	0.07	DL + LL
433	Turbular 273d	Beam	0.05	DL + LL
434	Turbular 273d	Beam	0.01	DL + LL + EL + TH_AC
436	Turbular 273d	Beam	0.08	DL + LL
437	Turbular 273d	Beam	0.03	DL + LL
439	Turbular 273d	Beam	0.07	DL + LL
440	Turbular 273d	Beam	0.01	DL + LL + EL + TH_AC
459	Turbular 273d	Beam	0.03	DL + LL + EL + TH_AC
460	Turbular 273d	Beam	0.01	DL + LL + EL + TH_AC
461	Turbular 273d	Beam	0.02	DL + LL + EL + TH_AC
462	Turbular 273d	Beam	0.01	DL + LL + EL + TH_AC
463	Turbular 273d	Beam	0.01	DL + LL + EL + TH_AC
464	Turbular 273d	Beam	0.01	DL + LL

465	Turbular 273d	Beam	0.01	DL + LL + EL + TH_AC
466	Turbular 273d	Beam	0.01	DL + LL
467	Turbular 273d	Beam	0.01	DL + LL + EL + TH_AC
468	Turbular 273d	Beam	0.01	DL + LL + EL + TH_AC
469	Turbular 273d	Beam	0.01	DL + LL + EL + TH_AC
470	Turbular 273d	Beam	0.01	DL + LL + EL + TH_AC
471	Turbular 273d	Beam	0.02	DL + LL + EL + TH_AC
472	Turbular 273d	Beam	0.01	DL + LL + EL + TH_AC
473	Turbular 273d	Beam	0.03	DL + LL + EL + TH_AC
474	Turbular 273d	Beam	0.01	DL + LL
476	Turbular 273d	Beam	0.02	DL + LL + EL + TH_AC
477	Turbular 273d	Beam	0.02	DL + LL + EL + TH_AC
479	Turbular 273d	Beam	0.00	DL + LL + EL + TH_AC
480	Turbular 273d	Beam	0.01	DL + LL + EL + TH_AC
482	Turbular 273d	Beam	0.02	DL + LL
483	Turbular 273d	Beam	0.02	DL + LL + EL + TH_AC
485	Turbular 273d	Beam	0.01	DL + LL + EL + TH_AC
486	Turbular 273d	Beam	0.01	DL + LL + EL + TH_AC
488	Turbular 273d	Beam	0.02	DL + LL
489	Turbular 273d	Beam	0.02	DL + LL
491	Turbular 273d	Beam	0.01	DL + LL + EL + TH_AC
492	Turbular 273d	Beam	0.01	DL + LL + EL + TH_AC
494	Turbular 273d	Beam	0.02	DL + LL + EL + TH_AC
495	Turbular 273d	Beam	0.02	DL + LL + EL + TH_AC
497	Turbular 273d	Beam	0.01	DL + LL

Graph of bending stress and shear stress under varies load combinations have been plotted in Figure 4.10 and 4.11. It is clearly showed that the maximum bending stress occurred at the load combination of dead loads and live loads, 245 307.52 kN/m<sup>2</sup> which still within the allowable bending stress, 480 677.45 kN/m<sup>2</sup>. This means the structure still able to resist the bending stress although the stress is quite higher. This also proved that the intensity of the earthquake is not strong enough to cause the structure to collapse. The reason for the result of load cases of dead load, live load, environmental load and time history load is slightly less than the load cases of dead and live load because of the counteractive between the stresses. Counteract in between the stresses may occur and act against stress and lead to the result of decreasing or neutralizing by its force.

Similar to the bending stress, the maximum shear stress occurred at the load case of dead loads and live loads, 14 796.77 kN which do not exceed the allowable stress, 130 464.21 kN. The load cases of dead load, live load, environmental load and time history load is slightly less than the load cases of dead and live load. For response

spectrum cases, it contributed the least bending stress and shear stress among all the cases.

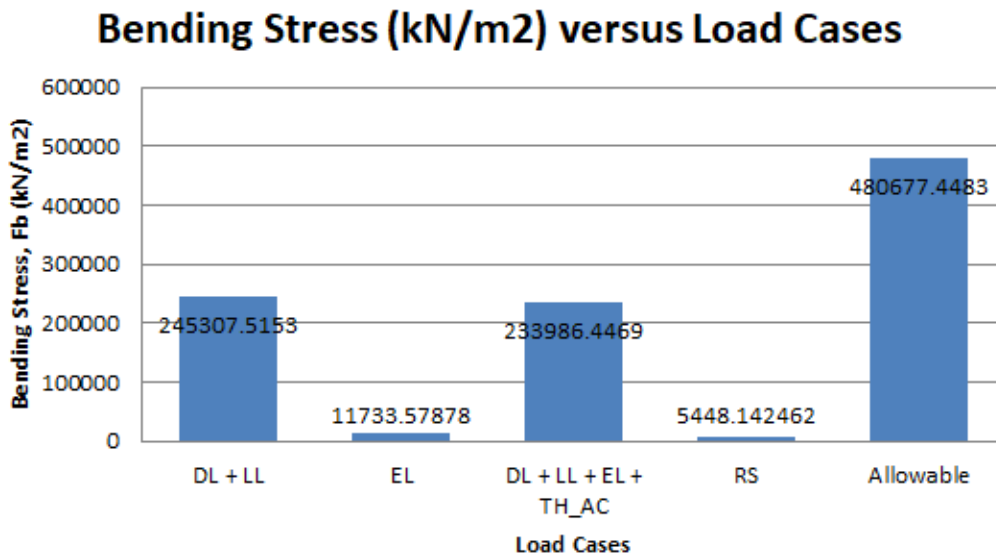


Figure 4.10 Graph of Bending Stress versus Load Cases

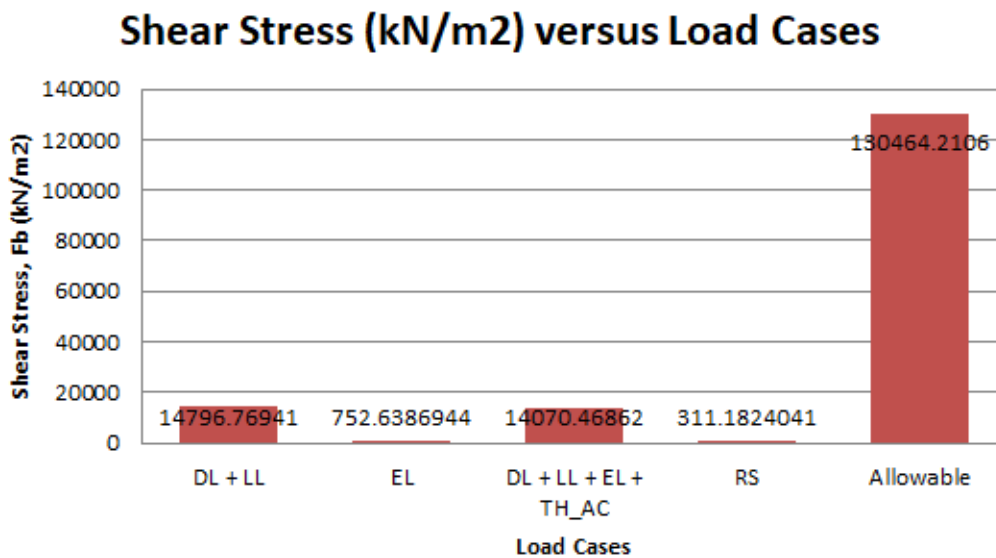


Figure 4.11 Graph of Shear Stress versus Load Cases

Joint displacement under varies load cases has been performed since it is the most critical part of the structure. Joint 37 has the maximum value of displacement among other joint connection. Hence, the result of the joint displacement for joint 37 has been tabulated and illustrated in Table 4.9 and Figure 4.12. The maximum

displacement is 0.001969 m in U1 direction under load cases of DL + LL + EL +TH\_AC. For U2 direction, it is observed that the maximum displacement is 0.001078 m caused by response spectrum case. However, DL + LL result in the maximum displacement in U3 direction, -0.002143m. Among all the directions, DL + LL in U3 direction is the maximum displacement.

It's clear that the static analysis gives higher values for maximum displacement of the structure among all load cases rather than other methods of analysis, especially in dynamic analysis.

Table 4.9 Joint Displacement in different load combination at joint 37

Load Combination	Joint	U1	U2	U3
DL + LL	37	-0.000276	0.000022	-0.002143
EL	37	0.001218	0.000149	0.000486
RS	37	0.001541	0.001078	0.000473
DL + LL + EL + TH_AC	37	0.001969	0.000178	-0.001299

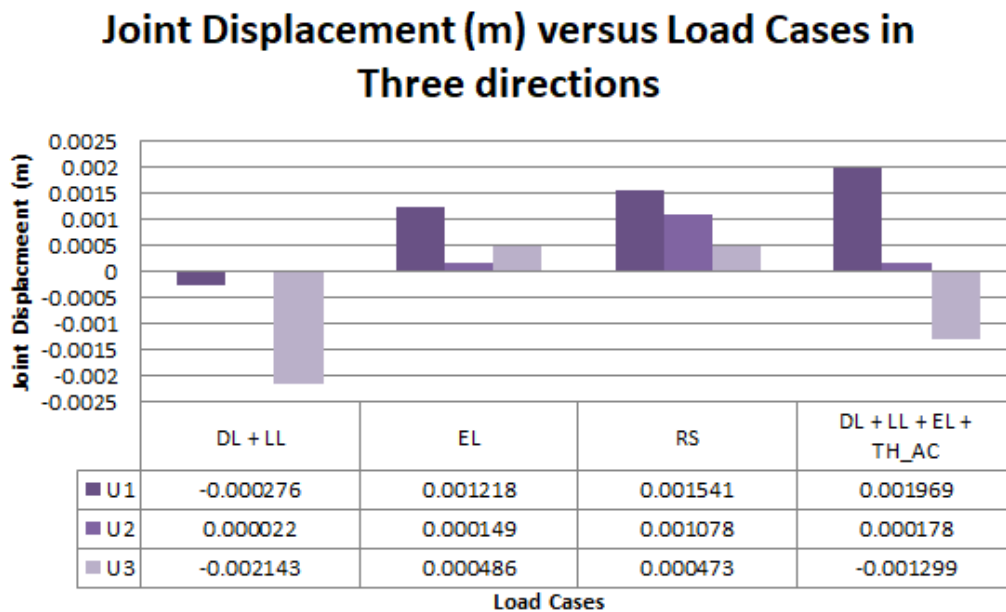


Figure 4.12 Graph of Joint Displacement versus Load Cases in Three Directions

Joint velocities under varies load cases also performed ad determined in this study. The result of the joint displacement for joint 37 has been tabulated and illustrated in Table 4.10 and Figure 4.13. RS load case has the maximum velocity for all U1, U2,

and U3 compared to other load cases. It can be observed that DL + LL load case and EL load case do not carry any movement to the structure as the load applied is a static and vertical load which result in zero velocity to the joint 37.

Table 4.10 Joint Velocities in different load combination at joint 37

Load Combination	Joint	U1	U2	U3
DL + LL	37	0	0	0
EL	37	0	0	0
RS	37	0.0946	0.0768	0.0285
DL + LL + EL + TH_AC	37	0.0280	0.0002	0.0088

**Joint Velocities (m/sec) versus Load Cases in Three directions**

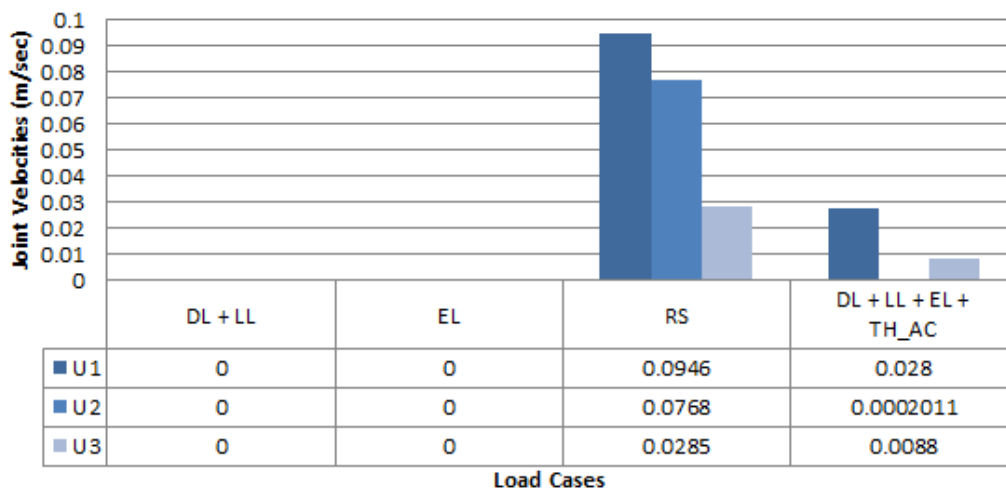


Figure 4.13 Graph of Joint Velocities versus Load Cases in Three Directions

Joint velocities under varies load cases also performed ad determined in this study. The result of the joint displacement for joint 37 has been tabulated and illustrated in Table 4.11 and Figure 4.14. RS load case has the maximum acceleration for all U1, U2, and U3 compared to other load cases which are  $5.8781 \text{ m/s}^2$ ,  $5.4686 \text{ m/s}^2$ , and  $1.7378 \text{ m/s}^2$ . It can be observed that DL + LL load case and EL load case do not carry any movement to the structure as the load applied is a static and vertical load which result in zero acceleration to the joint 37.

Table 4.11 Joint Acceleration in different load combination at joint 37

Load Combination	Joint	U1	U2	U3
DL + LL	37	0	0	0
EL	37	0	0	0
RS	37	5.8781	5.4686	1.7378
DL + LL + EL + TH_AC	37	1.1217	0.0081	0.3469

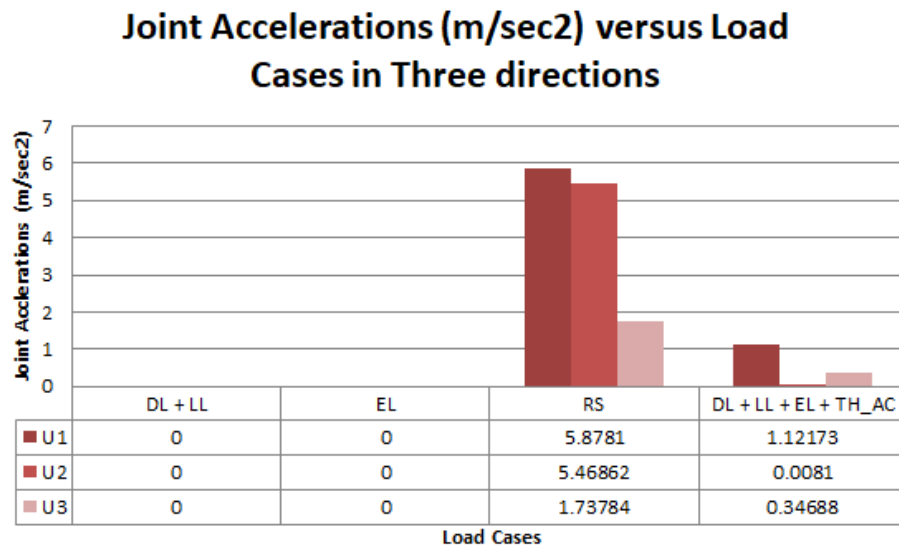


Figure 4.14 Graph of Joint Acceleration versus Load Cases in Three Directions

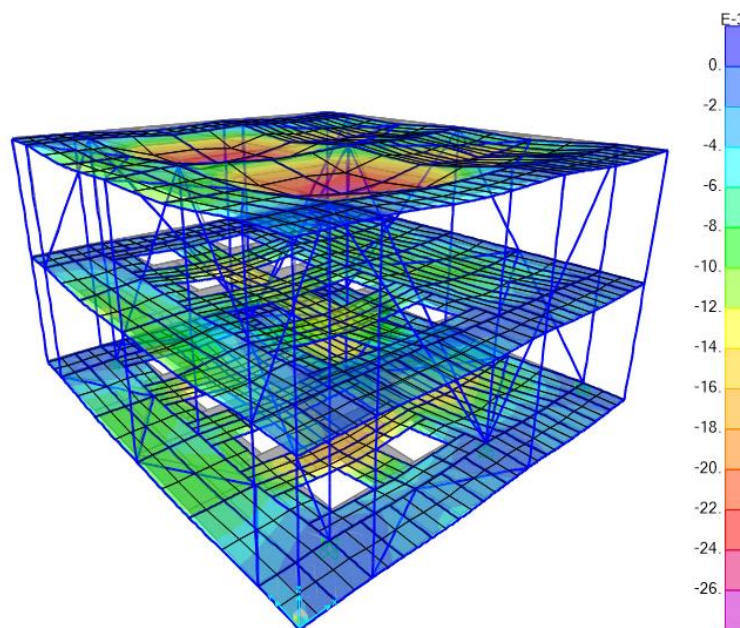


Figure 4.15 Deformed shape of DL + LL



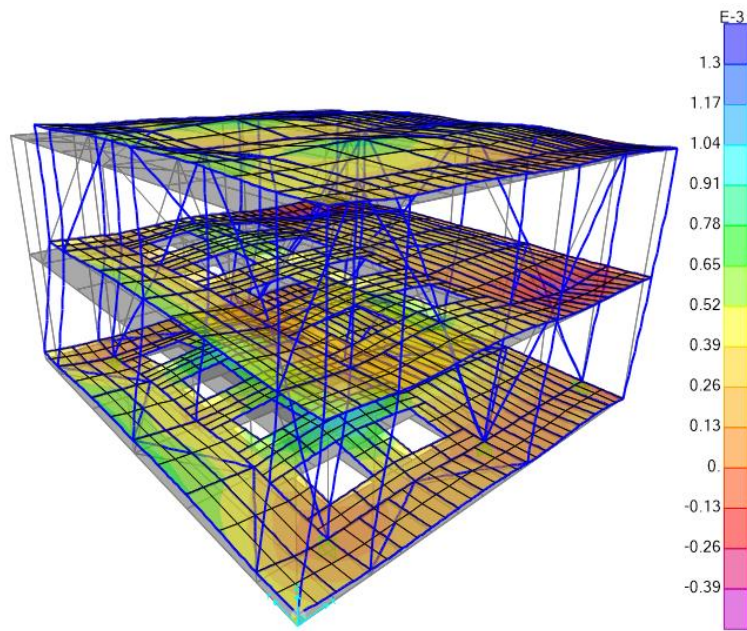


Figure 4.16 Deformed shape of EL

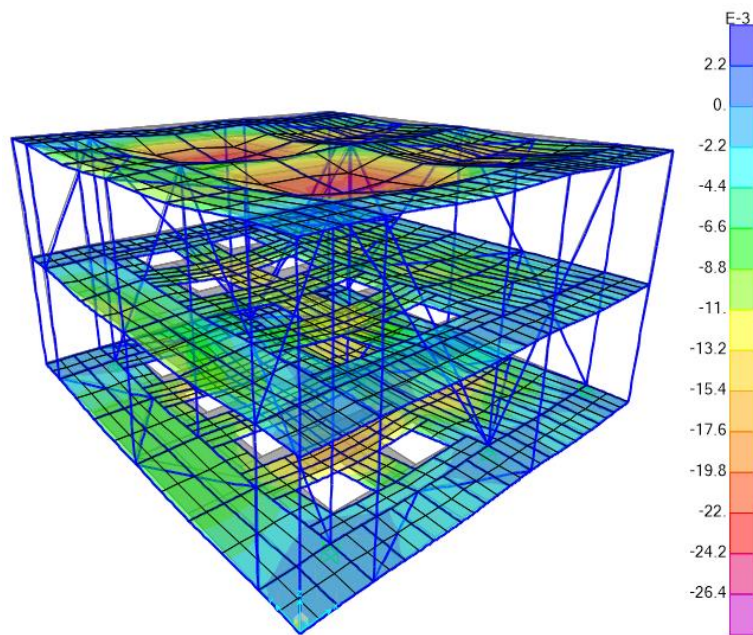


Figure 4.17 Deformed shape of DL + LL + EL + TH\_AC

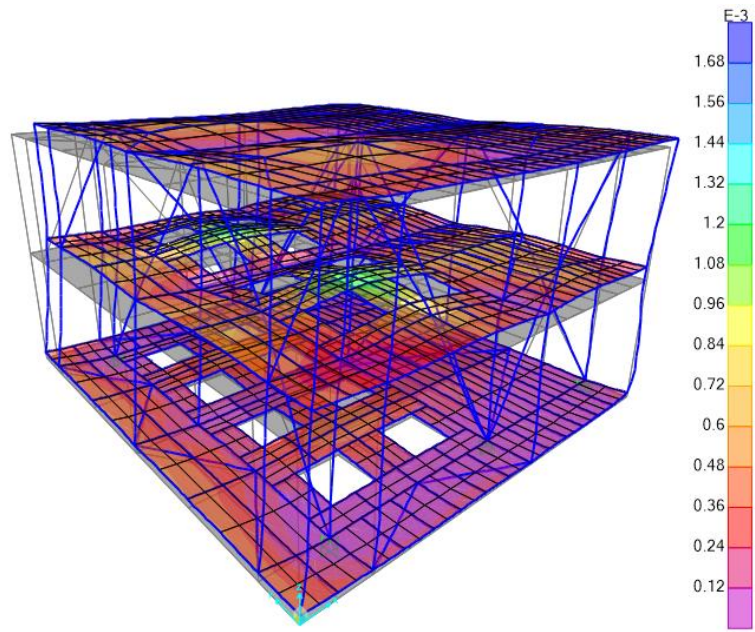


Figure 4.18 Deformed shape of RS

## **CHAPTER 5**

### **CONCLUSION**

#### **5.1 Conclusion**

As Malaysia is inching closer to seismic zones and will not be immune to earthquakes forever, this study is conducted based on a real-life project of wellhead offshore platform in Terengganu region to check the earthquake resistance capacity of wellhead offshore platform in Malaysia due to El Centro earthquake by using SAP 2000. All the specifications of the material, size and section details of the structure were followed by structural drawing. The objective of the study has been achieved, whereby the seismic performance of wellhead offshore platform in Malaysia has been computed and provided a desirable result for performance evaluation parameters in the offshore structures.

In order to determine the seismic response of a wellhead offshore structure, seismic analysis including free vibration analysis, time history analysis, response spectrum by utilizing the available historical seismic data from El Centro earthquake. The results obtained were the modal shape, natural period and natural frequency of wellhead offshore platform; maximum shear and bending moment in the member under various load cases; and critical joint displacement, velocity, and acceleration under different types of load combination.

It is recommended that further studies about the seismic analysis of the structure are carried out to continuously monitor the seismic response and the necessity of seismic design consideration for wellhead offshore structure to prevent structural failure. Besides that, this is also to prevent any uncertainties as Malaysia is affected by active seismic activity from the nearby inter-plate earthquakes, with regard to the recent Ranau, Sabah earthquake, other local faults may be reactivated in the coming future.

Based on the finding of the research, the conclusion that can be made in the following:

- i. The simulation of the wellhead offshore structure model is not fully 100% represent the actual structure. This is due to the earlier assumptions made on the restrains at the base condition and the joint connection of the offshore structure. The restraint at base condition of the wellhead offshore platform is assumed fixed to the ground as a replacement for piled and soil interaction is also neglected. Moreover, the connection of the offshore structure was not designed according to the EuroCode3 design specification. The stress that applied to the connection is assumed to be within the connection capacity thus connections of the members are not defined in SAP2000.
- ii. Wellhead offshore structures in Malaysia region are capable of resisting this type of seismic activity based on the study since the maximum shear stress and bending stress is within the allowable capacity checks after several combination load cases have been applied.
- iii. Element unity check has been performed; the final steel P-M interaction ratios are determined and displayed. All steel frames passed the stress/capacity check as the ratio is less than 1 as shown in table 4.8. The most critical frame member in this offshore model is a frame member 25 with 0.51 ratios.
- iv. From the free vibration analysis, the highest value of the natural period is 0.1060 sec of mode shape 1.
- v. The maximum shear force that happens at the most critical frame element 25 is -449.44 kN when loading combination dead load + live load being applied.
- vi. The maximum bending moment that occurred at the most critical frame element 25 is -667.58 kNm when loading combination dead load + live load being applied.
- vii. The highest value of displacement is -0.002143m in U3 direction which occurred in the dead load and lives load case at joint 37.
- viii. The highest value of velocity is 0.0946m/s in U1 direction which occurred in the response spectrum load case at joint 37.

- ix. The highest value of acceleration is  $5.8781 \text{ m/s}^2$  in U1 direction which occurred in the response spectrum load case at joint 37.

## 5.2 Recommendations

For the future studies, the consideration of the soil interaction and joint connection of the offshore structure should both be included in the analysis. This is because the earthquake loads transfer from the ground surface and transfer the horizontal loading to the upper surface. Hence, it might have slightly different effects on the results and actually happened on site if neglecting the soil interaction in the analysis. In fact, most of the failures of the steel structure occurred at the joint connection between the members. The main reason leading to the failure is due to the higher stress at the connection. Thus, the welded joint should be modeled in computational software, SAP 2000 according to EuroCode3 for detailed analysis.

In addition, for improving the accuracy on the seismic response study, the earthquake data should be always updated, so that the higher intensity of the earthquake would be considered for the design analysis of structure to prevent failure. For instances, according to United States Geological Survey (USGS), the earthquake with magnitude 5.9 occurred at the Ranau, Sabah lately has killed at least 18 people on Mount Kinabalu, some climbers have injured, some building has damaged seriously, water supply was disrupted in the area around Kundasang and Ranau, rockfalls triggered in the mountain area.

There are some short term and long term recommendations that might help Malaysia to prevent losses of life and building damages from the earthquake. Firstly, set up seismic monitoring stations in Malaysia. The current five numbers of seismic monitoring stations in Peninsular Malaysia should be increased to at least one (1) station per state so that sufficient data could be collected for better decisions making to the analysis in the future. Besides that, set up building acceleration instrumentation devices on the building to obtain the acceleration at different story height. It is recommended in ACI code that such devices have to be installed on at least three positions of high-rise structures, i.e. at the base, at mid-level, and at the top, in order to obtain accurate and reliable readings of the building response.

Furthermore, seismic vulnerability studies of existing important buildings or structures in high-risk areas are conducted. (a) This can be done by using appropriate seismic vibration measuring devices to the structures for recording seismic response to a certain degree of accuracy. Not only that, Institution of Engineer Malaysia (IEM) should always review current engineering design and construction standards and practices in Malaysia. This is important as the current standards do not consider the possible vibration forces, principally due to the earthquake.

For long-term measures, Board of Engineer Malaysia (BEM) and Institution of Engineer Malaysia (IEM) should develop or adopt a suitable code of practice for the construction industry with proper guidelines that are needed for the design engineers as a long-term solution. In addition, these proposed documents need to be updated and revised in every five (5) years, when new findings appear.

Some sensitive structures like bridges, transmission towers, dams and other residential buildings shall be checked for vulnerability when exposed to the seismic ground motion. Periodic Inspection should be conducted for buildings of over 10 years old and over five (5) stories under The Street, Drainage and Buildings Act. Ministry of Education Malaysia can also implement and introduce earthquake engineering as a subject in the Universities and other tertiary institutions of higher learning. Alternatively, it can be an extension or continuation to the university's general engineering study on dynamic analysis of rigid bodies, structural frames, and foundation subsoils.

Last but not least, CIDB research might accumulate a substantial research fund for earthquake engineering research and also include monitoring and risk assessment works. Research and development represent an important part of the initiation of earthquake engineering programme.

## REFERENCES

- A S Kharade; and S V Kapadiya. (2014). Offshore Engineering : an Overview of Types and Loadings on Structures. *International Journal of Structural and Civil Engineering Research*, 3(2).
- Afolalu, S. A., Ajayi, O. O., Ikumapayi, O. M., & Adejuyigbe, S. B. (2015). Modeling and Simulation of Wave load on Periodic Support for Isolation system of Offshore Platform, 6(5).
- Ahmad, S. W., Adnan, A., Nazir, R., Ramli, N. I., Ali, M. I., & Ramli, M. Z. (2017). Determination Of Earthquakes Design Ratio For Fixed Offshore Platform Due To Aceh Earthquakes In Malaysia. *International Journal of Civil Engineering and Geo-Environment*. Retrieved from <http://ijceg.ump.edu.my>
- American, P. I. (2007). Recommended Practice for Planning , Designing and Constructing Fixed Offshore Platforms — Working Stress Design. *API Recommended Practice*, 24–WSD(December 2000), 242. <https://doi.org/10.1007/s13398-014-0173-7.2>
- Bargi, Khosro; Hosseini, S.Reza; H.Tadayon, Mohammad; Sharifian, H. (2011). Seismic Response of a Typical Fixed Jacket-Type Offshore Platform (SPD1) Under Sea Waves. *Open Journal of Marine Science*, 01(02), 36–42. <https://doi.org/10.4236/ojms.2011.12004>
- Bernamea. (2010a). Mild earthquake in Kenyir. *The Star Online*. Retrieved from <https://www.thestar.com.my/news/nation/2010/03/11/mild-earthquake-in-kenyir/>
- Bernamea. (2010b). Mild quake in Batu Niah. *The Star Online*. Retrieved from <https://www.thestar.com.my/news/nation/2010/01/26/mild-quake-in-batu-niah/>
- Cheng, K.-H. (2016). Plate Tectonics and Seismic Activities in Sabah Area. *Transactions on Science and Technology*, 3(1), 47–58. Retrieved from [http://transectscience.org/pdfs/vol3/no1/3147\\_58.pdf](http://transectscience.org/pdfs/vol3/no1/3147_58.pdf)
- Datta, T. K. (2010). *Seismic Analysis Of Structures*. <https://doi.org/10.1016/B978-1-85617-501-2.00026-2>
- Department of Statistic Malaysia. (2018). Press Release Malaysia Economic Performance First Quarter 2018. *Department of Statistic Malaysia*, (May).
- Devold, H. (2002). *Oil and Gas Production Handbook - An introduction to oil and gas production*. *Oil and gas production handbook: an introduction to oil and gas production*.

- Elshafey, A. A., Haddara, M. R., & Marzouk, H. (2009). Dynamic Response of Offshore Jacket Structures under Random Loads. *Marine Structures*, 22(3), 504–521. <https://doi.org/10.1016/j.marstruc.2009.01.001>
- Fardis, M. N. (2004). Current Development and Future Prospects of the European Code for Seismic Design and Rehabilitation of Buildings : Eurocode 8. *13th World Conference on Earthquake Engineering*, 2(2025).
- Gerhard W. Leo. (1991). Oliverian Domes, Related Plutonic Rocks, and Mantling Ammonoosuc Volcanics of the Bronson Hill Anticlinorium, New England Appalachians. *U.S. Geological Survey Professional Paper*, 1516, 352. [https://doi.org/10.1016/0003-6870\(73\)90259-7](https://doi.org/10.1016/0003-6870(73)90259-7)
- Gioncu, V., & Mazzolani, F. (2011). *Earthquake Engineering for Structural Design*.
- Hatheway, A. W. (1996). *Fundamentals of Earthquake Engineering. Engineering Geology* (Vol. 43). [https://doi.org/10.1016/0013-7952\(95\)00070-4](https://doi.org/10.1016/0013-7952(95)00070-4)
- Joseph, T. (2009). Assessment of Kinematic Effects on Offshore Piled Foundations.
- Kramer, S. L. (1996). *Geotechnical Earthquake Engineering*.
- Li-Jeng, H., & Hong-Jie, S. (2014). Seismic Response Analysis of Tower Crane using SAP2000. *Procedia Engineering*, 79(1st ICM), 513–522. <https://doi.org/10.1016/j.proeng.2014.06.374>
- Light, G. U. V. (2011). An Introduction to the Petroleum Industry. *Energy Economics*, 1–8.
- Malaysian Meteorological Service. (2009). Seismic and Tsunami Hazards and Risks Study in Malaysia. *Mosti*, 50. <https://doi.org/10.1007/s13398-014-0173-7.2>
- Manafizad, A. N., Pradhan, B., & Abdullahi, S. (2016). Estimation of Peak Ground Acceleration (PGA) for Peninsular Malaysia using geospatial approach. *IOP Conference Series: Earth and Environmental Science*, 37, 012069. <https://doi.org/10.1088/1755-1315/37/1/012069>
- Marto, A., Tan, C. S., Kasim, F., & Mohd.Yunus, N. Z. (2013). Seismic Impact in Peninsular Malaysia. *The 5th International Geotechnical Symposium - Incheon*, (May), 22–24. <https://doi.org/10.13140/2.1.3094.9129>
- Maske, A. A., Maske, N. A., & Shiras, P. P. (2014). Seismic Response of Typical Fixed Jacket Type Offshore Platform Under Sea Waves : a Review. *International Journal of Advance Research In Science And Engineering IJARSE*, 3(3), 24–35.



- Mukhlas, N. A., Abdullah Shuhaimy, N., Johari, M. B., Mat Soom, E., Abu Husain, M. K., & Mohd Zaki, N. I. (2016). Design and Analysis of Fixed Offshore Structure – an Overview. *Malaysian Journal of Civil Engineering*, 28(3), 503–520.
- Noorliza Lat, C. H. E., & Ibrahim, A. T. (2009). Bukit Tinggi earthquakes: November 2007 - January 2008. *Bulletin of the Geological Society of Malaysia*, 55(55), 81–86. <https://doi.org/10.7186/bgsm2009013>
- Park, M. su, Koo, W., & Kawano, K. (2011). Dynamic Response Analysis of an Offshore Platform due to Seismic Motions. *Engineering Structures*, 33(5), 1607–1616. <https://doi.org/10.1016/j.engstruct.2011.01.030>
- Potty, N. S., Akram, M. K. M., & Khamidi, M. F. Bin. (2012). Risk-Based Assessment on Malaysia's Offshore Jacket Platform. *Malaysian Journal of Civil Engineering*, 24(1), 29–47.
- PWC. (2016). The Malaysian Oil & Gas Industry: Challenging Times, but Fundamentals Intact, (May), 12. Retrieved from [www.pwc.com/my](http://www.pwc.com/my)
- Ramtal D., & Dobre A. (2014). *Physics for JavaScript Games, Animation, and Simulations*. Apress. Apress, Berkeley, CA. [https://doi.org/https://doi.org/10.1007/978-1-4302-6338-8\\_8](https://doi.org/10.1007/978-1-4302-6338-8_8)
- Reddy, D.V and Swanmidas, A. S. . (2014). *Essential Of Offshore Structures: Framed and Gravity Platforms*. <https://doi.org/10.1017/CBO9781107415324.004>
- S. Nallayarasu. (1981). Offshore Structures: Analysis and Design. *Applied Ocean Research*, 3(3), 149. [https://doi.org/10.1016/0141-1187\(81\)90119-X](https://doi.org/10.1016/0141-1187(81)90119-X)
- S.Bedi, R. (2012). Shelter from tremors. *The Star Online*. Retrieved from <https://www.thestar.com.my/news/nation/2012/04/15/shelter-from-tremors/>
- Shreyasvi, C., & Shivakumaraswamy, B. (2015). A Case Study on Seismic Response of Buildings with Re-Entrant Corners. *International Journal of Engineering Research & Technology (IJERT)*, 4(05), 1071–1078.
- Southern California Earthquake Data Center. (2018). Significant Earthquakes and Faults. Retrieved from <http://scedc.caltech.edu/significant/imperial1940.html>
- Speight, J. G. (2015). *Handbook of Offshore Oil and Gas Operations*. <https://doi.org/10.1016/B978-1-85617-558-6/00001-5>
- Suriati, T., & Yusoff, T. (2015). Advantage Using Eurocode 3 for Design of Factory Frame, 5(11), 11–16.

U.S Energy Information Administration. (2017). Country Analysis Brief: Malaysia, 1–7.

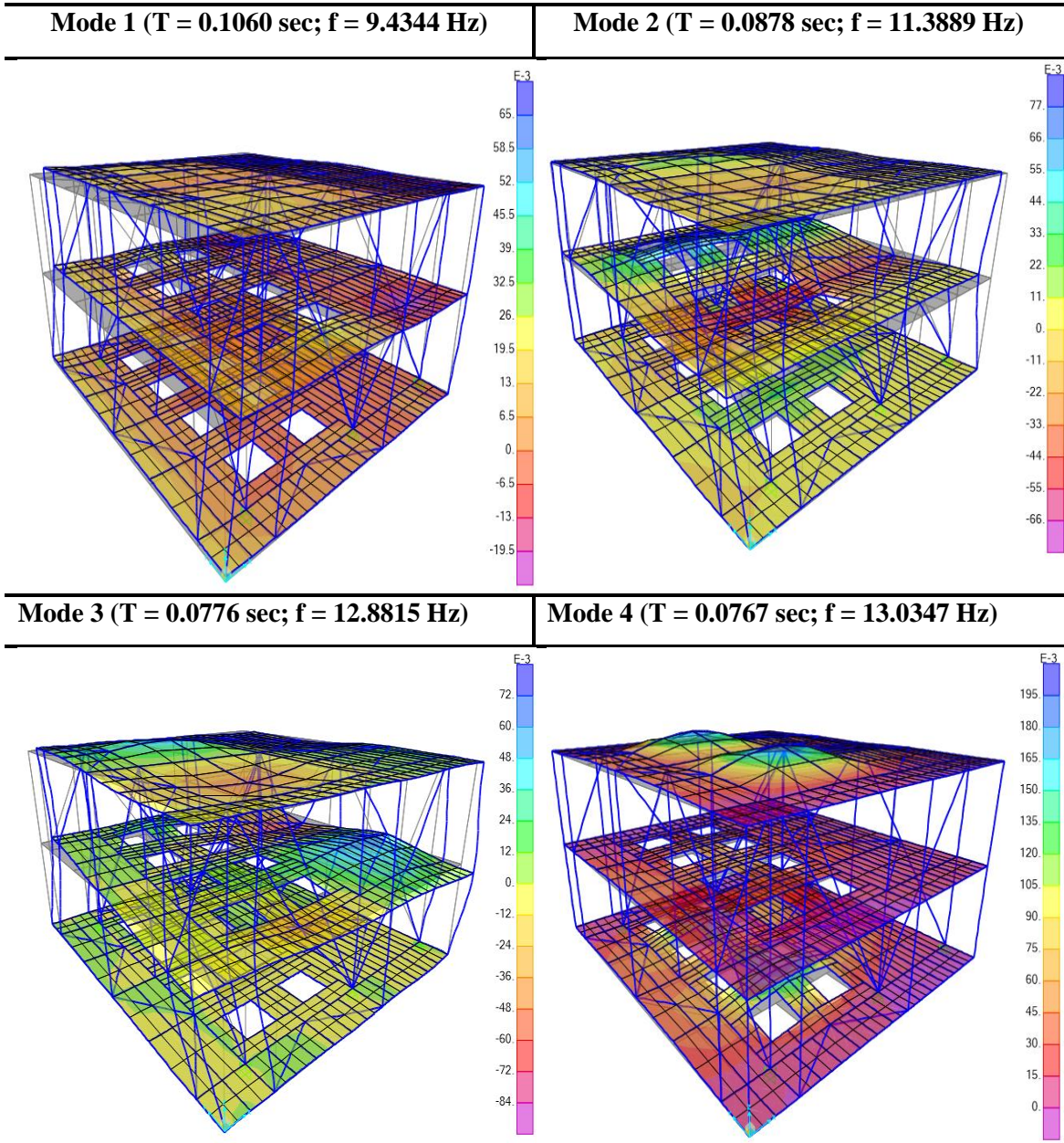
Zawawi, N. A. W. A., Liew, M. S., & Na, K. L. (2012). Decommissioning of the offshore platform: A sustainable framework. *CHUSER 2012 - 2012 IEEE Colloquium on Humanities, Science and Engineering Research*, (September 2015), 26–31.  
<https://doi.org/10.1109/CHUSER.2012.6504275>

Zhou, X.-Y., Yu, R.-F., & Dong, L. (2004). The Complex-Complete-Quadratic-Combination (CCQC) Method for Seismic Response of Non-Classically Damped Linear MDOF System. *13th World Conference on Earthquake Engineering*, (January 2004), Paper No. 848.

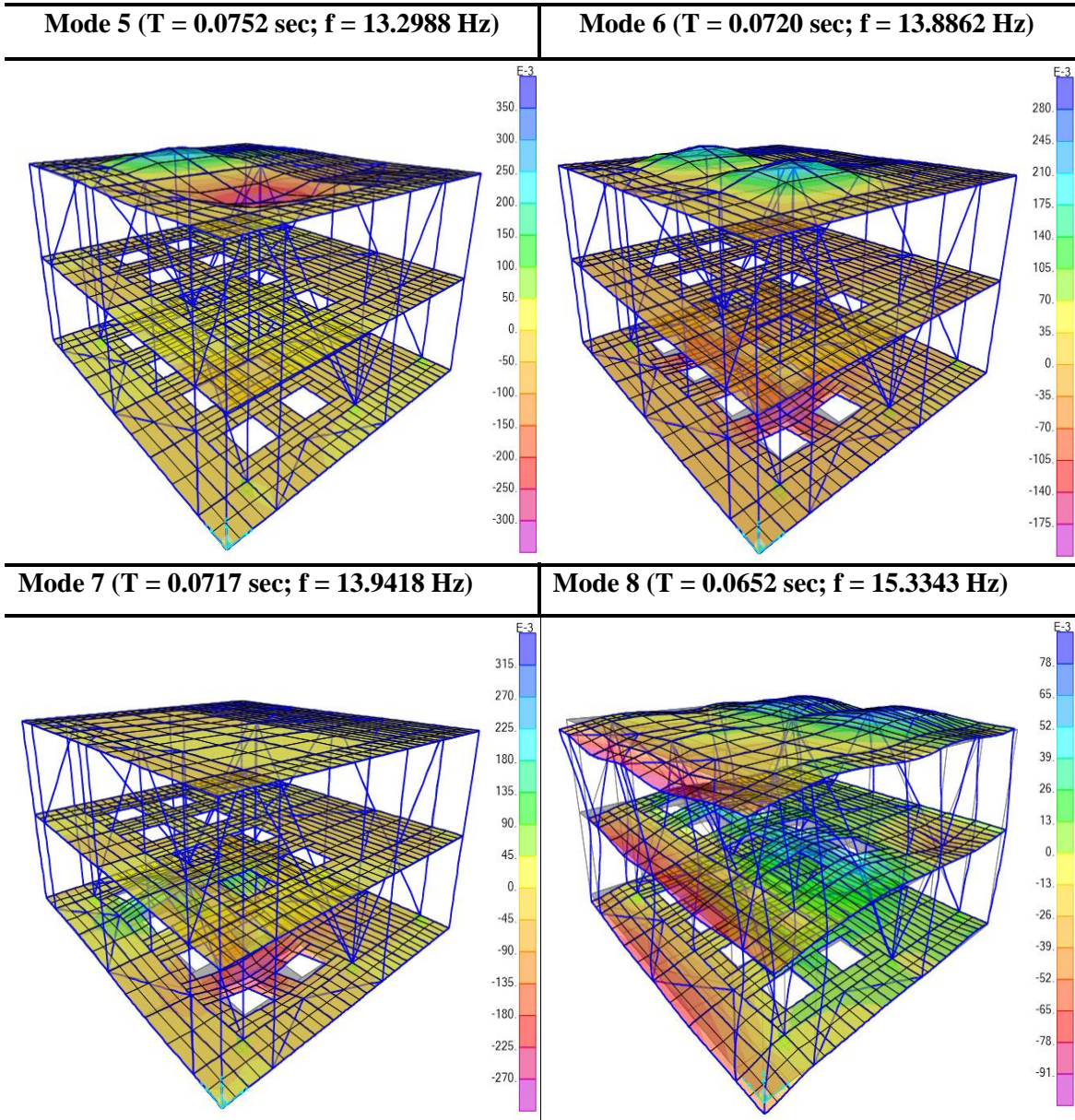
**APPENDIX A  
GRID SYSTEM DATA**

<b>X Grid Data</b>		<b>Y Grid Data</b>		<b>Z Grid Data</b>	
<b>Grid ID</b>	<b>Ordinate</b>	<b>Grid ID</b>	<b>Ordinate</b>	<b>Grid ID</b>	<b>Ordinate</b>
A	0.000	1	0.0000	Z1	0
B	1.981	2	1.4000	Z2	4
C	7.925	3	7.3625	Z3	8
D	13.366	4	13.3250		
		5	14.7250		

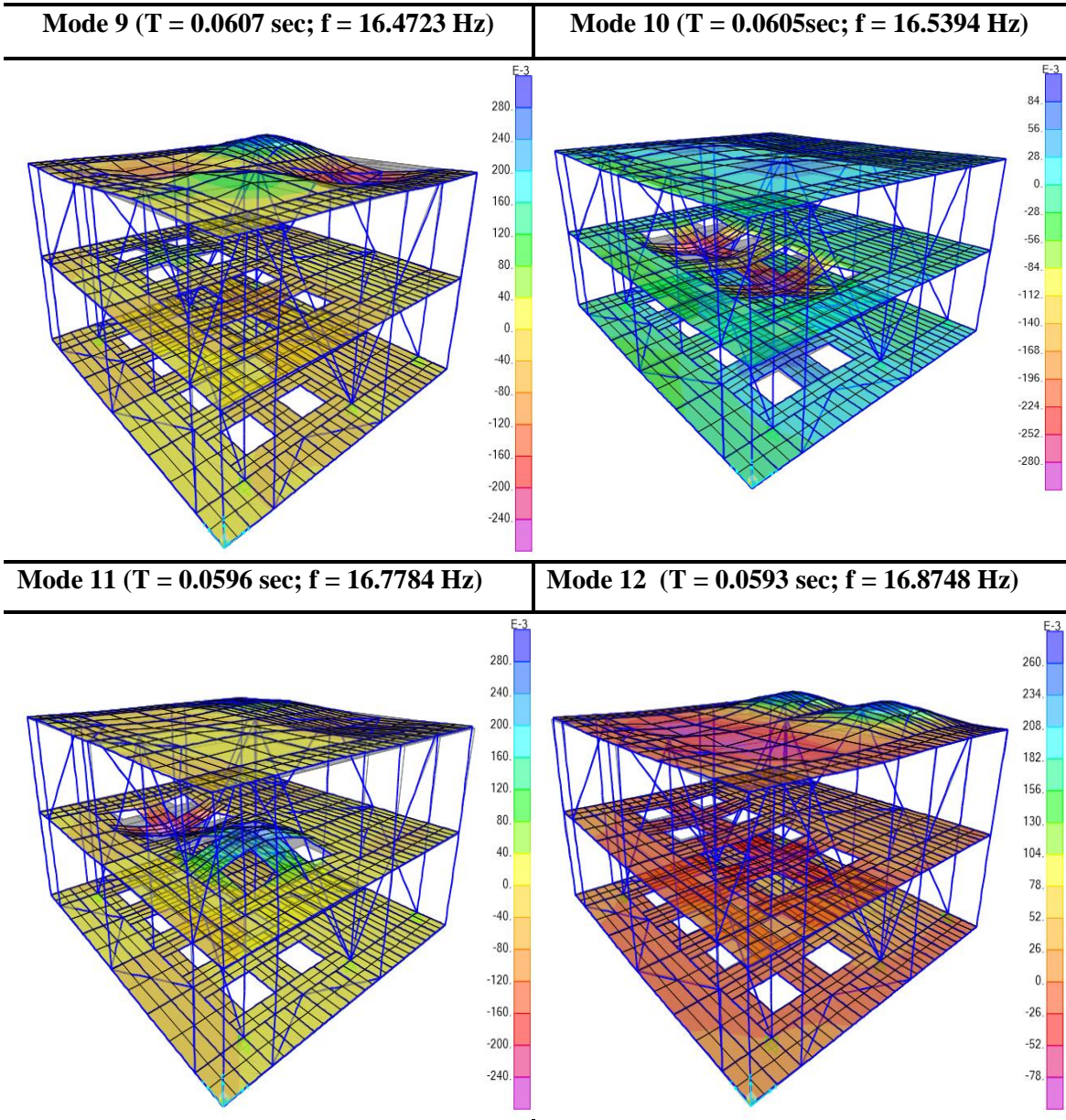
**APPENDIX B**  
**MODAL SHAPE OF OFSHORE PLATFORM**



APPENDIX B: CONTINUED



APPENDIX B: CONTINUED



## APPENDIX C MANUAL CALCULATION

### Load Description

The load combinations of dead load, deck loads, wind, wave, current and earthquake loads have been defined.

#### Self-weight and functional loads

The self-weight and functional loads of wellhead offshore platform are listed in Table 3.1.

Table 3.1      Dead loads and live load description

No.	Load description	Weight (MN)
1	Jacket appurtenances weight	0.339
2	Topside dead loads	0.393
3	Topside live loads	1.150
4	Piping & equipment weights	0.400
TOTAL		2.282

### Dead and Live Loads

$$\text{Dead load} = 0.339 + 0.393 + 0.400 = 1.132 \text{ MN}$$

$$\begin{aligned} \text{Uniform dead load} &= (1.132 \times 1000) \text{ kN} \div (14.725 \times 13.366) \text{ m}^2 \\ &= 5.752 \text{ kN /m}^2 \end{aligned}$$

$$\text{Live load} = 1.150 \text{ MN}$$

$$\begin{aligned} \text{Uniform live load} &= (1.150 \times 1000) \text{ kN} \div (14.725 \times 13.366) \text{ m}^2 \\ &= 5.843 \text{ kN /m}^2 \end{aligned}$$

## APPENDIX C: CONTINUED

### Environmental Loads

The environmental loads are based on the metocean data. Table 3.2 shows the environmental criteria for the offshore structure which located in Terengganu.

Table 3.2 Environmental criteria used at Terengganu

MSL	Types of data	Unit	Design condition
47.629 m	Wave height	m	10.79
	Wave period	s	10.90
	Current velocity	m/s	0.75
	Wind speed	m/s	21.80
	Maximum tide	m	2.00
	Storm surge	m	0.40

Therefore all the environmental loads which including wind, wave, and current action were calculated by using the provided environmental criteria and formula from American Petroleum Institute (API).

#### Wind load

The wind profile, gusts and wind drag force are calculated using following equations that are taken directly from the API RP 2A-WSD practice.

#### Wind profile and Gusts

$$U(z) = U_o \times [1 + C \times \ln(\frac{z}{32.8})]$$

$$z = 8000 \text{ mm} = 26.247 \text{ ft}$$

$$U_o = 21.8 \text{ m/s} = 71.522 \text{ ft/s}$$

$$\begin{aligned} C &= 5.73 \times 10^{-2} \times [1 + 0.0457 \times U_o]^{\frac{1}{2}} \\ &= 5.73 \times 10^{-2} \times [1 + 0.0457 \times 71.522]^{\frac{1}{2}} \\ &= 0.118 \end{aligned}$$



## APPENDIX C: CONTINUED

$$U(z) = 71.522 \text{ ft/s} \times [1 + 0.118 \times \ln(\frac{26.247}{32.8})] = 69.641 \text{ ft/s}$$

$$I_u(z) = 0.06 \times [1 + 0.0131 \times U_o] \times (\frac{z}{32.8})^{-0.22}$$

$$I_u(z) = 0.06 \times [1 + 0.0131 \times 69.641 \text{ ft/s}] \times (\frac{26.247}{32.8})^{-0.22}$$

$$= 0.121 \text{ ft/s}$$

$$u(z, t) = U(z) \times [1 - 0.41 \times I_u(z) \times \ln(\frac{t}{t_o})]$$

$$u(z, t) = 69.641 \times [(1 - 0.41 \times 0.121 \times \ln(\frac{60}{3600}))]$$

$$= 83.787 \text{ ft/s}$$

$$= \mathbf{25.54 \text{ m/s}}$$

### Wind Speed and Force Relationship

The wind drag force on object should be calculated as:

$$F = (\rho/2) \times u^2 C_s A$$

$C_s$  = Overall projected area platform = 1 (From table 3.3)

$\rho$  = 0.0023668 slug/ft<sup>3</sup> = 1.22 kg/m<sup>3</sup> (From API RP 2A-WSD, 2.3.2.c)

$$u = u(z, t) = 25.54 \text{ m/s}$$

$$A = 2\pi r_1 h = 2\pi(0.203)(8) = 10.204 \text{ m}^2$$

$$F = (1.22/2) \times (25.54)^2 (1)(10.204) = \mathbf{4.060 \text{ kN}}$$

### Wave load

Based on American Petroleum Institute (API), the drag coefficient,  $C_d$  and inertia coefficient,  $C_m$  are according to the following:

## APPENDIX C: CONTINUED

Table 3.4 Drag coefficient,  $C_d$  and Inertia Coefficient,  $C_m$

Marine Growth	Drag Coefficient, $C_d$	Shape Coefficient, $C_s$
Smooth	0.65	1.6
Rough	1.05	1.2

The wave load above sea water level was considered as rough:

$$\begin{aligned}
 F &= C_D \frac{w}{2g} A U|U| + C_m \frac{w}{g} V \left( \frac{\delta U}{\delta t} \right) \\
 &= 1.05 \left( \frac{10300}{2(9.81)} \right) (0.406)(0.75)|0.75| + \\
 &\quad 1.2 \left( \frac{10300}{9.81} \right) \left[ \frac{\pi(0.406)^2}{4} - \frac{\pi(0.3552)^2}{4} \right] \left( \frac{0.75}{100 \times 365 \times 24 \times 60 \times 60} \right) \\
 &= \mathbf{125.89 \text{ N/m}}
 \end{aligned}$$

While the wave load below sea water level was considered as smooth:

$$\begin{aligned}
 F &= C_D \frac{w}{2g} A U|U| + C_m \frac{w}{g} V \left( \frac{\delta U}{\delta t} \right) \\
 &= 0.65 \left( \frac{10300}{2(9.81)} \right) (0.406)(0.75)|0.75| + \\
 &\quad 1.6 \left( \frac{10300}{9.81} \right) \left[ \frac{\pi(0.406)^2}{4} - \frac{\pi(0.3552)^2}{4} \right] \left( \frac{0.75}{100 \times 365 \times 24 \times 60 \times 60} \right) \\
 &= \mathbf{77.929 \text{ N/m}}
 \end{aligned}$$

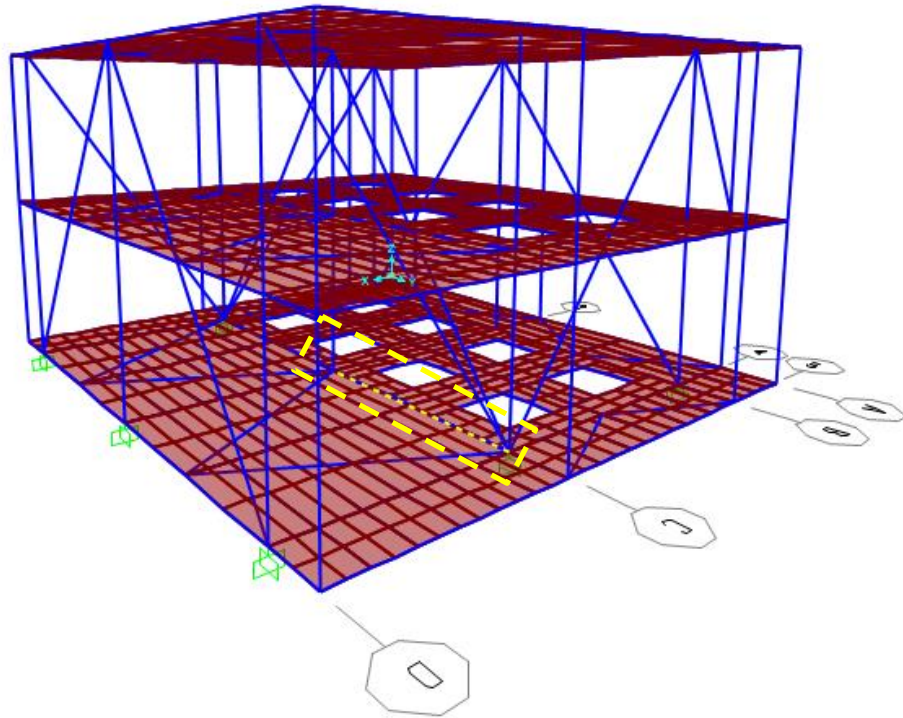
Current load

In order to calculate the current force on the structural members, no wave conditions need to be applied, by substitute the  $\frac{\delta U}{\delta t} = 0$ .

$$\begin{aligned}
 F &= C_D \frac{w}{2g} A U|U| \\
 &= 0.65 \left( \frac{10300}{2(9.81)} \right) (0.406)(0.75)|0.75| \\
 &= \mathbf{77.929 \text{ N/m}}
 \end{aligned}$$

## APPENDIX C: CONTINUED

### Design for Restrained Beam



### Load Combination: DL + LL

#### 1) Design Load

$$\text{Shear force, } V_{Ed} = -449.44 \text{ kN}$$

$$\text{Bending moment, } M_{Ed} = -667.58 \text{ kNm}$$

#### 2) Try Section

$$d = 406 \text{ mm} \quad I = 57400 \text{ cm}^4 = 5.74 \times 10^8 \text{ mm}^4$$

$$t = 25 \text{ mm} \quad W_{el} = 2690000 \text{ mm}^3$$

$$M = 235 \text{ kg/m} \quad W_{pl} = 3642000 \text{ mm}^3$$

$$A = 30000 \text{ mm}^2 \quad G = 81000 \text{ N/mm}^2$$

$$i = 135 \text{ mm} \quad E = 210000 \text{ N/mm}^2$$

## APPENDIX C: CONTINUED

### 3) Design Strength

Refer to Table 3.1 (continued), Eurocode 3 (Part 1-1)

For steel grade S355,

$$t = 25 \text{ mm} < 40 \text{ mm}$$

$$f_y = 355 \text{ N/mm}^2$$

$$f_u = 510 \text{ N/mm}^2$$

### 4) Section Classification

Referring to Table 5.2, Eurocode 3 (Part 1-1)

Tubular sections,

$$\varepsilon = \sqrt{\frac{235}{f_y}} = 0.81$$

$$\varepsilon^2 = (0.81)^2 = 0.66$$

$$\frac{d}{t} = \frac{406}{25} = 16.24 < 50\varepsilon^2 = 50(0.66) = 33$$

The section is classified as Class 1 since  $\frac{d}{t}$  meets Class 1 standard.

### 5) Shear Resistance of Section

i. Maximum external design shear force,  $V_{Ed} = -449.44 \text{ kN} = 449.44 \text{ kN}$

ii. Shear resistance of the section,  $V_{c,Rd}$

$$V_{c,Rd} = V_{pl,Rd}$$

$$V_{pl,Rd} = \frac{A_v \left( \frac{f_y}{\sqrt{3}} \right)}{\gamma_{M0}}$$

## APPENDIX C: CONTINUED

$$\gamma_{M0} = 1.00 \text{ (EC 3: Part 1, 6.1 NOTE 2B)}$$

$$f_y = 355 \text{ N/mm}^2$$

$$A_v = 2A/\pi = 2(30500)/\pi = 19417 \text{ mm}^2 \text{ (Circular Hollow Sections)}$$

$$\begin{aligned} \sim A &= \pi r_{\text{outer}}^2 - \pi r_{\text{inner}}^2 \\ &= \pi(203)^2 - \pi(177.5)^2 = 30500 \text{ m}^2 \end{aligned}$$

$$V_{\text{pl,Rd}} = \frac{(19417) \left( \frac{355}{\sqrt{3}} \right)}{1.00} = 3979695.6 \text{ N} = \mathbf{3979.70 \text{ kN}}$$

iii. Design Check

$$\frac{V_{ed}}{V_{c,Rd}} = \frac{449.44}{3979.70}$$

$$= \mathbf{0.11} \leq 1.0$$

The section is satisfactory.

6) Bending Moment Resistance of Section

i. Maximum external design moment,  $M_{Ed} = \mathbf{-667.58 \text{ kNm} = 667.58 \text{ kNm}}$

ii. Moment resistance for Class 1 cross section,  $M_{c,Rd}$

$$M_{c,Rd} = M_{\text{pl,Rd}}$$

$$M_{\text{pl,Rd}} = \frac{W_{\text{pl}} f_y}{\gamma_{M0}} \text{ (for Class 1)}$$

$$M_{\text{pl,Rd}} = \frac{(3642000)(355)}{1.00} = 1292910000 \text{ Nmm} = \mathbf{1292.91 \text{ kNm}}$$

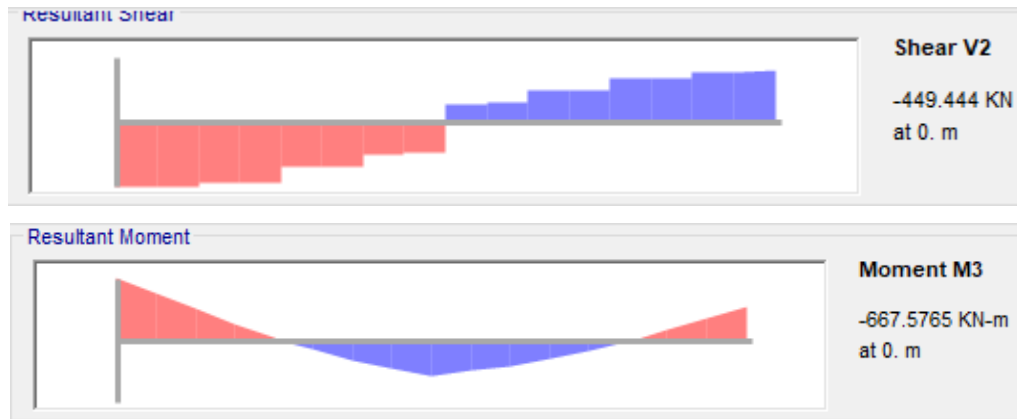
iii. Design Check

$$\frac{M_{ed}}{M_{c,Rd}} = \frac{667.58}{1292.91} = \mathbf{0.52} \leq 1.0. \text{ The section is satisfactory.}$$

## APPENDIX C: CONTINUED

### 7) Combined Bending and Shear Resistance

Referring to Shear Force and Moment diagrams, a section where the moment is maximum is considered, the mid-span section where  $V_{Ed} = -449.44$  kN and  $M_{Ed} = -667.58$  kNm.



a) Shear force at the maximum moment,  $V_{Ed} = -449.44$  kN

b)  $0.5 * V_{c,Rd} = 0.5 (3979.70) = 1989.85$  kN

c) Since  $V_{Ed} = 449.44$  kN  $<$   $0.5 V_{c,Rd} = 1989.85$  kN

The shear,  $V_{Ed}$  is small and it does not affect the moment resistance,  $M_{c,Rd}$ . The beam section is able to carry the most critical combination of bending and shear. No reduction in the yield strength of the steel,  $f_y$  and the design moment resistance remains,  $M_{c,Rd} = -1292.91$  kNm.

### 8) Resistance of Cross-sections

$$\frac{N_{ed}}{N_{Rd}} + \frac{M_{y,ed}}{M_{y,Rd}} + \frac{M_{z,ed}}{M_{z,Rd}} \leq 1$$

$$\frac{0.639}{10781.54} + \frac{667.58}{1292.91} + \frac{0.386}{1292.91} \leq 1$$

$$0.52 \leq 1 \text{ (ok!)}$$

## APPENDIX C: CONTINUED

### Load Combination: EL

#### 1) Design Load

$$\text{Shear force, } V_{Ed} = \mathbf{22.86 \text{ kN}}$$

$$\text{Bending moment, } M_{Ed} = \mathbf{31.93 \text{ kNm}}$$

#### 2) Try Section

$$d = 406 \text{ mm} \quad I = 57400 \text{ cm}^4 = 5.74 \times 10^8 \text{ mm}^4$$

$$t = 25 \text{ mm} \quad W_{el} = 2690000 \text{ mm}^3$$

$$M = 235 \text{ kg/m} \quad W_{pl} = 3642000 \text{ mm}^3$$

$$A = 30000 \text{ mm}^2 \quad G = 81000 \text{ N/mm}^2$$

$$i = 135 \text{ mm} \quad E = 210000 \text{ N/mm}^2$$

#### 3) Design Strength

Refer to Table 3.1 (continued), Eurocode 3 (Part 1-1)

For steel grade S355,

$$t = 25 \text{ mm} < 40 \text{ mm}$$

$$f_y = 355 \text{ N/mm}^2$$

$$f_u = 510 \text{ N/mm}^2$$

#### 4) Section Classification

Referring to Table 5.2, Eurocode 3 (Part 1-1)

Tubular sections,

$$\varepsilon = \sqrt{\frac{235}{f_y}} = 0.81$$

## APPENDIX C: CONTINUED

$$\varepsilon^2 = (0.81)^2 = 0.66$$

$$\frac{d}{t} = \frac{406}{25} = 16.24 < 50\varepsilon^2 = 50(0.66) = 33$$

The section is classified as Class 1 since  $\frac{d}{t}$  meets Class 1 standard.

### 5) Shear Resistance of Section

i. Maximum external design shear force,  $V_{Ed} = \mathbf{22.86 \text{ kN}}$

ii. Shear resistance of the section,  $V_{c,Rd}$

$$V_{c,Rd} = V_{pl,Rd}$$

$$V_{pl,Rd} = \frac{A_v \left( \frac{f_y}{\sqrt{3}} \right)}{\gamma_{M0}}$$

$$\gamma_{M0} = 1.00 \text{ (EC 3: Part 1, 6.1 NOTE 2B)}$$

$$f_y = 355 \text{ N/mm}^2$$

$$A_v = 2A/\pi = 2(30500)/\pi = 19417 \text{ mm}^2 \text{ (Circular Hollow Sections)}$$

$$\sim A = \pi r_{\text{outer}}^2 - \pi r_{\text{inner}}^2$$

$$= \pi(203)^2 - \pi(177.5)^2 = 30500 \text{ m}^2$$

$$V_{pl,Rd} = \frac{(19417) \left( \frac{355}{\sqrt{3}} \right)}{1.00} = 3979695.6 \text{ N} = \mathbf{3979.70 \text{ kN}}$$

iii. Design Check

$$\frac{V_{Ed}}{V_{c,Rd}} = \frac{22.86}{3979.70}$$

$$= \mathbf{0.01} \leq 1.0$$

The section is satisfactory.



## APPENDIX C: CONTINUED

### 6) Bending Moment Resistance of Section

i. Maximum external design moment,  $M_{Ed} = 31.93 \text{ kNm}$

ii. Moment resistance for Class 1 cross section,  $M_{c,Rd}$

$$M_{c,Rd} = M_{pl,Rd}$$

$$M_{pl,Rd} = \frac{W_{pl} f_y}{\gamma_{M0}} \text{ (for Class 1)}$$

$$M_{pl,Rd} = \frac{(3642000)(355)}{1.00} = 1292910000 \text{ Nmm} = 1292.91 \text{ kNm}$$

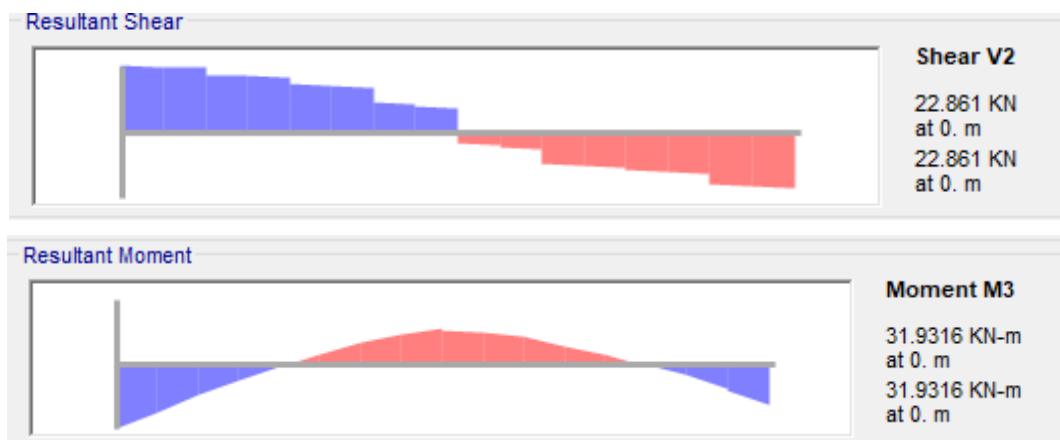
iii. Design Check

$$\frac{M_{ed}}{M_{c,Rd}} = \frac{31.93}{1292.91} = 0.03 \leq 1.0$$

The section is satisfactory.

### 7) Combined Bending and Shear Resistance

Referring to Shear Force and Moment diagrams, a section where the moment is maximum is considered, the mid-span section where  $V_{Ed} = 22.86 \text{ kN}$  and  $M_{Ed} = 31.93 \text{ kNm}$ .



a) Shear force at the maximum moment,  $V_{Ed} = 22.86 \text{ kN}$

b)  $0.5 * V_{c,Rd} = 0.5 (3979.70) = 1989.85 \text{ kN}$

## APPENDIX C: CONTINUED

c) Since  $V_{Ed} = 22.86 \text{ kN} < 0.5 V_{c,Rd} = 1989.85 \text{ kN}$

The shear,  $V_{Ed}$  is small and it does not affect the moment resistance,  $M_{c,Rd}$ . The beam section is able to carry the most critical combination of bending and shear. No reduction in the yield strength of the steel,  $f_y$  and the design moment resistance remains,  $M_{c,Rd} = 1292.91 \text{ kNm}$ .

8) Resistance of Cross-sections

$$\frac{N_{ed}}{N_{Rd}} + \frac{M_{y,ed}}{M_{y,Rd}} + \frac{M_{z,ed}}{M_{z,Rd}} \leq 1$$

$$\frac{1.461}{10781.54} + \frac{31.93}{1292.91} + \frac{0.932}{1292.91} \leq 1$$

$$0.03 \leq 1 \text{ (ok!)}$$

### Load Combination: DL + LL + EL + TH\_AC

1) Design Load

$$\text{Shear force, } V_{Ed} = -427.38 \text{ kN}$$

$$\text{Bending moment, } M_{Ed} = -636.77 \text{ kNm}$$

2) Try Section

$$d = 406 \text{ mm} \quad I = 57400 \text{ cm}^4 = 5.74 \times 10^8 \text{ mm}^4$$

$$t = 25 \text{ mm} \quad W_{el} = 2690000 \text{ mm}^3$$

$$M = 235 \text{ kg/m} \quad W_{pl} = 3642000 \text{ mm}^3$$

$$A = 30000 \text{ mm}^2 \quad G = 81000 \text{ N/mm}^2$$

$$i = 135 \text{ mm} \quad E = 210000 \text{ N/mm}^2$$

3) Design Strength

## APPENDIX C: CONTINUED

Refer to Table 3.1 (continued), Eurocode 3 (Part 1-1)

For steel grade S355,

$$t = 25 \text{ mm} < 40 \text{ mm}$$

$$f_y = 355 \text{ N/mm}^2$$

$$f_u = 510 \text{ N/mm}^2$$

### 4) Section Classification

Referring to Table 5.2, Eurocode 3 (Part 1-1)

Tubular sections,

$$\varepsilon = \sqrt{\frac{235}{f_y}} = 0.81$$

$$\varepsilon^2 = (0.81)^2 = 0.66$$

$$\frac{d}{t} = \frac{406}{25} = 16.24 < 50\varepsilon^2 = 50(0.66) = 33$$

The section is classified as Class 1 since  $\frac{d}{t}$  meets Class 1 standard.

### 5) Shear Resistance of Section

i. Maximum external design shear force,  $V_{Ed} = -427.38 \text{ kN} = 427.38 \text{ kN}$

ii. Shear resistance of the section,  $V_{c,Rd}$

$$V_{c,Rd} = V_{pl,Rd}$$

$$V_{pl,Rd} = \frac{A_v \left( \frac{f_y}{\sqrt{3}} \right)}{\gamma_{M0}}$$

$$\gamma_{M0} = 1.00 \text{ (EC 3: Part 1, 6.1 NOTE 2B)}$$

## APPENDIX C: CONTINUED

$$f_y = 355 \text{ N/mm}^2$$

$$A_v = 2A/\pi = 2(30500)/\pi = 19417 \text{ mm}^2 \text{ (Circular Hollow Sections)}$$

$$\begin{aligned} \sim A &= \pi r_{\text{outer}}^2 - \pi r_{\text{inner}}^2 \\ &= \pi(203)^2 - \pi(177.5)^2 = 30500 \text{ mm}^2 \end{aligned}$$

$$V_{\text{pl,Rd}} = \frac{(19417) \left( \frac{355}{\sqrt{3}} \right)}{1.00} = 3979695.6 \text{ N} = \mathbf{3979.70 \text{ kN}}$$

### iii. Design Check

$$\begin{aligned} \frac{V_{\text{ed}}}{V_{\text{c,Rd}}} &= \frac{427.38}{3979.70} \\ &= \mathbf{0.11} \leq 1.0 \end{aligned}$$

The section is satisfactory.

## 6) Bending Moment Resistance of Section

i. Maximum external design moment,  $M_{\text{Ed}} = \mathbf{-636.77 \text{ kNm} = 636.77 \text{ kNm}}$

ii. Moment resistance for Class 1 cross section,  $M_{\text{c,Rd}}$

$$M_{\text{c,Rd}} = M_{\text{pl,Rd}}$$

$$M_{\text{pl,Rd}} = \frac{W_{\text{pl}} f_y}{\gamma_{M0}} \text{ (for Class 1)}$$

$$M_{\text{pl,Rd}} = \frac{(3642000)(355)}{1.00} = 1292910000 \text{ Nmm} = \mathbf{1292.91 \text{ kNm}}$$

### iii. Design Check

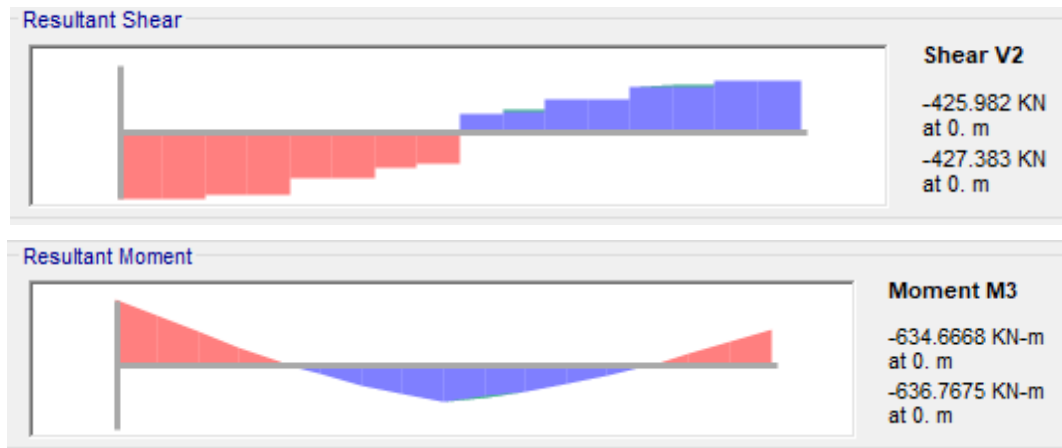
$$\frac{M_{\text{ed}}}{M_{\text{c,Rd}}} = \frac{636.77}{1292.91} = \mathbf{0.49} \leq 1.0$$

The section is satisfactory.

## APPENDIX C: CONTINUED

### 7) Combined Bending and Shear Resistance

Referring to Shear Force and Moment diagrams, a section where the moment is maximum is considered, the mid-span section where  $V_{Ed} = -427.38$  kN and  $M_{Ed} = -636.77$  kNm.



a) Shear force at the maximum moment,  $V_{Ed} = -427.38$  kN

b)  $0.5 \cdot V_{c,Rd} = 0.5 (3979.70) = 1989.85$  kN

c) Since  $V_{Ed} = -427.38$  kN  $<$   $0.5 V_{c,Rd} = 1989.85$  kN

The shear,  $V_{Ed}$  is small and it does not affect the moment resistance,  $M_{c,Rd}$ . The beam section is able to carry the most critical combination of bending and shear. No reduction in the yield strength of the steel,  $f_y$  and the design moment resistance remains,  $M_{c,Rd} = -1292.91$  kNm.

### 8) Resistance of Cross-sections

$$\frac{N_{ed}}{N_{Rd}} + \frac{M_{y,ed}}{M_{y,Rd}} + \frac{M_{z,ed}}{M_{z,Rd}} \leq 1$$

$$\frac{1.216}{10781.54} + \frac{636.77}{1292.91} + \frac{1.642}{1292.91} \leq 1$$

$$0.49 \leq 1 \text{ (ok!)}$$

**Load Combination: RS**

## APPENDIX C: CONTINUED

### 1) Design Load

$$\text{Shear force, } V_{Ed} = \mathbf{9.45 \text{ kN}}$$

$$\text{Bending moment, } M_{Ed} = \mathbf{14.83 \text{ kNm}}$$

### 2) Try Section

$$d = 406 \text{ mm} \quad I = 57400 \text{ cm}^4 = 5.74 \times 10^8 \text{ mm}^4$$

$$t = 25 \text{ mm} \quad W_{el} = 2690000 \text{ mm}^3$$

$$M = 235 \text{ kg/m} \quad W_{pl} = 3642000 \text{ mm}^3$$

$$A = 30000 \text{ mm}^2 \quad G = 81000 \text{ N/mm}^2$$

$$i = 135 \text{ mm} \quad E = 210000 \text{ N/mm}^2$$

### 3) Design Strength

Refer to Table 3.1 (continued), Eurocode 3 (Part 1-1)

For steel grade S355,

$$t = 25 \text{ mm} < 40 \text{ mm}$$

$$f_y = 355 \text{ N/mm}^2$$

$$f_u = 510 \text{ N/mm}^2$$

### 4) Section Classification

Referring to Table 5.2, Eurocode 3 (Part 1-1)

Tubular sections,

$$\varepsilon = \sqrt{\frac{235}{f_y}} = 0.81$$

$$\varepsilon^2 = (0.81)^2 = 0.66$$

## APPENDIX C: CONTINUED

$$\frac{d}{t} = \frac{406}{25} = 16.24 < 50\varepsilon^2 = 50(0.66) = 33$$

The section is classified as Class 1 since  $\frac{d}{t}$  meets Class 1 standard.

### 5) Shear Resistance of Section

i. Maximum external design shear force,  $V_{Ed} = \mathbf{9.45 \text{ kN}}$

ii. Shear resistance of the section,  $V_{c,Rd}$

$$V_{c,Rd} = V_{pl,Rd}$$

$$V_{pl,Rd} = \frac{A_v \left( \frac{f_y}{\sqrt{3}} \right)}{\gamma_{M0}}$$

$$\gamma_{M0} = 1.00 \text{ (EC 3: Part 1, 6.1 NOTE 2B)}$$

$$f_y = 355 \text{ N/mm}^2$$

$$A_v = 2A/\pi = 2(30500)/\pi = 19417 \text{ mm}^2 \text{ (Circular Hollow Sections)}$$

$$\begin{aligned} \sim A &= \pi r_{\text{outer}}^2 - \pi r_{\text{inner}}^2 \\ &= \pi(203)^2 - \pi(177.5)^2 = 30500 \text{ mm}^2 \end{aligned}$$

$$V_{pl,Rd} = \frac{(19417) \left( \frac{355}{\sqrt{3}} \right)}{1.00} = 3979695.6 \text{ N} = \mathbf{3979.70 \text{ kN}}$$

iii. Design Check

$$\begin{aligned} \frac{V_{Ed}}{V_{c,Rd}} &= \frac{9.45}{3979.70} \\ &= \mathbf{0.002} \leq 1.0 \end{aligned}$$

The section is satisfactory.

### 6) Bending Moment Resistance of Section

## APPENDIX C: CONTINUED

i. Maximum external design moment,  $M_{Ed} = 14.83 \text{ kNm}$

ii. Moment resistance for Class 1 cross section,  $M_{c,Rd}$

$$M_{c,Rd} = M_{pl,Rd}$$

$$M_{pl,Rd} = \frac{W_{pl} f_y}{\gamma_{M0}} \text{ (for Class 1)}$$

$$M_{pl,Rd} = \frac{(3642000)(355)}{1.00} = 1292910000 \text{ Nmm} = 1292.91 \text{ kNm}$$

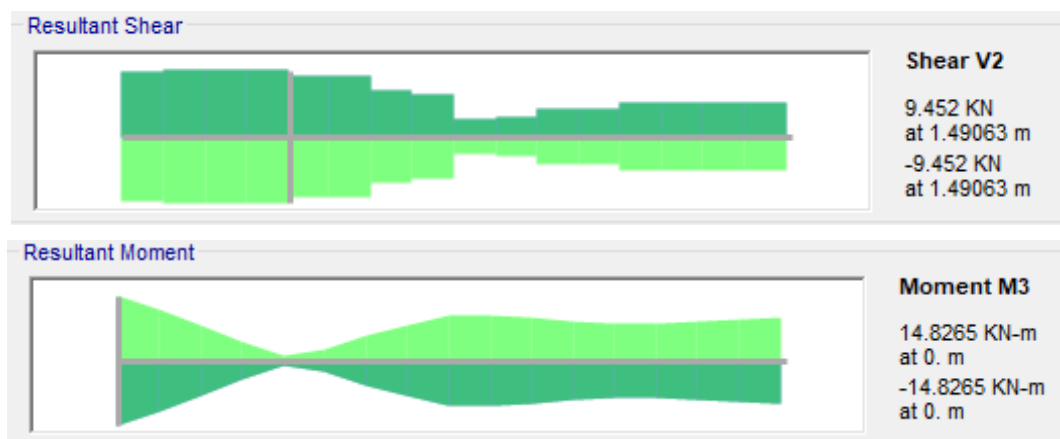
iii. Design Check

$$\frac{M_{ed}}{M_{c,Rd}} = \frac{14.83}{1292.91} = 0.011 \leq 1.0$$

The section is satisfactory.

### 7) Combined Bending and Shear Resistance

Referring to Shear Force and Moment diagrams, a section where the moment is maximum is considered, the mid-span section where  $V_{Ed} = -449.44 \text{ kN}$  and  $M_{Ed} = -667.58 \text{ kNm}$ .



a) Shear force at the maximum moment,  $V_{Ed} = 9.45 \text{ kN}$

b)  $0.5 * V_{c,Rd} = 0.5 (3979.70) = 1989.85 \text{ kN}$

c) Since  $V_{Ed} = 9.45 \text{ kN} < 0.5 V_{c,Rd} = 1989.85 \text{ kN}$



## APPENDIX C: CONTINUED

The shear,  $V_{Ed}$  is small and it does not affect the moment resistance,  $M_{c,Rd}$ . The beam section is able to carry the most critical combination of bending and shear. No reduction in the yield strength of the steel,  $f_y$  and the design moment resistance remains,  $M_{c,Rd} = -1292.91$  kNm.

### 8) Resistance of Cross-sections

$$\frac{N_{ed}}{N_{Rd}} + \frac{M_{y,ed}}{M_{y,Rd}} + \frac{M_{z,ed}}{M_{z,Rd}} \leq 1$$

$$\frac{4.268}{10781.54} + \frac{14.83}{1292.91} + \frac{0.519}{1292.91} \leq 1$$

$$0.011 \leq 1 \text{ (ok!)}$$